UNIVERSITY OF GÖTTINGEN

DOCTORAL DISSERTATION

Effects of solid additives and inorganic ligands on the efficiency of metallic iron-based water treatment systems

Dissertation for the award of the degree

Doctor rerum naturalium (Dr.rer.nat.) of the Georg-August-Universität Göttingen

within the doctoral program Geoscience of the Georg-August University School of Science (GAUSS)

Submitted by
Ran Tao from
Jiangsu
Province, China

Göttingen, 2023

Thesis Committee:

Priv.-Doz. Dr. Chicgoua Noubactep (Department of Applied Geology, Georg-August University of Göttingen),

Prof. Dr. Rui Hu (School of Earth Science and Engineering, Hohai University),

Prof. Dr. Thomas Ptak (Department of Applied Geology, Georg-August University of Göttingen),

Members of the Examination Board:

First Reviewer: Priv.-Doz. Dr. Chicgoua Noubactep (Department of Applied Geology, Georg-August University of Göttingen),

Second Reviewer: Prof. Dr. Thomas Ptak (Department of Applied Geology, Georg-August University of Göttingen),

Further members of the Examination Board:

Prof. Dr. Hans Ruppert (Department of Sedimentology & Environmental Geology, Georg-August University of Göttingen),

Prof. Dr. Hongbiao Gu (School of Transportation Science & Engineering, Nanjing Tech University),

Prof. Dr. Tobias Licha (Professor of Hydrogeochemistry, Ruhr University Bochum)

Date of the oral examination: 15.01.2024

Abstract

Metallic iron (Fe^0) or zero-valent iron (ZVI) has been extensively used for water remediation during the past three decades. It has been proven to be effective in treating waters polluted with chlorinated aliphatics, dyes, heavy metals, pathogens, radionuclides and more. Fe^0 is an abundant, low-cost, and non-toxic reactive metal. Its environmental reactivity is justified by the negative electrode potential of the redox couple Fe^{II}/Fe^0 ($E^0 = -0.44$ V). These characteristics of Fe^0 have been exploited in a wide range of remediation technologies, including both permeable reactive barriers (PRBs) for in-situ groundwater remediation, and filtration systems (Fe^0 filters) for decentralized water treatment. Fe^0 PRBs and Fe^0 water filters employ Fe^0 and other solid aggregates (e.g. MnO_2, pyrite, sand) to passively remediate polluted waters in a reactive zone. A polluted water flowing through a reactive zone packed with Fe^0 is ideally satisfactorily decontaminated, meaning that the contaminant concentrations in the outflow are below regulatory levels (called maximum contamination level - MCL).

The voluminous literature on "water remediation using Fe^0" is characterized by the huge number of parameters which have been shown to affect the efficiency of Fe^0/H_2O remediation systems under environmental conditions. Relevant parameters include: (i) Fe^0 type, (ii) nature and concentration of pollutants, (iii) pH value, (iv) O_2 concentration, (v) water salinity, (vi) water flow velocity (contact time), and (vii) ambient temperature. These factors are interrelated and have been frequently demonstrated as important from isolated sets of experiments. However, because of the lack of (i) a reference Fe^0 material, and (ii) a unified experimental procedure, it is practically impossible to compare data obtained with different contaminants, different natural waters and using different Fe^0 samples. A major shortcoming of published results from batch experiments is that they have been achieved within very short equilibration times (some few hours or days). More so, they have been mostly achieved under mixing and stirring conditions that do not represent the conditions in filtration systems while additionally considering Fe^0 as a reducing agent. The net result is that it is doubtful whether the reported limitations of the Fe^0 technology have been accurately identified.

To address these gaps, the present thesis was designed to: (i) theoretically discuss the importance of hybrid Fe^0/aggregate systems for the sustainability of Fe^0 filters (Objective 1), and (ii) experimentally investigate the influence of five common anions (Cl^-, F^-, HCO_3^-, HPO_4^{2-}, and SO_4^{2-}) on the efficiency of Fe^0/H_2O remediation systems (Objective 2). Objective 1 was achieved by a critical literature review, and published as such (review article). Objective 2 was achieved through a series of quiescent batch experiments lasting for up to 45 days using the methylene blue method (MB method). Each system was characterized by the extent of dye discoloration, the final iron concentration and the final pH value. Experiments were conducted in assay tubes containing 20 or 22 mL of MB, 0.1 of Fe^0, 0.5 g of sand, and various concentrations of anions. The MB method is an innovative procedure which enables monitoring the availability of solid iron corrosion products (FeCPs) in a Fe^0/sand/H_2O system. The results are summarized in two research articles.

Results from Objective 1 indicate that hybrid systems which are likely to be sustainable (e.g. Fe^0:sand < 10% (v/v)) are yet to be investigated. Experimental results (Objective 2) showed that all five tested anions basically inhibit the remediation process as Fe salts are formed within individual systems, thereby delaying the availability of FeCPs which are the effective contaminant scavengers. For the chloride and sulfate, the present work has established that Cl^- and SO_4^{2-} basically delay the process of contaminant removal in Fe^0/H_2O systems because the stability of Fe-salts (e.g. $FeCl_2$, $FeCl_3$, $FeSO_4$) delay the availability of solid iron corrosion products. The results also present a better explanation of the ambivalent role of HCO_3^- (e.g. inhibitory at high concentrations, and enhancing at lower ones). In fact, the impact of HCO_3^- is not limited to a concentration-dependent buffering effect but reveals the kinetics of the formation of a $FeCO_3$ scale on Fe^0. As expected, phosphate inhibition of Fe^0 reactivity was observed, since phosphate could form inner-sphere complexes with dissolved Fe and co-precipitates on the Fe^0 surface, which inhibits electron transfer from Fe^0 to protons (H^+ from water dissociation). Lastly, fluoride is demonstrated as a strong inhibitor of Fe^0 reactivity because of the formation of very stable FeF_6^{3-} complexes, delaying the precipitation of FeCPs.

Based on the results achieved in this thesis, one of the most productive areas for future work would involve investigating the suitability of lower than 10% (vol/vol). Related small-scale experiments should last for several months or years to interpret the unexpected long-term corrosion kinetics. In addition, better experimental protocols to characterize the influence of co-solutes on the Fe^0 remediation systems is possible. More systematic research is needed to design efficient and sustainable real world Fe^0-based systems characterized by multi-anion-compositions. Replicating the experiments conducted herein with relevant mixtures of anions (e.g. HCO_3^--Cl^--SO_4^{2-} or HCO_3^--F^--SO_4^{2-}), representative for natural waters seems to be to logical next step.

Keywords: Co-existing solutes, Groundwater remediation, Porosity loss, Reactivity loss, Zero-valent iron.

Acknowledgements

It has been more than 6 years since I first arrived in Germany. I finished my master study in 2019 and worked on my Ph.D. since 2020.03. This road was not easy as previously expected. The Covid, the pressure from paper submission, the failure of experiments as well as the expectations from my family and friends all hit and inspired me. And finally, I arrived.

I would like to express my best appreciations to my family, my supervisors, my colleagues and all my friends who were in company with me in these challenging times.

I would like to thank Prof. Dr. Thomas Ptak for your tremendous support during my master and Ph.D. period. We had great time working together on the field courses every year. I am so appreciating that you could always give me constructive suggestions for my manuscripts and researches.

I am so grateful to Priv.-Doz. Dr. Chicgoua Noubactep for not only being a supervisor, but also a friend during these four years. Your academic support for my research, your encouragement when I am disappointed and your patience for my mistakes helped me to continue working.

I would like to thank Prof. Rui Hu for providing me professional suggestions and information for my research. My work was better presented under your guidance. And I am happy that you are always standing by me when I need help.

I would like to thank all the committee members, for reading my Ph.D. thesis and attending my defense. It is my glory.

I am also grateful to my colleagues, Huichen Yang, Minhui Xiao and Xuesong Cui for your help in my experiments and the accompany during the times in Gottingen.

Special appreciations to my parents. Thank my mother Qin Yu and my father Rong Tao for your selfless love on me, the financial support during my Germany period and your endless and thoughtful kindness. Without your support, I can’t achieve so much.

Contents

List of Figures

List of Tables

Chapter 1: Introduction

1.1 Background

The quest for safe drinking water and a clean environment has motivated the application of metallic iron (Fe^0) in environmental remediation (Baker 1934, Henderson and Demond 2007, Noubactep 2018a, Noubactep 2020, Noubactep 2024). This technology is a century old (Bischof 1973, Bischof 1877, Devonshire 1890, Mwakabona et al. 2017) but it has regained interest during the 1990s when Gillham and colleagues realized that halogenated hydrocarbons (RCl) dissolved in groundwater disappeared in Fe^0-based sampling vessels (Reynold et al. 1990, Lee et al. 2004, Gillham 2010, Naidu et al. 2014). The observation was interpreted as RCl reduction by Fe^0 after Equation 1.1 (Gillham and O'Hannesin 1994, Matheson and Tratnyek 1994, Weber 1996, Gillham 2010). Suggesting that RCl is reduced to RH by electrons from Fe^0, an electrochemical reaction.

$$Fe^0 + RCl + H^+ \Rightarrow Fe^{2+} + Cl^- + RH \qquad (1.1)$$

This observation was in turn the motivation for the development of subsurface permeable reactive barriers (PRBs) which are regarded as one of the most promising available technologies for groundwater remediation (Naidu et al. 2014, Lawrinenko et al. 2023b, Plessl et al. 2023, Singh et al. 2023).

Currently, Fe^0-based filtration is also considered to be one of the most affordable and applicable technologies for decentralized safe drinking water supply (Naseri et al. 2017, Noubactep 2018a, Mueller et al. 2023, Bandyopadhyay 2024). In other words, the Fe^0 technology can significantly contribute to achieving the two United Nations (UN) Sustainable Development Goals (SDGs) focusing explicitly on freshwater: (i) Goal 6 "*Ensure availability and sustainable management of water and sanitation for all*", and (ii) Goal 14 "*Conserve and sustainably use the oceans, seas and marine resources for sustainable development*" (Hering et al. 2016). Hering et al. (2016) anticipated that, given the timeframe of the then only 15 years (in 2016) to achieve the 17 SDGs by 2030, scientists were required to effectively translate existing knowledge into practical solutions. Now, this timeframe has been reduced to less than a decade, i.e. 7 years.

Translating existing knowledge on "water remediation using Fe^0" into practical efficient Fe^0 water filtration systems implies a profound understanding of the variables (e.g. factors, parameters) that influence their operation and performance in the field (Sun et al. 2016, Naseri et al. 2017, Li et al. 2019, Noubactep 2018b, Noubactep 2019, Noubactep 2024). Relevant factors include: (i) Fe^0 characteristics (e.g. reactivity, shape, size), (ii) operating conditions (e.g. Fe^0 loading, Fe^0 admixing with other aggregates, water flow velocity), (iii) solution chemistry (e.g. common major anions and cations, dissolved O_2, natural organic matter - NOM), and (iv) ambient temperature (Sun et al. 2016, Naseri et al. 2017). All these factors have been demonstrated in individual investigations to exert significant negative or positive effects on the performance of Fe^0 towards contaminant removal (Su and Puls 2001, Klausen et al. 2003, Westerhoff and James 2003, Bi et al. 2009a, Sun et al. 2016). It is obvious, that depending on the removal mechanisms of the respective contaminants and other environmental conditions, an individual variable may exhibit different effects (Sun et al. 2016). For this reason, a reference Fe^0 material (Cui et al. 2023) and a unified experimental procedure (Naseri et al. 2017) seem to be the starting point for achieving more reliable results (Xiao et al. 2023, Xiao et al. 2024). It is therefore not surprising that the effects of many of these factors on the performance of Fe^0 systems have not been well understood despite three decades of intensive research (Sun et al. 2016, Lawrinenko et al. 2023a, Plessl et al. 2023, Singh et al. 2023). The present work was designed to address two aspects: (i) the significance of hybrid Fe^0/aggregate systems for the sustainability of Fe^0 filters, and (ii) the effects of common anions on the contaminant removal efficiency. Such a fundamental understanding should shape the design of future research for more efficient Fe^0 filters.

1.2 State-of-the-art knowledge

Filtration in Fe^0-based systems represents an efficient technology for the remediation of polluted waters, but the evidence in the literature lacks an understanding of their long-term performance. This section gives an overview of the state-of-the-art knowledge of the two aspects investigated in this work.

1.2.1 The suitability of hybrid Fe^0/aggregate systems

The fundamental characteristic of Fe^0 used in Fe^0-based filtration systems is the volumetric expansive nature of the iron corrosion process (Pilling and Bedworth 1923, Caré et al. 2008, Caré et al. 2013). In fact, each solid iron corrosion product (FeCPs or "oxides") is larger in volume than the parent metal (iron): i.e., $V_{oxide} > V_{iron}$. According to Caré et al. (2008) the volumes of individual oxides are 2.1 to 6.4 times larger than Fe^0. This implies that under environmental conditions ($pH > 4.5$), the initial porosity of any Fe^0-based filter is progressively filled by in-situ generated FeCPs, leading to porosity loss. This porosity loss is necessarily coupled to reductions in the hydraulic conductivity (permeability loss) of the Fe^0 filter (Handerson and Demond 2007, Ruhl et al. 2012, Domga et al. 2015, Bilardi et al. 2023). This evidence has been considered in the Fe^0 literature only around 2010, approximately some 15 years after the installation of the first commercial full-scale Fe^0 PRB in Sunnyvale, California/USA (Singh et al. 2023). Even after this realization, mixing Fe^0 with granular materials to build hybrid Fe^0/aggregate systems is discussed, just as a strategy to improve the hydraulic behavior of Fe^0 filters. However, mixing non-expansive aggregates to Fe^0 should be regarded as a pre-requisite for sustainable filtration systems (Domga et al. 2015, Naseri et al. 2017). In other words, Fe^0 filters without aggregates are not sustainable because they will lose porosity and hydraulic conductivity, resulting in clogging (Hussam 2009, Bilardi et al. 2023, Noubactep 2020, Noubactep 2021, Noubactep 2024).

Following this highly pragmatic approach, many inert (e.g. gravel, sand) and reactive (e.g. magnetite, pyrite) materials have been proposed and tested to sustain the reactivity and the permeability of Fe^0 filters as recently reported by Bilardi et al. (2023). However, works using pure Fe^0 beds (100 % Fe^0) are still performed (Yu et al. 2023). Thus, there is a need for a critical review of how hybrid Fe^0/aggregate systems have been investigated in order to shape future experimental methodologies. It is important to recall that the breakthrough in understanding the suitability of Fe^0/aggregate systems for sustainable Fe^0-based systems was achieved using the methylene blue method (Miyajima 2012, Miyajima and Noubactep 2012). The methylene blue method (MB method) is a low-cost but efficient tool for characterizing the extent of FeCPs availability within a Fe^0/H_2O system.

The MB method uses MB as an indicator of reactivity for the Fe^0/H_2O system (Miyajima 2012, Btatkeu-K. et al. 2016, Konadu-Amoah et al. 2021). The MB method is hinged on the historic findings by Mitchell et al. (1955) that the efficiency of pure sand to adsorb MB declines as iron oxides progressively cover the surface of sand. The suitability of the MB method to characterize Fe^0/H_2O systems is based on the evidence that: (i) sand is a good adsorbent for MB, and (ii) iron oxide-coated sand has a poor affinity for MB discoloration (Miyajima 2012). The method characterizes MB discoloration by sand as it is in-situ coated by FeCPs in Fe^0/H_2O/sand system. In order words, the MB method enables the detection of the decline of Fe^0 reactivity (reactivity loss), which is related to porosity loss. In fact, Miyajima (2012) has also demonstrated the ability of the MB method to trace the clogging of Fe^0 filters (permeability loss). Miyajima (2012) unequivocally demonstrated for the first time, that admixing Fe^0 with non-expansive aggregates is a pre-requisite for sustainable Fe^0 filters. Prior to 2012, admixing Fe^0 with other aggregates was regarded as "material dilution" with possible impacts on reaction rates and contaminant removal efficiency despite beneficial cost reduction (Kenneke and McCutcheon 2003, Kaplan and Gilmore 2004, Song et al. 2005, Bi et al. 2009a). This misconception originated from the falsified view that Fe^0 is a reducing agent for many dissolved species (Matheson and Tratnyek 1994, Weber 1996, Lawrinenko et al. 2023a, 2023b). Unfortunately, this view is still prevailing

(Lawrinenko et al. 2023a, Noubactep 2021, Noubactep 2023, Noubactep 2024) and has affected the understanding of both key aspects addressed in this work. For the sake of clarity, Chapter 3 will present the background of the experimental methodology in more details. An overview of the achieved results is given in Chapter 5 and the published review article appended to this work.

1.2.2 Effects of common anions on the efficiency of Fe^0-based systems

Typical anions present in natural water include (hydro)carbonate (CO_3^{2-} or HCO_3^-), chloride (Cl^-), nitrate (NO_3^-), phosphate ($H_2PO_4^-$ or HPO_4^{2-}), silicate (SiO_3^{2-}) and sulfate (SO_4^{2-}). The nature and the concentration of anions in the aqueous matrix are reported to dictate the remediation performance of Fe^0-based systems (Klausen et al. 2003, Kim et al. 2007, Sun et al. 2016). As summarized in a recent review article by Sun et al. (2016), NO_3^- is redox-active and "consumes Fe^0" through cathodic attack while non-redox anions may form solid precipitates that subsequently deposit on the Fe^0 surface. Such precipitates form (i) a physical barrier for mass transfer to (and from) the Fe^0 surface, and (ii) a conduction barrier for electrons from the Fe^0 surface (Henserson and Demond 2007, Hu et al. 2021). Sun et al. (2016) also reported that Cl^- and to some extent SO_4^{2-} may enhance the performance of Fe^0 remediation systems either by (i) facilitating the breakdown of passivating oxide scales and/or (ii) enabling the formation of new reactive phases within the system. Moreover, for individual anions ambivalent or mixed effects are reported while varying their initial concentrations or the reaction (even for the same contaminant).

This presentation is based on Sun et al. (2016) as it was the most recent overview article at the start of this work. However, the start-of-the-art knowledge has not changed despite 7 additional years since 2016 (Roccamante et al. 2022). The discussion of the influences of common anions on the performance of Fe^0 remediation systems is mostly falsified by the view that Fe^0 is a reducing agent under environmental conditions (Equation 1.1) (Matheson and Tratnyek 1994, Hu et al. 2021, Lawrinenko et al. 2023a). In addition, it would be suitable to investigate the performance of Fe^0 remediation systems as influenced by common anions while excluding any redox interaction except for the Fe^0 oxidation by water (H^+) (Equation 1.2).

$$Fe^0 + 2\,H^+ \Rightarrow Fe^{2+} + H_2 \qquad (1.2)$$

The MB method fulfils these requirements while excluding NO_3^- from the investigated systems will account for the requirement related to the redox reactivity of anions. Note that works under experimental conditions similar to those used herein have demonstrated that SO_4^{2-} is not redox reactive (Gatcha-

Bandjun et al. 2017, Tsamo et al. 2018). The background of this knowledge is summarized in Chapter 3 and the achieved results discussed in Chapter 5.

1.2.3 Knowledge gaps on both aspects and their interlinkages

Sections 1.2.1 and 1.2.2 demonstrate that there are gaps in knowledge regarding the operating mode of Fe^0 filters and their long-term efficiency. Actually, accurately evaluating the sustainability of such systems is essential, both for future researchers and policymakers. However, previous and current evaluations either neglect or insufficiently address interlinkages among factors influencing the performance of the systems. In particular, investigating the influences of admixing Fe^0 and other aggregates has been performed in the perspective that the aggregates will reduce the efficiency of the systems (Rahman et al. 2013, Bilardi et al. 2023). Similarly, investigating the effects of common anions on the Fe^0/H_2O system has been almost limited to discuss how, and to which extent, the electron transfer from Fe^0 is impacted (Sun et al. 2016). This situation has led to unclear identification of leverage points to enhance the sustainability of Fe^0 filters. Thus, there is a need to identify and establish complex interlinkages among key factors affecting the sustainability of Fe^0 filters as used in subsurface PRBs and systems for decentralized safe drinking water supply. The results would: (i) help researchers to design better experiments in future, and (ii) enable policymakers to take well-informed decisions before implementing Fe^0 filters.

1.3 Research objectives

The goal of this thesis is to shape practical applications of Fe^0 filtration systems by:

(i) theoretically discussing the suitability of hybrid Fe^0/aggregate systems for filter design, and

(ii) experimentally investigating the influences of five common groundwater anions (Cl^-, HCO_3^-, F^-, HPO_4^{2-}, and SO_4^{2-}) on the performance of Fe^0-based systems for water decontamination.

An important feature of the study design is to use the methylene blue method in batch experiments without any attempt to mechanically homogenize the solutions. This experimental design provides an affordable and replicable setup to investigate processes associated with contaminant removal under the diffusion-driven conditions occurring in Fe^0 filters. Non-agitated or quiescent batch experiments also facilitates the formation of the oxide scale which would otherwise be disturbed through agitation.

The working hypothesis for experimental investigations is based on Equation 1.3 and states that the addition of any anion delays or inhibits the process of MB discoloration. This is because MB discoloration is achieved by adsorption and co-precipitation with FeCPs.

$$Fe^0, H_2O, \text{anions}, O_2 \Rightarrow \text{Fe-salts or Fe-complexes} + \text{FeCPs} \qquad (1.3)$$

Because all anions tested (Cl^-, HCO_3^-, F^-, HPO_4^{2-}, SO_4^{2-}) form salts (e.g. $FeCl_3$) or complexes (e.g. FeF_6^{3-}) with Fe^{2+} and/or Fe^{3+}, the availability of FeCPs should be typically delayed.

1.4 Research methodology

Quiescent batch experiments are used to monitor the extent of MB discoloration by various Fe^0/sand systems (MB method) as influenced by the presence and the amounts of individual anions for an experimental duration of up to 45 days. The MB method traces the dynamics within the Fe^0/H_2O system by exploiting the differential adsorptive affinity of MB onto sand and sand coated with iron corrosion products (FeCPs). It evaluates the degree of Fe^0 corrosion in various Fe^0/anion/H_2O systems. The extent of MB discoloration in various Fe^0-based systems was characterized in parallel quiescent batch experiments for 0 to 45 days. Parallel experiments with Orange II as a model contaminant allowed an improved discussion of the results. Additional experiments using 4 different Fe^0 types were conducted. Each system was characterized by: (i) final pH value, (ii) final Fe concentration, and (iii) extent of dye discoloration.

A detailed description of background of the experimental methodology is given in Chapter 3. Chapter 4 provides details on material and methods used.

1.5 Outline of the thesis

This introductory chapter has given the theoretical background of the study, together with the current state-of-the-art knowledge on (i) designing hybrid Fe^0/aggregate systems, and (ii) the influences of common groundwater anions on the efficiency of Fe^0-based remediation systems. The remaining of the thesis is presented as follows:

- Chapter 2 gives an overview of the named state-of-the-art knowledge as reflected by the published literature;
- Chapter 3 presents the background of the used experimental methodology to outline its novelty;
- Chapter 4 summarizes the experimental conditions used;
- Chapter 5 present the achieved results and give a discussion;

- Chapter 6 provides a general conclusion of this work and gives some suggestions for further research;
- A list of all references used in all chapters; and
- An appendix closes the presentation.

The appendix includes a list of journal articles that were authored or co-authored by me and directly related to the presented work. In summary, two papers were published, and one manuscript is submitted. The appendix also includes all experimental results achieved in the framework of this thesis.

Chapter 2: Literature review

This chapter summarizes the state-of-the-art knowledge on: (i) the design of hybrid Fe^0/H_2O filtration systems, and (ii) the effect of common anions on the performance of such systems. Both aspects are tied by the evidence that the extent of iron corrosion and thus the extent to which available pores are filled depends on how anions influence the solubility of Fe^{2+} and its transport within and eventually out of the filter. This chapter is not repeating the reasoning used in introducing the appended two articles (Tao et al 2022, Tao et al 2023) and one submitted manuscript (Tao et al. 2024). Rather, a critical overview is given that (i) is based on the chemistry of the system (Equation 2.1), and (ii) considers the current state of the knowledge, including views published after these articles.

$$Fe^0 + 2\ H^+ \Longrightarrow Fe^{2+} + H_2 \qquad (2.1)$$

Equation 2.1 recalls the reaction of the oxidative dissolution of Fe^0 that is the fundamental reason for using this readily available and cost-effective material in water remediation (James et al. 1992, Henderson and Demond 2007, Noubactep and Caré 2010a, Noubactep and Caré 2010b, Wu et al. 2017). The application of Fe^0–based filtration systems have been reported to suffer from reactivity loss and permeability loss (Henderson and Demond 2007, Guan et al. 2015, Wu et al. 2017, Saadatpour et al. 2023, Singh et al. 2023). Discrepancies on the extent of the importance of both aspects have been reported in the literature and can be collectively attributed to the fact that both aspects have been considered separately. However, given that Equation 1 describes the oxidation of Fe^0 by water, it must be considered that each individual Fe^0 particle experiences reactivity loss and the extent to which it is consumed contribute to reducing the pore space (porosity loss and the permeability loss) (Domga et al. 2015, Yang et al. 2020, 2021, 2022).

Equation 2.1 is also a compass to evaluate the extent to which contaminants are removed and the permeability decreases. The ambivalent nature of iron corrosion for the sustainability of Fe^0-based filters has been difficult to consider in previous works (Wu et al. 2017, Bilardi et al. 2023, Saadatpour et al. 2023): iron corrosion induces water treatment (beneficial), and the same reaction causes porosity loss (harmful) (Henserson and Demond 2007, Domga et al. 2015). This makes designing efficient and sustainable Fe^0 filters challenging (Miyajima 2012, Rahman et al. 2013, Yang 2022). The three fundamental questions to answer are: (i) how much iron oxidizes (e.g. per unit time)? (Question 1), (ii) which amount or which fraction of dissolved Fe is transported out of the column? (Question 2), and (iii) which amount of dissolved Fe is precipitated and available to act as contaminant scavengers? (Question 3). Questions 1 to 3 can only be answered together, ideally while using a holistic spatiotemporal approach (Yang 2022). This makes the conventional approach of separately characterizing the nature and amount of FeCPs and the extent of porosity loss at specific times, for instance at the end of a short-term experiment (Wielinski et al. 2022) unreliable or at least non accurate (Yang 2022). The methylene blue method used in this work has been demonstrated a powerful tool to solve this critical problem (Btatkeu-K et al. 2016, Konadu-Amoah et al. 2022).

2.1 The suitability of Fe^0/aggregates hybrid systems

2.1.1 General aspects

To predict spatiotemporal changes of porosity of a Fe^0-based filter, it suffices to consider the time-dependent extent of the following (Yang 2022, Bilardi et al. 2023): (i) Fe^0 corrosion (Equation 2.1), (ii) precipitation of solid iron corrosion products (e.g. Fe oxides and hydroxides - FeCPs), (iii) precipitation of other minerals (e.g. $CaCO_3$, $FeCO_3$), (iv) accumulation of H_2, and (v) accumulation of contaminants. It can be operationally considered that H_2 escapes out of the system. The contribution of other minerals and contaminants to porosity loss can also be neglected. This can be considered as an oversimplification but it shows that iron corrosion by water alone do provoke porosity loss and this was experimentally documented by Luo et al. (2013) using deionized water.

The other characteristic feature of Fe^0 corrosion to consider is its volumetric expansive nature (Whitney 1903, Pilling and Bedworth 1923, Caré et al. 2008, Zhao et al. 2011). Because the volume of the corrosion products (FeCPs - oxides) is greater than that of the original metal ($V_{oxide} > V_{iron}$), the formation of the FeCPs induces a reduction in the pore volume (porosity loss), and this occurs for each Fe^{2+} from Equation 2.1 unless it is complexed, for instance by Cl^- (e.g. $FeCl_3$), F^- (e.g. FeF_6^{3-}) or natural organic matters. However, even in cases such stable complexes are formed, they are transported away from the Fe^0 particles which continue to corrode. In other words, stable complexes sustain the reactivity of Fe^0, which is available in large stoichiometric amount in a Fe^0-based filter. Clearly, when strong complexing agents (e.g. Cl^-, F^-) are available, more Fe^0 is corroded. The net result is a comparative delay in porosity loss. Under static conditions (batch studies), strong complexing agents delay the availability of FeCPs and thus the decontamination process (section 2.2).

2.1.2 Fe^0 corrosion in porous media

A reliable approach for a knowledge-driven design of sustainable and stable Fe^0 filters goes through a holistic analysis of the Fe^0/H_2O system (Noubactep 2009b, Cao et al. 2021a). A Fe^0 filter is a porous bed containing granular Fe^0 in a pure (Fe^0 alone) or in a hybrid system (e.g. Fe^0/pyrite, Fe^0/sand). A porous bed is characterized by an initial porosity, e.g. 36 % for compact spheres (Caré et al. 2013, Rahman et al. 2013) which necessarily decreased over the time as contaminants are eliminated from inflowing polluted waters.

Iron corrosion in a Fe^0 filter is an electrochemical process as discussed above (Equation 2.1). The 4 components are (Xiao et al. 2023, Xiao et al. 2024): (i) iron dissolution at an anodic site of Fe^0 (releasing Fe^{2+} and leaving electrons behind), (ii) transport of released Fe^{2+} through the electrolyte (polluted water) away from the Fe^0 surface, (iii) transfer of electrons to a cathodic site on the surface of uncorroded Fe^0, and (iv) H^+ reduction at the cathode. The corrosion rate is influenced by several factors including: (i) the rate with which species H^+ and Fe^{2+} are consumed or released (intrinsic reactivity), (ii) their transport through the pore system within the filter (solution chemistry), (iii) the occurrence of further chemical reactions such as complexation, oxidation, precipitation (pH value solution chemistry), and (iii) the occurrence of physical processes such as adsorption, ion exchange, and size-exclusion (pH value, solution chemistry) (Nesic 2007, Noubactep 2015, Angst 2019). Items (i) to (iv) locally affect the electrolyte chemistry at the Fe^0 surface, which in turn affects the electrochemical reaction kinetics of the uncorroded Fe^0. It is essential to mention that H_2 and Fe^{2+} (Equation 2.1) are stand-alone reducing agents for several organic (Jiao et al. 2009) and inorganic pollutants (Farrell et al. 2001). Moreover, several Fe^{II} and Fe^{II}/Fe^{III} species generated in Fe^0/H_2O systems are stand-alone natural reducing agents (Scherer et al. 2000, Henderson and Demond 2007).

Another characteristic feature of Fe^0 filters is the presence of a porous medium which significantly influences all processes involved in the progression of iron corrosion (Equation 2.1). The most important being that (i) there is limited space to store expansive corrosion products, and (ii) transport processes are all limited (e.g. restricting convection). A potential beneficial role of a porous medium adjacent to the Fe^0 surface is that different local properties at the Fe^0/H_2O interface create new electrochemical cells to sustain corrosion.

Summarized, to design a Fe^0 filter, the following is needed: (i) a filter container, (ii) a reactive Fe^0 sample, and (iii) one or several filling materials (e.g. MnO_2, pumice, sand) or reactive aggregates (e.g. MnO_2, pyrite). Because Fe^0 corrosion is volumetric expansive is nature, a pure Fe^0 filter (100 % Fe^0) can be efficient but not sustainable (Hussam 2009, Domga et al. 2015). In other words, sustainable Fe^0 filters are hybrid in nature (e.g. Fe^0/sand). Practically, Fe^0 proportion, Fe^0 type, Fe^0 shape, initial porosity, nature, shape and size of admixing aggregates, and water quality are interrelated parameters which all influence progressive generation and accumulation of iron corrosion products (FeCPs) within the pores of any Fe^0 filter. Filter function can be influenced by sediment influx and deposition. Consequently, determining the rate of sedimentation and the period before sediment accumulation obstructs the filter's ability to function effectively is crucial. While designing a filter, enough storage capacity for FeCPs should be considered so that FeCPs accumulation does not affect the filter's function during its planned operational life. One proven efficient approach has been the use of porous Fe^0 materials (Bischof 1973, Hussam and Munir 2007, Hussam 2009).

2.1.3 Fundamental flaws in designing Fe^0 filters

The literature reports on "detailed analysis of the rate of surface precipitate buildup" (Wilkin et al. 2002) in Fe^0 filters as a critical step in understanding how long long-term systems can be sustainably designed (Li et al. 2005, Li et al. 2006, Li and Benson 2010). However, the reasoning was rooted on the Fe^0 amount available for the reductive transformation of selected contaminants (Sarr 2001, Wilkin et al. 2002). In this approach, depending on the environmental conditions (e.g. aquifer chemistry, composition of Fe^0 filter), different types of minerals and surface coatings have been discussed (Li et al. 2006, Li and Benson 2010, Guan et al. 2015). The impacts of microbiological processes (e.g. presence of bacteria and their mediated processes) have also been largely discussed (Gu et al. 1999, Scherer et al. 2000, Henderson and Demond 2007). In this context, Wilkin et al. (2002) presents a subsurface Fe^0 filter as a "large reservoir of iron" for contaminant transformation whose action can be enhanced by microorganisms including iron-reducing, sulfate-reducing, and/or methanogenic bacteria. Wilkin et al. (2002) also suggested that such enhancement may occur at the "expense of faster corrosion", thereby inducing a faster clogging of the Fe^0 filter.

The approach presented by Wilkin et al. (2002) is commonplace in the Fe^0 literature and was mainly a recommendation of the Interstate Technology & Regulatory Council (ITRC 2005, 2011). Accordingly, to explore the bio-geochemical processes occurring within a Fe^0 filter, and thus understand the reasons of reactivity loss and permeability loss, sophisticated structural analytical techniques and detailed coring and water sampling programs are needed (Gaspar et al.2002, McGuire et al.2003, Li et al 2019, Wielinski et al. 2022). However, in the absence of any theory of the system (Section 1), there is no guide to orient the discussion of achieved results. In addition, most of the observations made from coring and water sampling programs are just static snap-shots and their measurements are inaccurate (Brenner 2010). Thus, they cannot enable the generation of non-trivial models of the dynamic processes within Fe^0 filters, especially as these occur over an enormous range of time scales - from some few days or weeks (lab experiments) to several months or years (pilot studies and field implementations). Moreover, each Fe^0 material has its own intrinsic corrosion rate (Reardon 1995), meaning that two different materials will fill the same pore space within different time scales.

The approach recommended by the ITRC for subsurface Fe^0-based permeable reactive barriers (Fe^0 PRBs) aimed at: (i) characterizing the surface precipitates and minerals formed within and down gradient of the Fe^0 PRBs, (ii) developing conceptual models to predict the type and rate of precipitate formation, (iii) identifying relevant microbiological activities impacting the service life of Fe^0 PRBs, and (iv) developing applicable and cost-effective protocols for long-term performance monitoring of Fe^0 PRBs.

Ideally, a Fe^0 PRB should support complete groundwater remediation while maintaining an acceptable hydraulic conductivity over its planned service life. However, inherent temporal and spatial variability of chemical, microbial, and physical processes within the Fe^0 PRB are difficult to correlate with permeability loss and reactivity loss using the conventional approach (Wielinski et al. 2022). This correlation has not been successfully established by the ITRC approach (Santisukkasaem and Das 2019, Wielinski et al. 2022), suggesting that an alternative approach is needed to design sustainaible Fe^0 filters, including Fe^0 PRBs (Wielinski et al. 2022). The service life of a Fe^0 filter is essentially determined by how fast minerals precipitate within its pore space, which in turn, determines the rate of porosity and permeability loss. This reveals the paramount importance of the corrosion rate (Fe^0 intrinsic reactivity) of used materials in aqueous environments (Lufingo et al. 2019, Cui et al. 2023). Since 1995, the corrosion rate of Fe^0 materials has been widely characterized (Reardon 1995, 2005). However, this has been done in a too pragmatic approach (Lufingo et al. 2019) and for too short experimental durations (Li et al. 2019, Konadu-Amoah et al. 2023). This points to the need for (i) an alternative approach based on the fundamentals of iron corrosion science, and (ii) considering reasonably long timescales representative of real field applications. The presentation herein insists on the fact that the oxidative dissolution of each individual Fe^0 contributes to reducing the pore space (porosity loss) and inducing reactivity loss. This occurs to different extents depending on the prevailing environmental conditions (e.g. anoxic/oxic, Fe^0 mass, Fe^0/aggregate ratio, pH value, water chemistry).

A proof that the conventional approach has not worked is the development of Artificial Neural Network (ANN) for evaluating permeability decline in Fe^0 PRBs (Santisukkasaem et al. 2015, Santisukkasaem and Das 2019). These authors clearly stated that all other approaches were not successful (Moraci et al. 2016). However, the ANN is not a physically based approach as it relies on the network's ability to understand given information and outputs from physically based relationships derived using other methods (Santisukkasaem et al. 2015). Fortunately, a physical approach has been presented which is able to address both permeability loss and reactivity loss in a very simple and low-cost experimental setup: The methylene blue (MB) discoloration method (MB method) (Btatkeu-K. et al. 2016, Konadu-Amoah et al. 2022).

2.1.4 Ways out of the "valley of confusion"?

The literature evidences difficulties in understanding the long-term permeability of Fe^0 filters (Bilardi et al. 2023). It is now established that sustainable Fe^0 filters are hybrid in nature, wherein, Fe^0 is admixed with non-expansive aggregates (e.g. Fe^0/MnO_2, Fe^0/pyrite, Fe^0/sand). It is established that factors influencing the sustainability of Fe^0 filters include: (i) reactive Fe^0 (intrinsic reactivity), (ii) Fe^0 shape and size, (iii) nature and extent of contamination, (iv) geochemical and hydrogeological characteristics of the aquifer, and (v) groundwater flow velocity. Bilardi et al. (2023) analyzed the relative importance of these parameters and showed that "admixing Fe^0 with non-expansive granular materials" is the most suitable tool to design "long-term hydraulically efficient" Fe^0 filters. This corresponds to the findings of Noubactep and Care (2010a, b), showing that despite hundreds of new peer-reviewed scientific publications, little progress has been made during the past 12 to 14 years. The reason for this sad situation is the proliferation of pragmatic, but independent investigations without any opportunity to compare achieved results. In particular, concerning the impact of Fe^0/sand ratio, the rationale for working with 50 % (w/w or v/v) is rarely specified, while (i) the Fe^0 intrinsic reactivity is not characterized (Cui et al. 2023), (ii) evidence exists that far lesser Fe^0/sand ratios are efficient (Tepong-Tsinde 2021), and (iii) experiments are performed for too short experimental times (Yang et al. 2022, Xiao et al. 2023, Xiao et al. 2024).

The Fe^0 remediation technology involves immersing small Fe^0 particles (< 5 mm thick) in water-saturated zones for long times. This is a novel situation for environmental scientists since there are no comparable data in the scientific literature, for example, on the long-term corrosion kinetics (Yang et al. 2022). Therefore, new experimental procedures are needed for obtaining better data, reflecting the true Fe^0 corrosion kinetics. The starting point is certainly the characterization of the intrinsic reactivity of available Fe^0 materials (e.g. iPutec GmbH & Co. KG in Germany, Connelly-GPM in the USA or Högnäs in Sweden). Such Fe^0 materials can be intensively characterized for their long-term ability to: (i) generate H_2 under well-defined conditions (e.g. tap water, spring water, and saline water), (ii) release Fe^{2+} in selected solutions (e.g. ascorbic acid, ethylenediaminetetraacetic acid - EDTA), and (iii) remove some selected probe contaminants under well-defined operational conditions. The discussion of a large number of data, obtained under such controlled experimental conditions (e.g. items (i) to (iii)), would reveal some common underlying trends for interactions within Fe^0/H_2O systems that provide a confidence for design that is non-material-specific. Accordingly, when a significant body of data exists on removal rates for selected contaminants by materials depicting certain characteristics, site-specific treatability studies may only be required to fine-tune design criteria for the optimal performance of Fe^0 filters. Such data would provide a good starting point for the design of future laboratory, pilot, and field-scale studies for investigating the remediation Fe^0/H_2O system (McGeough et al. 2007, Naseri et al. 2017).

A key feature of the presentation herein is that it is about Fe^0 corrosion by water (H^+) and not by any contaminant. This means that polluted water contains one or several species that can enhance or impede Fe^0 corrosion. The question is, how are individual contaminants removed during Fe^0 corrosion in the presence of polluted water? This approach is supported by reports on Fe^0 corrosion in deionized water (Luo et al. 2013, Xin et al. 2016), and the removal of several species without redox-reactivity in Fe^0/H_2O (You et al. 2005, Jia et al. 2007, Miyajima 2012, Btatkeu et al. 2016).

According to the viewpoints discussed above, the following three key conclusions and perspectives are put forward:

- Fe^0 is not a stand-alone reducing agent under environmental conditions (pH ≥ 4.5);
- Permeability loss and reactivity loss are two inherent properties of Fe^0 in a porous system. The occurrence of both processes is intimately related to the intrinsic reactivity of the materials used and the pore space available;
- An in-depth characterization of the long-term reactivity of selected Fe^0 materials under relevant operational conditions is regarded as a key step in designing the next-generation Fe^0 filters.

2.2 Effects of common anions on the performance of Fe^0/H_2O systems

2.2.1 General aspects

Predicting the influences of common anions on the efficiency of Fe^0 filters is a very complex task. Ideally, the temporal changes of the generation of Fe^{2+} (corrosion rate) should be known together with amount of each anion and the stability of the Fe^{II} and Fe^{III} complexes likely to be formed within the porous system. Furthermore, the amount of FeCPs available should be considered and the competitive adsorptive affinity of anions and all other co-solutes (including contaminants) discussed. Under ambient atmospheric conditions, Fe^{2+} from Equation 2.1 is oxidized by molecular O_2 to Fe^{3+} (Equation 2.2). Depending on the relative stability of the Fe^{II} or Fe^{III} salts and complexes, the following reaction can be considered for the considered anions (Equations 2.3 to 2.7):

$$4\ Fe^{2+} + 4\ H^+ + O_2 \Rightarrow 4\ Fe^{3+} + 2\ H_2O \qquad (2.2)$$
$$Fe^{2+} + CO_3^{2-} \Rightarrow FeCO_3 \qquad (2.3)$$
$$Fe^{3+} + 3\ Cl^- \Rightarrow FeCl_3 \qquad (2.4)$$
$$Fe^{3+} + 6\ F^- \Rightarrow FeF_6^{3-} \qquad (2.5)$$
$$Fe^{3+} + PO_4^{3-} \Rightarrow FePO_4 \qquad (2.6)$$
$$Fe^{2+} + SO_4^{2-} \Rightarrow FeSO_4 \qquad (2.7)$$

Because O_2 (8 mg/L in air, replenished upon consumption) and Fe^0 are present in stoichiometric abundance, iron oxides and hydroxides will also be formed, for example following the two simplified steps (Equation 2.8 and 2.9) according to Mos et al. (2018):

$$Fe^{2+}, Fe^{3+}, H_2O \Rightarrow GR \qquad (2.8)$$
$$Fe^{2+}, GR \Rightarrow Fe_3O_4, H_2O \qquad (2.9)$$

Under natural conditions, at least seven different iron hydroxides and oxides are likely to be formed and are mutually transformed to each other through a myriad of dynamic biotic and abiotic reactions (Chaves 2005, Raghav et al. 2015). Additionally, these transformations are influenced by the presence and concentration of individual co-solutes (including anions and contaminants) (Rose et al. 1996, 1997a, 1997b). For all these reasons, investigating any Fe^0/anion/H_2O system is a very complex task. The situation is exacerbated by extending the system to consider a given contaminant (e.g. Fe^0/anion/contaminant/H_2O system) while considering any specific (redox or adsorptive) interaction of the contaminants with other components of the system.

2.2.2 Investigating the Fe^0/anion/H_2O system

Section 2.2.1 has demonstrated the complexity of investigating the influences of common anions on the performance of Fe^0/H_2O systems. In essence, the impact of all co-solutes on the process of iron corrosion has to be characterized from the hydrolysis of Fe^{2+} (Equation 2.1) to the re-crystallization of oxides through nucleation and precipitation (Equations 2.8 and 2.9). This analysis suggests that characterizing the solid phases at individual times cannot help in solving the enigma of the Fe^0/H_2O system. On the other hand, the similitude between the Fe^0/H_2O system and Fe^0 electrocoagulation has been acknowledged (Bojic et al. 2007, 2009, Noubactep and Schöner 2010). This implies that, like for coagulation and electrocoagulation, it is better to characterize the influences of anions on the whole process of decontamination, before subsequently discuss the importance of redox processes (Crawford et al. 1993a, 1993b). This assertion is supported by reports better justifying the efficiency of Fe^0-based remediation systems by the affinity of contaminants to FeCPs (Scott et al. 2011, Phukan 2015, Phukan et al. 2015, Phukan et al. 2016).

The presentation until now suggests that any innovative approach to investigate the influences of common anions on the performance of the Fe^0/H_2O system goes through an operational reference. For example, the local tap water can be used as a reference system and the same augmented by various amount of each anion or mixture of anions. The present work has used this approach combined to the MB method (Chapter 3). The next section illustrates the extent of confusion existing in the Fe^0 remediation literature.

2.2.3 Fundamental flaws in investigating Fe^0/anion/H_2O systems

The literature evidences fundamental difficulties in understanding the processes occurring in Fe^0/anion/H_2O systems (Sun et al 2016). Factors influencing the efficiency of Fe^0/anion/H_2O systems in batch studies include: (i) Fe^0 intrinsic reactivity, (ii) Fe^0 shape and size, (iii) solution chemistry, including the nature and extent of contamination, and (iv) the mixing type and the mixing intensity.

There has been a large number of systematic studies designed to elucidate the effects of common anions on the decontamination process in Fe^0/H_2O systems (Sun et al. 2016). However, controversial results have been typically reported, even for the same probe contaminant and the same Fe^0 (Jiao et al. 2009, Sun et al. 2016). This is usually justified by the evidence that varying experimental procedures are employed for the collection of data. For batch experiments, these procedures differ in Fe^0 pre-treatment, Fe^0 particle size (e.g. granular, powder, nanoscale), admixing agents used (e.g. FeS_2, MnO_2, pumice, sand), volume of the experimental vessels (mL), volume of solution added (mL), equilibration time allowed, and ambient temperature (Vidic et al. 1990, Naseri et al. 2017). The major pitfall in conventional batch experiments has been the disturbance of the "natural" layering sequence Fe^0/oxide/H_2O in which the Fe^0 surface is permanently shielded by an oxide scale. In fact, while performing batch experiments, mixing intensities of up to more than 400 rpm are used to explicitly keep all particles in suspension and avoid mass transfer limitations (Devlin et al. 1998, Polasek 2007, Miyajima 2012). Such procedures certainly deliver reproducible results, however, without practical significance for filtration systems. In Fe^0 filters, transport in the vicinity of Fe^0 is diffusion-driven (Miyajima and Noubactep 2012). For this reason, quiescent experiments are recommended for treatability studies (Naseri et al. 2017). Our research group has been using exclusively quiescent batch experiments (mostly Fe^0/sand mixtures) for the past 15 years (since 2009) for experimental durations of up to 90 days (3 months). A major result has been that expressing the performance of Fe^0/H_2O systems in terms of adsorption capacity (e.g. mg of contaminant per g of Fe^0) is not acceptable (Naseri et al. 2017). This is because (i) Fe^0 is not depleted, (ii) its corrosion rate is not known, and (iii) no standard experimental protocol has been established.

The presentation until here clearly justified why confusing reports are typically reported in the literature. An illustration thereof is given based on the review article by Sun et al. (2016). The types and concentration aqueous anions dictate the performance of Fe^0-based systems (Klausen et al. 2003, Wilkin et al. 2003, Liu et al. 2007). Generally, some anions are redox-active (e.g. NO_3^-, SO_4^{2-}) species and others species non redox reactive. The interaction of each anion with species from Fe^0 corrosion and other co-solutes (including the contaminants) may lead the surface being coated by an interfacial barrier to both electron and mass transfer. In other words, these anions inhibit the performance of the Fe^0/H_2O system through "mineralogical modification" (Sun et al. 2016). In contrast, some other anions may enhance the performance of Fe^0/H_2O systems either by facilitating the breakdown of oxide scale on Fe^0 coatings or by enabling the formation of new reactive phases. However, Sun et al. (2016) acknowledged that individual anions "may concurrently serve different roles, and the net effect could vary with concentration, exposure time" and also the nature of the contaminant. It is obvious that this argumentation is based on the view that electrons from the Fe^0 body can reductively transformed dissolved contaminants, a view that contradicts the science of the system as established in 1903 (Whitney 1903, Xiao et al. 2023). As stated earlier, this chapter is not reviewing the literature on this issue, interested readers are referred to Sun et al. (2016). Chapter 2 has rather justified the reason why a new experimental approach was necessary. The background of this approach is presented in the next Chapter.

Chapter 3: Background of the experimental methodology

Published studies on the interactions between common anions and corroding Fe^0 appear to be mixed, reporting on both enhancement and inhibition of the efficiency of decontamination in the presence of individual anions. To shed light on the complex interactions between Fe^0 and relevant anions, this chapter (i) presents an analysis of the contaminant-free Fe^0/H_2O system, and (ii) theoretically discusses the interactions in the $Fe^0/MB/H_2O$ system (MB method). The MB method is also discussed in more details.

An analysis of the contaminant-free system provides information on possible reactants (e.g. adsorbents, ligands, reducing agents) that are available within the system. Based on the analysis of the contaminant-free system, the $Fe^0/MB/H_2O$, using MB as a tracer, enables the validation (or the falsification) of the working hypothesis, and thus provides sound information on interactions occurring in the remediation Fe^0/H_2O system. The chapter closes with clarifying the working hypothesis.

3.1 Chemistry of the contaminant-free Fe^0/H_2O system

A holistic analysis of contaminant-free system provides a guide for the interpretation of achieved results. It enables a scientific discussion of processes likely to occur, and justify which ones are more likely to take place under given experimental conditions (Noubactep 2009b, Cao et al. 2021a). The initial reaction of aqueous iron corrosion is electrochemical in nature and operates through a corrosion cell with an anode (Fe^0 oxidation) and cathode (electron transfer) (Whitney 1903, Whitman et al. 1924, Groysman 2010). At the anodic electrode of this cell, Fe^0 releases ferrous ions (Fe^{2+}) into the solution according to the reaction described by Equation 3.1. A corresponding reduction occurs at the cathodic electrode (cathodic area) of the non-corroded Fe^0 (Groysman 2010, Noubactep 2014, Noubactep 2016a, 2016b, 2016b, 2016d). The most usual cathodic reaction is the deposition of hydrogen ions as atomic hydrogen, and the subsequent liberation as hydrogen gas (Equation 3.2). Equation 3.3 summarizes the electrochemical dissolution of Fe^0 in water. This is consistent with the differences of the electrode reaction of the corresponding redox reactions: –0.44 V for Fe^{II}/Fe^0 and 0.00 V for H^+/H_2.

$$Fe^0 \Leftrightarrow Fe^{2+} + 2\ e^- \qquad (3.1)$$

$$2\ H^+ + 2\ e^- \Leftrightarrow H_2 \qquad (3.2)$$
$$Fe^0 + 2\ H^+ \Rightarrow Fe^{2+} + H_2 \qquad (3.3)$$

In the broad iron literature, it is considered that dissolved oxygen (O_2) corrodes Fe^0 to form ferrous ions (Equation 3.4) and other Fe^{II} species. More so, it is considered that beside reactions illustrated in Equations 3.3 and 3.4, a number of other reduction reactions are possible "under very special conditions" (Whitman et al. 1924). These special conditions include the electrodeposition of Cu^{2+} under acidic conditions (Aghazadeh et al. 2012), the acidic reduction of MnO_2 (Bafghi et al. 2008), or the synthesis of aniline around a pH value of 4.0 (Werner 1959). A relevant reaction in the context of this thesis is the reduction of nitrate (NO_3^-). As a rule, according to the Electrochemical Series, the oxidant of each redox couple having a standard electrode potential higher than –0.44 V ($E^0 > -0.44$ V) can oxidize Fe^0. This way of thinking has also largely guided previous research on "using Fe^0 for environmental remediation and water treatment" in general, and the installation of subsurface Fe^0 PRBs in particular (Matheson and Tratnyek 1994, Richardson and Nicklow 2002, Singh et al. 2023, Zhang et al. 2023). Unfortunately, while using the Electrochemical Series, researchers have overlooked the statement "under very special conditions" of Whitman et al. (1924). In fact, using Fe^0 for water treatment implies a pH value > 4.5. This corresponds to the pH range of natural waters used as drinking water sources. Under these conditions, the Fe^0 surface is permanently shielded by an oxide scale, and thus, not accessible to O_2 and all other oxidizing agents. This knowledge was established by Dr. Willis Rodney Whitney (Whitney 1903) and recognized by an award 44 years later by the the National Association of Corrosion Engineers (NACE - USA) (Whitney 1947). Clearly, reaction after Equation 4 is thermodynamically favourable, but physically impossible. This is because the oxide scale on Fe^0 acts as (i) a conduction barrier for electrons from Fe^0, and (ii) a physical barrier for dissolved pollutants (Hu et al. 2021, Xiao et al. 2023, Xiao et al. 2024).

$$2\ Fe^0 + 4\ H^+ + O_2 \Rightarrow 2\ Fe^{2+} + 2\ H_2O \qquad (3.4)$$

The presentation until now shows that, in contaminant-free Fe^0/H_2O systems, O_2 is reduced by Fe^{II} species, according to a chemical reaction (Equation 3.5). Fe^{3+} from Equation 3.5 spontaneously form hydroxides that polymerize and precipitate as FeCPs, unless some co-solutes delay or hinder the precipitation of FeCPs (Equation 3.6).

$$4\ Fe^{2+} + 4\ H^+ + O_2 \Rightarrow 4\ Fe^{3+} + 2\ H_2O \qquad (3.5)$$
$$Fe^{2+} + H_2O + \text{Na-salt} \Rightarrow \text{Fe-salts} + \text{FeCPs} \qquad (3.6)$$

Relevant co-solutes for natural waters are common anions (e.g. Cl^-, F^-, HCO_3^-, HPO_4^{2-}, NO_3^-, and SO_4^{2-}), cations (e.g. Ca^{2+}, K^+, Mg^{2+}, Na^+), and natural organic matters (NOMs). This study focuses on the effects of anions on the reactivity of Fe^0/H_2O systems. NO_3^- was excluded because of its redox reactivity under the experimental conditions (Westerhoff and James 2003). Although SO_4^{2-} is potentially redox active, its redox activity under conditions closed to the ones used herein has not been documented (Tsamo et al. 2018). The five remaining anions are: Cl^-, F^-, HCO_3^-, HPO_4^{2-}, and SO_4^{2-}, of which HCO_3^- (Equation 3.7) and HPO_4^{2-} (Equations 3.8 and 3.9) have the capacity to change the acidity of the solution. At pH > 4.5, both reactions are theoretically possible.

$$HCO_3^- + OH^- \Rightarrow CO_3^{2-} + H_2O \qquad (3.7)$$
$$HPO_4^{2-} + OH^- \Rightarrow PO_4^{3-} + H_2O \qquad (3.8)$$
$$HPO_4^{2-} + H^+ \Rightarrow H_2PO_4^- + H_2O \qquad (3.9)$$

Overall, in light of the foregoing analysis of the contaminant-free Fe^0/H_2O system, the following insights are evident:
(i) the correct wording should be pollutant-free Fe^0/H_2O system, this is because O_2 and co-solutes (anions, cations, and NOM) are contaminants, but usually non-polluting in the concentration range of natural waters;
(ii) O_2 and co-solutes more or less strongly impact the extent of iron corrosion and thus the availability of FeCPs for the elimination of pollutants;
(iii) Anions form complexes (e.g. FeF_6^{3-}) and salts (e.g. $FeCl_3$) with Fe ions (from Equation 3.1) and delay the availability of FeCPs. For this reason, whether minerals coat the Fe^0 surface or not, the fundamental influence of any anion on the performance of Fe^0 filters should be a depression of contaminant removal. This corresponds to the working hypothesis of this thesis.

Real polluted natural waters to be treated with Fe^0 remediation systems are usually multi-component systems containing several: (i) co-solutes (e.g. anions, solutes, NOM), and (ii) contaminants. Both co-solutes and contaminants can be redox reactive, making real system more complex and difficult to analyse. A simplification adopted in this work corresponds the non-consideration of NO_3^- as it is redox active and the investigation of the $Fe^0/MB/H_2O$ system. MB is used here as a tracer of reactivity and not as a model pollutant (Miyajima 2012).

3.2 Influences of common anions on the $Fe^0/MB/H_2O$ system

The previous section has recalled that the chemical reactivity of a Fe^0/H_2O system depends on (i) the intrinsic reactivity of the used Fe^0 material (corrosion rate) (Cui et al. 2023), (ii) the nature of the interactions between primary iron corrosion products (e.g. Fe^{2+}, H_2) and co-solutes (Wang et al. 2021, Abd El-Monaem et al.

2024), and (iii) the extent of the availability of FeCPs (oxides or salts – Equation 3.6) (Konadu-Amoah et al. 2022).

(a) adsorption onto FeCPs

(b) occlusion by FeCPs

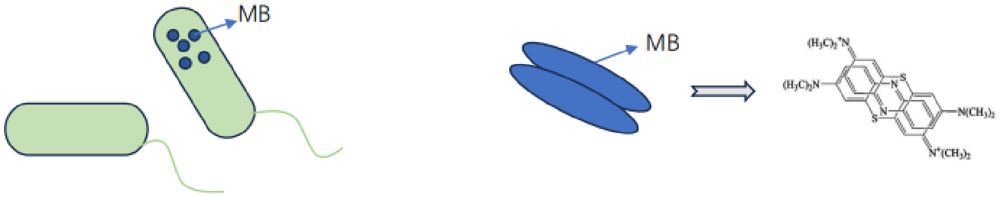

(c) microbial degradation

(d) reductive discoloration

Figure 3. 1 Mechanisms by which methylene blue (MB) can be discoloured in Fe^0/H_2O systems: (a) adsorption at the surface of solid iron corrosion products (FeCPs), (b) occlusion by precipitation FeCPs, (c) microbial degradation (not considered herein), and (d) dimerization under reducing conditions (not relevant for the used experimental conditions).

As stated already, redox reactive NO_3^- is not considered in this work for a sake of simplification. Investigating MB discoloration in Fe^0/H_2O systems as influenced by the presence of any other anion can be regarded as monitoring the process of MB occlusion by in-situ generated FeCPs (co-precipitation) (Figure 3.1) (Duff et al. 2002). The redox discoloration of MB is not considered because if anoxic conditions are established within the system, it is rather an intensification of the blue colour that is expected to occur (redox indicator) (Farjami et al. 2010). Relevant interactions include the extent to which the affinity of MB to FeCPs is influenced by the pH value (Mitchell et al.1955, Kara et al. 2021, Lu et al. 2023, Abd El-Monaem et al. 2024). These interactions are in turn modified by the nature of individual anions (Equations 3.7 to 3.9) because the speciation of anions is pH-dependent and the affinity of each anion to FeCPs depends on the point of zero charge (pzc or pH_{pzc}) of these solid phases (Kosmulski 2016, Kara et al. 2021).

Discussing the adsorptive interactions of each species within a Fe^0/H_2O system as influenced by an anion primarily corresponds to considering the pH shift induces by the addition of the anion. The difference between the actual pH value and the pH_{pzc} (ΔpH) is very useful in discussing adsorption processes (Kosmulski 2016). ΔpH is particularly important in this work, because FeCPs is a mixture of iron oxides and hydroxides with various adsorptive affinities (Sikora and Macdonald 2000, Duff et al. 2002, Chaves 2005, Nesic 2007, Zhang et al. 2023).

Solution chemistry is of great importance to the behaviour of the $Fe^0/MB/H_2O$ systems. As demonstrated by previous works this process can be regarded as local coagulation in the vicinity of Fe^0 (Bojic et al. 2007, Noubactep 2007, 2008, Bojic et al. 2009, Noubactep 2012, 2013a). The nature and concentration of the anions influence the speciation of iron, the precipitation of iron salts coupled with the adsorption and coprecipitation behavior of MB during precipitation ("local coagulation"). Research on the influence of common anions on MB discoloration in Fe^0/H_2O systems is still limited. Only one independent paper by Tsamo et al. (2018) was found. The results of Tsamo et al. (2018) will be considered in the discussion (Chapter 5). The remaining papers are those of Dr. Noubactep's research group, including one by the current author (Tao et al. 2023) which is part of this thesis. While some previous works have attributed observed MB discoloration in the presence of Fe^0 to redox properties (Frost et al. 2010, Hamdy et al. 2018), Miyajima clearly demonstrated that the only redox effect would be an intensification of the blue colour and not a discoloration, thus reductive discoloration is not considered in this thesis. This is because the redox conditions of this study are not reductive enough to evidence the redox-indicator property of MB. Similarly, because MB is not readily biodegradable (Ghaedi et al. 2015, Kara et al. 2021), MB discoloration by any microbiological process is not likely to occur under the used experimental conditions. Therefore, the two remaining discoloration mechanisms are (Figure 3.1): adsorption onto FeCPs and co-precipitation with FeCPs (occlusion).

This thesis uses quiescent batch tests to evaluate MB discoloration in the presence of Fe^0 under varying concentrations of Cl^-, F^-, HCO_3^-, HPO_4^{2-}, and SO_4^{2-}. The experimental results will be interpreted in terms of: (i) the variaton of pH value, and the iron concentration and (ii) the incidence on the extent of MB discoloration. No solid phase analysis (e.g. FTIR, XDR, XPS) will be performed. This is because such analysis gives only a static snapshot corresponding to a single time, while required information should help to understand dynamic processes lasting for years (Btatkeu-K et al. 2016, Konadu-Amoah et al. 2022). One key issue will consist on answering the question whether there is inhibition or enhancement of MB discoloration in the presence of individual anions. The working hypothesis is that there must be some suppressive effect on MB discoloration in the presence of all anions, because the formation of corresponding iron salts delays the availability of contaminant scavengers (FeCPs). Another inhibition path is the competitive adsorption of each ion onto FeCPs.

3.3 The MB method

The MB method is an innovative approach to characterize dynamic processes in Fe^0/H_2O systems. The method was introduced 11 years ago by Miyajima (2012) after the observation that a MB discoloration front (e.g. uniform adsorption onto sand) is altered in the zone containing Fe^0 (reactive zone). Miyajima (2012) reported that the Fe^0-packed columns generating more FeCPs within a short height were the ones exhibiting the most rapid MB breakthrough. This observation was justified by considering the historical work of Mitchell et al. (1955). Mitchell et al. (1955) reported that sand is an excellent adsorbent for MB but iron oxide-coated sand has no affinity for the same (Figure 3.2). In other words, in the experiments of Miyajima (2012), the earliest MB breakthrough was observed in the columns with the highest Fe: sand ratios (short reactive zone), or the lowest amount of sand. Based on these observations, Miyajima and colleagues developed the MB method (Miyajima and Noubactep 2012, Miyajima and Noubactep 2013, Miyajima and Noubactep 2015).

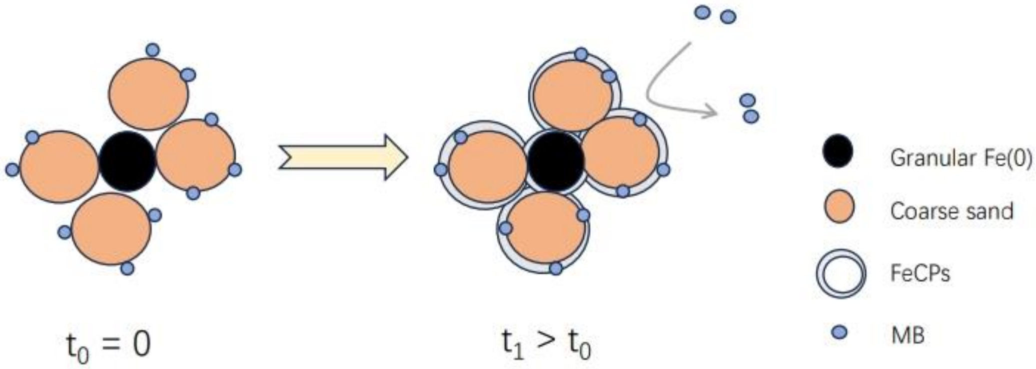

Figure 3. 2 Illustration of the time-dependent process of methylene blue (MB) discoloration in Fe^0/sand systems. From the start of the experiment ($t_0 = 0$), Fe^0 corrosion produces solid iron corrosion products (FeCPs) which progressively coat the sand surface. At $t_1 > t_0$, available sand is completely coated with FeCPs and MB is no more attracted. From t_1 on, MB is eliminated from the aqueous phase solely by occlusion within the matrix of precipitating FeCPs (co-precipitation).

The MB method has been successfully applied to advance the understanding of processes occurring in the Fe^0/sand system (Btatkeu-K et al. 2016, Konadu-Amoah et al. 2022). As illustrated in Figure 3.2, the MB method can be used to characterize the dynamics of the generation of FeCPs. Clearly, MB is used as an indicator of reactivity (Miyajima 2012, Miyajima and Noubactep 2015). MB is a cationic dye that is readily adsorbed onto the negatively charged surface of sand. When sand is progressively coated by positively charged FeCPs, its adsorptive affinity for MB decreases (Mitchell et al.1955, Miyajima 2012). In each experiment, the kinetics and the extent to which a given amount of sand is covered by FeCPs is characteristic for the Fe^0 material used (intrinsic reactivity) (Melchers et al. 2018, Yang et al. 2021). In other words, by using different Fe^0 materials, different amounts of Fe^0 and sand, several aspects of the reactivity of Fe^0/H_2O systems can be qualitatively assessed (Btatkeu-K et al. 2014a, 2014b, Gatcha-Bandjun et al. 2017). In particular, the MB method has clarified the issue of whether admixing Fe^0 to sand is inhibitory or beneficial for the sustainability of Fe^0 filtration systems (Miyajima and Noubactep 2012, 2013a). It is essential to recall that the MB method does not involve any solid phase analysis.

The MB method has been used to elucidate the following: (i) the ion-selective nature of Fe^0/H_2O systems (Phukan 2015, Phukan et al. 2015), (ii) the reasons why Cl^- ions enhance the efficiency of Fe^0/H_2O systems (Tepong-Tsindé et al. 2015, Gatcha-Bandjun et al. 2017, Tepong-Tsindé 2021), (iii) the reasons why MnO_2 addition enhances the efficiency of Fe^0/H_2O systems (Btatkeu-K et al. 2014a, Cao et al. 2021a, 2021b), and (iii) the mechanism of PO_4^{3-} removal in Fe^0/H_2O systems (Konadu-Amoah 2023, Konadu-Amoah et al. 2023).

3.4 Working methodology

The methodology used in this work consists in following the MB discoloration process in Fe^0/H_2O systems in the presence of various concentrations of Cl^-, F^-, HCO_3^-, HPO_4^{2-}, and SO_4^{2-} (Fig 3.3). The primary reaction in each Fe^0/H_2O system is the oxidation of Fe^0 to ferrous ions (Eq. 3.1). Depending on the nature of the anion added, there is at least five competitive paths for Fe^{2+} consumption: (i) precipitation of FeCPs, (ii) Fe^{2+} adsorption onto FeCPs, (iii) Fe^{2+} complexation with anions (e.g. Cl^-, F^-), (iv) Fe^{2+} precipitate with relevant anions (HCO_3^-, HPO_4^{2-}, and SO_4^{2-}), and (v) Fe^{2+} oxidation by dissolved O_2. All these processes will influence the availability of “free” FeCPs for MB discoloration by adsorption and co-precipitation (Fig 3.3). On the other hand, different anions shift the solution pH in characteristic manners and thus, modify the adsorptive affinity of FeCPs (iron hydroxides).

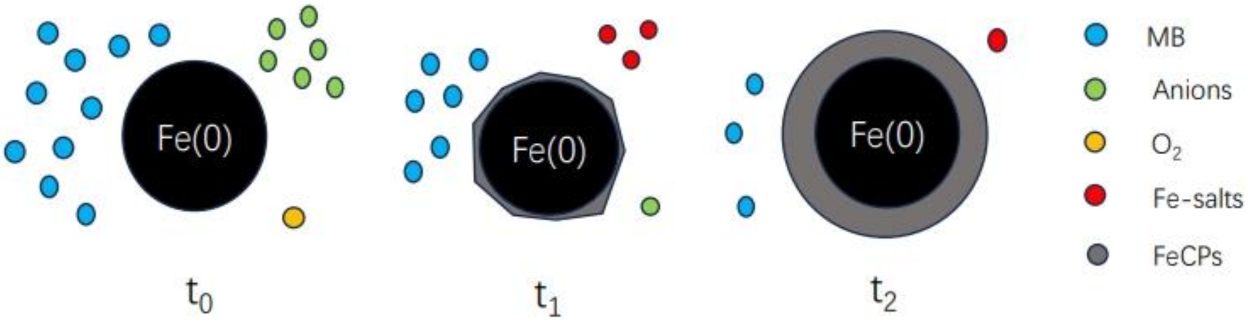

Figure 3. 3 Illustration of the processes of MB discoloration in the Fe^0/anion/H_2O system. The time-dependent availability of FeCPs is summarized as follows: (i) $t_0 = 0$: Fe0 is immersed in the MB solution containing O2 and the anions, (ii) $t_1 > t_0$: Fe^0 is covered by FeCPs and Fe-complexes are generated, and (ii) $t_2 > t_1$: the oxide scale on Fe^0 (FeCPs) is thicker, more MB is occluded.

The tap water of the city of Göttingen is used as reference system and the concentration of individual anions are added in nine (9) step to reach the saturation concentration. The rationale for using tap water as reference system is that its chemical composition roughly corresponds to that of groundwater. In fact, its treatment to drinking standard is almost limited to reduce reducing the concentration of Fe and Mn. As regarding the concentrations of anions tested, they were selected to be representative for natural waters and wastewaters as well. Chapter 4 gives details on the experimental setup.

Chapter 4: Materials and methods

This chapter summarized the experimental conditions for the experiments performed in this work.

4.1 Solutions

The used reagents methylene blue (MB—Basic Blue 9 from Merck, Darmstadt, Germany), methyl orange (MO—from Merck, Darmstadt, Germany), reactive red 120 (RR 120—from SIGMA company, St. Louis, USA), and orange II (OII—from ACROS Organics, New Jersey, USA) were all of analytical grade. The physico-chemical characteristics of the four dyes are summarized in Table 4.1. The working solution for each dye was 10 mg L^{-1}. The MB solutions were prepared by diluting a stock solution of 1000 mg L^{-1}. The other three dye solutions were prepared by dissolving accurately weighed corresponding materials in tap water.

Table salt from a local supermarket of Kaufland/Germany was used as the NaCl source, while commercial chemicals were used as sources of other anions. The chemicals were NaF, $NaHCO_3$, Na_2HPO_4, and Na_2SO_4, provided by Merck, Darmstadt (Germany). To prepare the working solutions, weighed salts were dissolved in tap water. The salt concentration of the tap water was considered as part of the background electrolyte (operational reference).

The average composition of this water is (mg L^{-1}): Cl^-: 9.7; NO_3^-: 7.7; SO_4^{2-}: 30.0; HCO_3^-: 88.5; Na^+: 6.0; K^+: 0.5; Mg^{2+}: 7.3; Ca^{2+}: 32.6, and its initial pH was 8.3. With this composition, tap water is a proxy for natural groundwater. The concentration of individual salts was increased to saturation level to explore the anions levels relevant to surface waters and various wastewaters.

Table 4. 1 Physico-chemical properties of the used dyes. Solubility data are from the cited references. Adapted fromTao et al. (2023).

Dye	**MW (g mol^{-1})**	**Formula**	**Nature**	**Type**	**λmax (nm)**	**Solubility (g L^{-1})**
Methylene blue	319.85	$C_{16}H_{18}ClN_3S$	cationic	basic	664.5	43.6
Methyl orange	327.33	$C_{14}H_{14}N_3NaO_3S$	anionic	acid	464.0	5.0
Orange II	350.32	$C_{16}H_{11}N_2NaO_4S$	anionic	Acid	486.0	64.5
Reactive red 120	1338.1	$C_{44}H_{30}Cl_{2}N_{14}O_{20}S_6$	anionic	acid	515.0	70.0

4.2 Solids

4.2.1 Metallic Iron (Fe^0)

A total of 4 commercially available Fe^0 materials were selected and used in this study. The selection was based on their differential reactivity as determined in previous work (Ndé-Tchoupé et al. 2020). The Fe^0 materials used were of different geometric shapes and sizes. These Fe^0 materials are referred to as: (i) ZVI1 is a material from iPutec GmbH Rheinfelden, Germany: (ii) ZVI2 is a directly reduced sponge iron material (DRI) from ISPAT GmbH, Hamburg, Germany; (iii) ZVI3 is scrap iron from the metal recycling company Metallaufbereitung Zwickau/Germany; and (iv) ZVI4 is a spherical iron sample from the Chinese company Tongda Alloy Material Factory. Table 4.2 summarizes the main characteristics of the 4 Fe^0 materials together with their iron content, as specified by the supplier. ZVI1 has been typically used by our research group since 2005 and represents the most widely used Fe^0 material for field applications in Europe (Birke et al. 2015). Therefore, ZVI1 is used here as an operational reference.

Table 4. 2 Code and main characteristics of the tested Fe^0 materials according to the supplier. n.s. = not specified; granular = mechanically broken pieces; sponge = particles with pitted surfaces; scrap = waste generated in any forms: spherical = standard sphere with a smooth surface. k_{AA} is the initial dissolution kinetics of each Fe^0 in a 2 mM ascorbic acid solution (Ndé-Tchoupé et al. 2020).

Code	**Shape**	**Size**	**Color**	**k_{AA}**	**Fe**	**Supplier**
		(mm)		**(µg h^{-1})**	**(%)**	
ZVI1	granular	0.05–5.00	black	13.2 ± 0.5	n.s.	iPutec GmbH
ZVI2	sponge	1.00–2.00	black	11.5 ± 1.3	90.0	ISPAT GmbH
ZVI3	scrap	0.05–2.00	black	12.3 ± 0.7	n.s.	Metallaufbereitung Zwickau
ZVI4	spherical	2.00	grey	2.8 ± 0.1	99.99	Tongda Alloy Material Factory

4.2.2 Sand

The sand used in this work was a commercial material for aviculture (parrot sand) (“Papageien sand” from RUT—Lehrte/Germany). “Papageien sand” was used as received without any further pre-treatment or characterization. The particle size varied between 0.5 - 2.0 mm. Sand was considered in this study because of its worldwide availability and its use as an additive in Fe^0/H_2O systems (Miyajima et al. 2012, Konadu-Amoah et al. 2023). The high adsorption capacity of sand for cationic MB was systematically documented as early as 1955 (Mitchell et al. 1955, Phukan 2015). Figure 4.1 shows a photograph of sand materials from three columns flushed with Orange II, methylene blue and reactive red 120 respectively.

Figure 4. 1 Photograph of sand materials from three columns flushed with Orange II, methylene blue and reactive red 120 respectively. Pictures are from the work of Phukan 2015.

4.3 Experimental Procedure

Batch experiments were performed under static conditions (no agitation) in assay tubes for 0 to 45 days. Figure 4.2 shows the used tubes on a corresponding test tube rack.

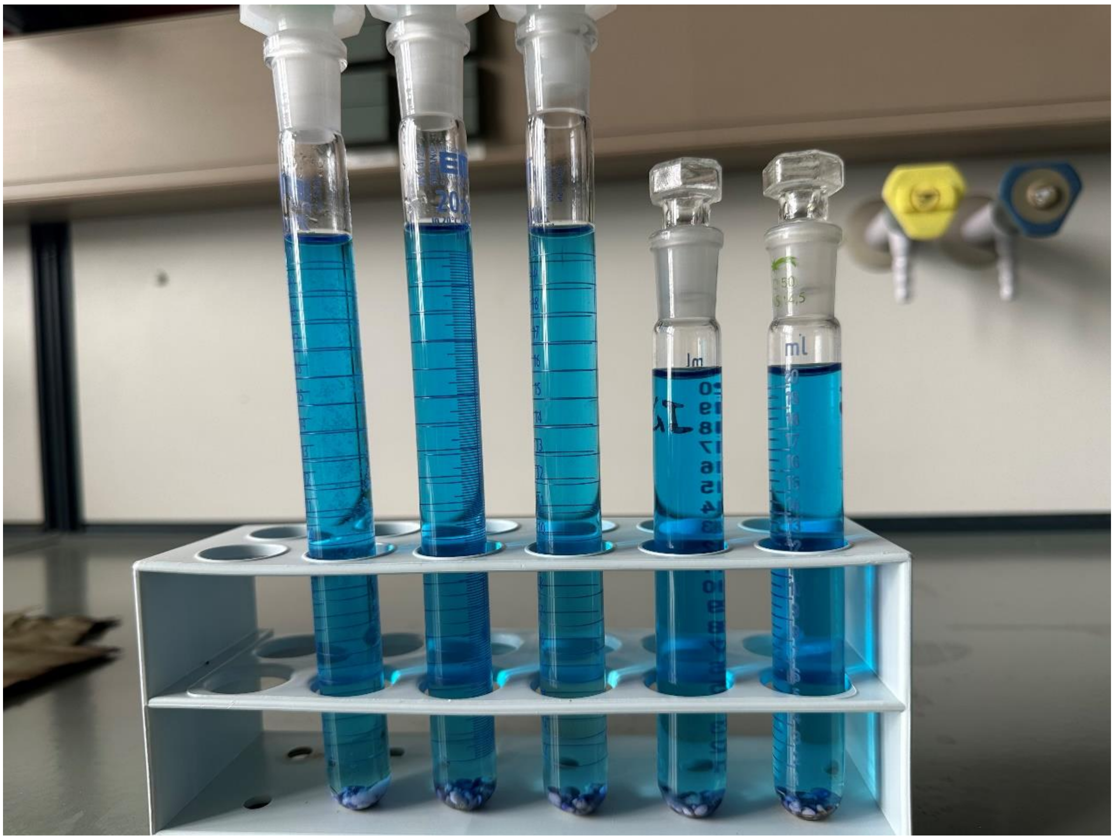

Figure 4. 2 Photograph of experimental set-up of batch experiments.

4.3.1 Chloride experiments

The batches consisted of 0.0 to 0.5 g of sand, 0.0 to 0.5 g of Fe^0, and mixtures thereof in 22.0 mL of a 10.0 mg L^{-1} of dye (MB, MO, OII, and RR 120) solution. Three different systems were investigated in parallel experiments for dye discoloration: (i) Fe^0 alone, (ii) sand alone, and (iii) Fe^0 + sand. The NaCl concentrations tested ranged from 0.0 to 40 g L^{-1}, corresponding to 0 to 24.3 g L^{-1} Cl^- (0 to 685 mM NaCl), without taking into account the Cl^- content of tap water (0.011–0.015 g L^{-1}). An operational reference (blank experiment) was included in each experiment. Mixtures with Fe^0 characterize the effect of sand on the availability of "free" iron corrosion products and hence their effect on dye discoloration (Konadu-Amoah et al. 2023). "Free" iron corrosion products are iron oxide-hydroxides precipitating from the bulk solution and capable of fixing (enmeshing) contaminants (Miyajima et al. 2012). The influence of different types of Fe^0 (ZVI1—ZVI4) on MB discoloration was also investigated. An additional set of dye discoloration experiments with MB and MO was performed by varying the Fe^0 loading (0.23 to 45 g L^{-1}) for 45 days.

The results of the above experiments are presented by Tao et al. (2023).

4.3.2 Commonly occurring ions experiments

The batches consisted of 0.0 to 0.5 g of sand, 0.1 g Fe^0, and mixtures thereof in 20.0 mL of a 10.0 mg L^{-1} of dye (MB and O-II) solution. The Fe^0/Sand system was investigated in different parallel experiments for dye discoloration. The five salt concentrations tested varied from each other, which were dependent on respective maximum solubility at room temperature. The maximum concentrations of salts used in this research were listed as following: (i) NaCl 40.0 g L^{-1} (684 mM); (ii) NaF 20.7 g L^{-1} (500 mM); (iii) $NaHCO_3$ 48.0 g L^{-1} (571 mM mM); (iv) Na_2SO_4 97.2 g L^{-1} (684 mM); (v) Na_2HPO_4 38.5 g L^{-1} (271 mM), without taking into account the background content of tap water. The operational reference (blank experiment) was the one performed in tap water. The rational for selecting these anion concentrations was to make sure that experiments are performed in stable solutions such that any precipitation reaction results from interactions within the system. The influence of different types of Fe^0 (ZVI1 – ZVI4) on MB discoloration was investigated. An additional experimental set for O-II was performed to better understand the impact of the contaminant nature in the Fe^0/salt system. O-II is very closed to MB in its molecular size but is negatively charged while MB is positively charged.

The influence of varying anion concentration salts was also investigated. For this purpose, 10 different salts concentrations were tested, the largest concentration (C_{max}) for each salt corresponds to i) maximum concentration used in previous work (e.g. Cl^-, SO_4^{2-}) ii) the half value of saturation solution at room temperature (e.g. F^-, HCO_3^-, HPO_4^{2-}) and the concentration of the remaining solutions were selected to keep the same equidistance among the corresponding points (Table 4.3). An additional experiment characterized the extent MB discoloration as the contact time varied from 0 to 30 days.

The results of the above experiments are presented by Tao et al. (2024).

The efficiency of each system in discoloring dyes was characterized at laboratory temperature (approximatively 22 °C). The initial pH value of the tap water was ~8.3. After equilibration, up to 5.0 mL of the supernatant solution was carefully collected for analysis (e.g. dye, iron). Each experiment was performed in triplicate.

Results are presented as means with the standard deviations (error bars) as a measure of data dispersion.

Table 4. 3 Concentrations of the synthetic solutions prepared for the investigation of the impact of anions on the efficiency of Fe^0/H_2O systems for dye discoloration. P (%) is the normalized anion concentration relative to the maximum concentration (e.g. 684 mM L^{-1} for NaCl).

Number	P	NaCl	NaF	$NaHCO_3$	Na_2SO_4	Na_2HPO_4
	(%)	(mM L^{-1})	(mM L^{-1})	(mM L^{-1})	(mM L^{-1})	(mM L^{-1})
1	0.00	0	0	0	0	0
2	5.0	34	24	29	35	13
3	10.0	68	51	57	68	27
4	15.0	103	75	86	103	41
5	20.0	137	99	114	137	54
6	25.0	171	126	143	171	68
7	38.0	257	186	214	257	101
8	50.0	342	249	286	342	136
9	75.0	513	375	429	513	204
10	100.0	684	500	571	684	271

4.4 Analytical Procedure

Aqueous dye and iron concentrations were determined using a Cary 50 UV–Vis spectrophotometer (Cary 300) (Figure 4.3). The working wavelengths for iron, MB, MO, OII, and RR 120 were 510.0, 664.5, 464.0, 486.0, and 515.0 nm, respectively. Cuvettes with a 1.0 cm light path were used. The spectrophotometer was calibrated for dye and iron concentrations ≤ 10.0 mg L^{-1}. The determination of iron was realized with the o-phenanthroline method (Saywell and Cunningham 1937, Fortune and Mellon 1938). The pH value was measured with a combined glass electrode (WTW Co., Germany).

Figure 4. 3 Photograph of the used Spectrophotometer (Cary 50 UV-Vis spectrophotometer).

4.5 Expression of Experimental Results

In order to characterize the degree of dye discoloration of the tested systems, the treatment efficiency (E) was calculated as the following equation. After the determination of the residual dye concentration (C), the corresponding percentage discoloration (E value) was calculated as follows:

$$E = [1 - (C/C_0)] \times 100\%$$

where C_0 is the initial aqueous contaminant concentration (10.0 mg L^{-1} for each dye) and C is the corresponding concentration at the end of the experiment.

Chapter 5: Results and discussion

This chapter summarizes the results obtained in this thesis. The corresponding two articles and one submitted manuscript are appended. The five main operational parameters for the successful design of a Fe^0 filter to treat a given polluted water are: (i) the volume and quality of water to be produced per unit time (e.g. day), (ii) the nature (e.g. charcoal, Fe^0, gravel) and the characteristics of the filtering media (e.g. form, reactivity, size), (iii) the used amount of filtering media (e.g. size of filter, number of filters in series), (iv) the nature and extent of pollution (e.g. co-solutes, contaminants of concern, pH value), and (v) the water flow velocity, which in turn determines the contact time. This work has (i) theoretically discussed the importance of admixing Fe^0 to other aggregates (hybrid systems), and (ii) experimentally investigated the influences of five commons anions on the performance of Fe^0/H_2O systems.

5.1 Hybrid Fe^0/aggregate systems

5.1.1 General aspects

A common feature of all Fe^0-based filtration systems is clogging (porosity loss and permeability loss) resulting from the accumulation of in-situ generated FeCPs within the pore volume (Henderson and Demond 2007, Henderson and Demond 2011, Henderson and Demond 2013, Noubactep 2013b, Noubactep 2013c, Noubactep 2013d, Guan et al. 2015, Bilardi et al. 2023). This means that Fe^0 filters are designed to experience porosity loss (Caré et al. 2013, Domga et al. 2015). The extent of porosity loss in each system depends on the Fe^0 intrinsic reactivity (corrosion rate) and the solution chemistry, including the nature of contaminants and their concentrations. The initial porosity and its time-dependent change are also crucial for the performance of Fe^0-based filters (Yang et al. 2021, Yang et al. 2022, Tao et al. 2023).

A survey of the history of Fe^0 filters reveals tangible observations made before 2010, that would have led to the proper consideration of the contribution of iron corrosion to the process of permeability loss (Table 5.1). In particular, Oldright et al. (1928) recommended many thin Fe^0 beds in series, rather than a thicker one with the same amount of sponge iron to avoid material wastage. They rationalized their recommendations by the larger volume of lead (Pb^0) replacing iron (Fe^0) in the porous system. These authors could have considered the volumetric expansive nature of iron corrosion at pH values > 4.5 as reported 25 years before by Whitney (1903).

Table 5. 1 Timeline of the main experimental observations relating the importance of porosity loss due to iron corrosion before 2010.

Year	Event	References
1882	Spongy iron filters are clogged at the water works of Antwerp (Belgium) because of cementation of iron and gravel.	(Devonshire 1890)
1903	Whitney reported on the expansive volumetric nature of iron corrosion	(Whitney 1903)
1923	Pilling and Bedworth established the rule of volumetric expansive nature of iron corrosion	(Pilling and Bedworth 1923)
1928	Bed clogging is attributed to Fe replacement by Pb	(Oldright et al. 1928)
1951	It is observed that column clogging occurs rapidly if fine iron filings are used in place of the steel wool. Using extremely fine grade of steel wool should also be avoided.	(Lauderdale and Emmons 1951)
1986	Filtration beds containing 100 % iron filings are very efficient at removing selenium from drainage water, but clogging occurred very rapidly.	(Anderson 1886)
1992	Using steel wool as Fe^0 source for phosphate removal, it is demonstrated that Fe^0/peat performed better than Fe^0/sand.	(James et al. 1992)
1993	Filtration systems containing 10 to 25 % Fe^0 particles (iron fillings) mixed to pelletized jute do not experience any permeability loss.	(Wakatsuki et al. 1993)
2001	Fe^0/pyrite filters are essentially more efficient for water treatment than pure Fe^0 filters.	(Zhang et al. 2004)
2007	Filtration systems containing less than 5 % Fe^0 (steel wool) do not experience any permeability loss.	(Erickson et al. 2007)
2000-2009	Household arsenic filters with pure Fe^0 layers are mostly efficient but not sustainable due to clogging. Only filters using porous materials (CIM = composite iron material) were sustainable.	(Hussam 2009)
2009	TCE removal rates are higher in an 85 % Fe^0 filter than in the 100 % system.	(Bi et al. 2009)

Table 5.1 shows that, besides sand and gravel, which are considered standard admixing agents (Westerhoff and James 2003), researchers have considered other aggregates including jute, peat and pyrite. It is certain that peat was used as another potential remediation material for PO_4^{3-}. However, the aspect of sustained

permeability should have received more attention. This in particularly true because systems using pelletized jute (Wakatsuki et al. 1993) and peat (James et al. 1992) experienced no permeability loss. It can be postulated, that bio-aggregates (e.g. jute, peat, wood chips) are better than compact minerals (e.g. gravel, sand) for sustained permeability. This is because bio-aggregates are likely to undergo decomposition over time, thereby improving porosity and permeability of the system and offsetting the effects of cementation.

5.1.2 Rationalizing the suitability of hybrid Fe^0/aggregate systems

Table 5.1 is limited to the period before 2010 as it corresponds to the date that the research group of Dr. Noubactep started its systematic investigation on hybrid Fe^0 systems. The very first result published in 2010 was that using porous Fe^0 materials like sponge iron or porous composites yields more sustainable systems (Noubactep and Caré 2010a, 2010b). For the same reasons, using pumice instead of sand yield more sustainable filters. The rationale is that the internal pores of individual grains are good "reservoirs" for in-situ generated FeCPs (Noubactep and Caré 2010a, Rahman et al. 2013). On the other hand, the rationale for Fe^0/sand being more sustainable than pure Fe^0 is that there are less expansive Fe^0 particles in the system compared to the pure Fe^0 system (a fraction is replaced by non-expansive sand), and thus delayed clogging (Figure 5.1). Upon clogging, the residual amount of unreacted Fe^0 is pure material wastage (Domga et al. 2015, Caré et al. 2013). In other words, the expression 'Fe^0 dilution' for hybrid systems is a thinking mistake. Of course, there are less Fe^0 particles in hybrid systems, but it is rather a prerequisite for sustainability and optimal material usage (Domga et al. 2015, Caré et al. 2013). This means that using pre-treatment Fe^0/sand zones was a thinking mistake as quantitative contaminant removal has been reported in such systems for more than one century, even when porous Fe^0 (e.g. spongy iron) was used (Baker 1948).

The presentation until here recalls that only mixed layer hybrid systems are sustainable, but as pointed out by Domga et al. (2015), pure Fe^0 filters can still be designed for particular uses, for instance in an emergency. In such cases, modular designs comprising at least one Fe^0 filter are recommended and selected Fe^0 units can be regularly replaced, for example on a monthly basis. For water supply of households and small communities however, more sustainable systems are required, a rule of thumb is to develop systems capable at operating for 6 to 12 months without maintenance (Tepong-Tsindé 2021, Noubactep et al. 2009, Noubactep and Schöner 2010, Tepong-Tsindé et al. 2019). The remaining discussion will focus on the suitability of admixing aggregates.

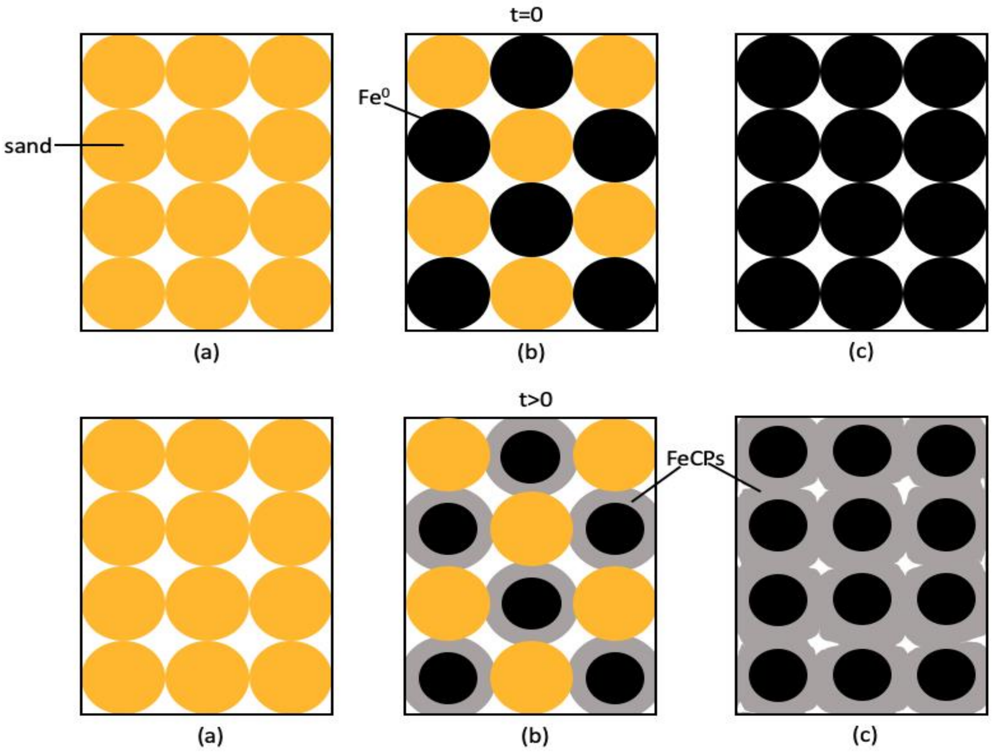

Figure 5. 1 Schematic representation of the cross-section of three different filters containing: (a) sand alone, (b) Fe^0/sand (1:1), and (c) Fe^0 alone. The pure Fe^0 systems completely clogs when the Fe^0/sand system has just experienced 50% porosity loss. In all three systems, permeability loss due to inflowing colloids and suspended particles is also possible.

5.1.3 Investigating the remediation Fe^0/aggregate filtration system

This section virtually considers that Fe^0 and aggregates are from the same sizes (Figure 5.1), and polluted water have the same chemistry. Only the nature of the aggregate is discussed. Table 5.2 gives an overview of the main aggregates that have been used to date.

Table 5.2 lists up two 12 different materials that have been demonstrated in individual studies to significantly impact the efficiency of hybrid systems relative to pure Fe^0. Discrepancies between studies are obvious because non-characterized Fe^0 materials are employed, although testing methods were made available for decades (Reardon 1995, Noubactep et al. 2005a, Lufingo et al. 2019, Ndé-Tchoupé et al. 2020). On the other hands each aggregate is tested as an independent success story without any effort to have an operational reference system (e.g. Fe^0/sand). To the best of the authors' knowledge, only Ndé-Tchoupé et al. (2020) used Fe^0/sand systems as reference to discuss the suitability of Fe^0/pozzolan. Therefore, it is a tangible fact that no normalisation of published data is possible. This sad situation is illustrated herein by the Fe^0/FeS_2 system in an historical perspective.

Table 5. 2 Representative materials used as aggregates in Fe^0/aggregate systems.

Aggregate	**Rationale for use**	**Comments**	**Reference**
Biochar	Adsorbs and accumulates contaminants	Also used as support for nano-Fe^0	(Zhang and Wu 2017)
Fe oxides	Adsorbs and accumulates contaminants	Fe_3O_4 is used the most	(Huang et al. 2012)
Fe sulfides	Shifts pH to lower values	FeS_2 is used the most	(Lü et al. 2018)
GAC	Builds galvanic cells with Fe^0	GAC coating with FeCPs will hinder electron transfer	(Tseng et al. 2011)
Lapillus	Stores FeCPs	Pores are not interconnected	(Bilardi et al. 2019)
Mn oxides	Sustains Fe^0 corrosion	Delay contaminant removal	(Cao et al. 2021c)
Peat	Accumulates contaminants	More efficient than sand	(James et al. 1992)
Pozzolan	Stores FeCPs	More efficient than sand	(Ndé-Tchoupé et al. 2018)
Pumice	Stores FeCPs	Pores are not interconnected	(Moraci and Calabrò 2010)
Sand	Reduces the Fe^0 cost	Reference additive	(Bi et al. 2009b)
Wood chips	Accumulates contaminants	Mostly used in PO_4^{3-} removal	(Wilopp et al. 2010)
Zeolite	Accumulates contaminants	Also used as support for nano-Fe^0	(Fronczyk 2020)

Pyrite (FeS_2) was introduced in the Fe^0 remediation literature as a pH shifting agent by Lipczynska-Kochany et al. (1994). The objective was to address “the deactivation of the metal surface” which was reported to be a barrier to the practical application of the then considered new technique. Between 1995 and 2005, many other researchers reported on the improved efficiency of Fe^0/FeS_2 system relative to pure Fe^0 (Wolfe and Cipollone 2001, Butler and Hayes 2001, Noubactep et al. 2003, Noubactep et al. 2005b, Noubactep et al. 2006). In particular, Wolfe and Cipollone (Wolfe and Cipollone 2001) secured a patent for remediation Fe^0/FeS_2 systems. Later on, Henderson and Demond (Henderson and

Demond 2011) used a pure Fe^0 bed length of 25 cm to investigate permeability and concluded that Fe^0 filters are not sustainable. Henderson and Demond (2013) concluded that FeS-based filters are better than Fe^0 ones with regard to permeability loss. This conclusion was based on four lines of evidence: (i) their excellent literature review (Henderson and Demond 2007), (ii) the results with the pure Fe^0 filters (Henderson and Demond 2011), (iii) results of a 25 cm bed of FeS-coated sand (Henderson and Demond 2013), and (iv) geochemical modeling. However, the same authors (Henderson and Demond 2011, Henderson and Demond 2013) have considered inflowing groundwater and not expansive iron corrosion as the cause of permeability loss. Additionally, no Fe^0/FeS system was investigated.

Since 2018, more systematic investigations on the suitability of the Fe^0/FeS systems were made available (Lü et al. 2018, Du et al. 2019, Lü et al. 2019, Du et al. 2020). However, they have not considered past efforts. and the experiments were performed for too short experimental duration while using poorly characterized Fe^0 and FeS materials (Hu et al. 2021). Additionally, the discussion of the operating mode of FeS_2 in improving the efficiency of Fe^0/H_2O systems is biased by considering Fe^0 as a reducing agent under operational conditions (Hu et al. 2021, Xiao et al. 2020a, 2020b). The results of Hu et al. (2021) support that FeS_2: (i) delay (not suppress) pH increase in Fe^0/H_2O systems, and (ii) boost the production of reactive Fe^{2+}. However, their results clearly demonstrated that any discussion supporting the electron transfer from Fe^0 is highly speculative and even wrong because despite pH decrease, quantitative contaminant removal was only observed when the final pH value was higher than 4.5 (Xiao et al. 2020a, 2020b). Thus, arguments like "FeS_2 activates the Fe^0 surface through replacing partially the passive oxide film with iron sulfide (FeS)" (Du et al. 2019) are non-acceptable. There is even evidence, that the addition of Fe^0 to pyrite can suppress its oxidation over the time (Seng et al. 2019, Tabelin et al. 2019). In other words, the documented enhanced efficiency of FeS-ammended Fe^0/H_2O systems should be further investigated to optimize its use in modular systems. The frequency of exchanging Fe^0/FeS units depends on the characteristics of used aggregates.

To sum up, despite 30 years of intensive investigations on the remediation Fe^0/FeS system, available knowledge is largely fragmented (Hu et al. 2021, Xiao et al. 2020a, 2020b). The situation is not better for all other aggregates, including sand. Therefore, real systematic investigations with well-characterized Fe^0 and aggregates are needed to optimize the design of efficient Fe^0 filters for safe drinking water provision, wastewater treatment and environmental remediation (Yang et al. 2021, Naseri et al. 2017).

5.2 Influences of chloride on the efficiency of Fe^0/H_2O systems

5.2.1. Influence of Cl^- Concentration on MB Discoloration in Fe^0/H_2O Systems

Figure 5.2 compares the time-dependent extent of MB discoloration under the experimental conditions for three different NaCl concentrations: 0.0, 8.0, and 40.0 g L^{-1}. It can be seen that for each contact time (i) MB discoloration is maximal in the NaCl free system (confirming the working hypothesis) and (ii) MB discoloration increases with increasing contact time. A closer look at the NaCl-containing systems shows that for $t < 30$ days, the 8 g L^{-1} NaCl system performed better than the 40 g L^{-1} system. Between 30 and 40 days, both systems performed similarly, and at $t > 40$ days, the 40 g L^{-1} NaCl system performed better than the 8 g L^{-1} system. However, both systems still performed lower than the NaCl-free system.

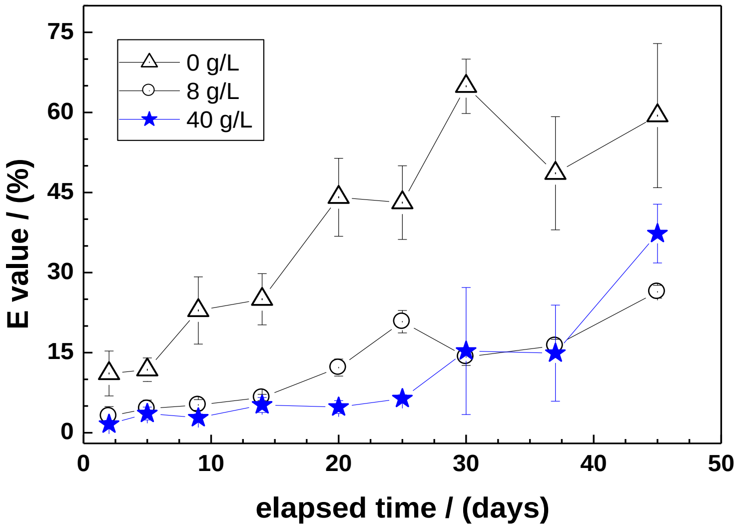

Figure 5. 2 Time-dependent extent of methylene blue discoloration in Fe^0/sand systems as a function of the NaCl concentration using ZVI1. Experimental conditions: $m_{iron} = 0.1$ g; $m_{sand} = 0.5$ g; $V_{solution} = 22$ mL; (MB) = 10 mg L^{-1}. The lines shown are not fitting functions, they simply connect the points for ease of visualization.

Figure 5.2 suggests that there is some ambivalence in the effects of Cl^- on the performance of Fe^0/H_2O systems for water treatment. The first reason may be an overall decrease in performance due to the absence or a reduced availability of FeCPs for contaminant adsorption and co-precipitation. This is evident when comparing NaCl free and NaCl-containing systems. Second, for the two NaCl-containing systems, there is first a decrease correlated with the amount of NaCl, then a phase in which both systems show the same performance. As the duration of the experiment increases, a stage is reached where the system with the higher

NaCl level performs better than the others. Although this improved performance is still lower than that of the NaCl-free system, these results suggest that the improved MB discoloration performance for the 40 g L^{-1} NaCl system corresponds to the often-reported improved performance of Fe^0/H_2O systems in the presence of Cl^- (Kim et al. 2007, Pullin et la. 2017, Hwang et al. 2015).

In this study, quiescent batch experiments in which diffusion transport is the dominant transport mechanism for dissolved species from the bulk solution to the vicinity of the Fe^0 surface have revealed the fundamental effects of the presence of Cl^- on the efficiency of Fe^0/H_2O systems for water treatment. Consistent with the chemistry of the system, Cl^- ions form stable dissolved complexes with Fe^{2+} and Fe^{3+}, delaying the formation of FeCPs for contaminant adsorption and/or co-precipitation. This observation clearly validates the working hypothesis: The presence of Cl^- delays the removal of contaminants in Fe^0/H_2O systems.

5.2.2 Influence of Cl^- Concentration on Dye Discoloration in Fe^0/H_2O Systems

Figure 5.3 summarizes the extent of dye discoloration after 45 days as the NaCl concentration varied from 0 to 40 g L^{-1}. It can be seen that the presence of Cl^- ions inhibit the discoloration of all dyes. A monotonic decrease in E values with increasing NaCl concentration is then observed for (NaCl) < 30 g L^{-1}, alongside a slight increase for (NaCl) = 40 g L^{-1}. This ambivalent situation is related to the relative amounts of Fe(II) and Fe(III) chlorocomplexes and the availability of FeCPs. Taken together, the results presented in Figure 5.2 and 5.3 suggest that it is possible to properly design a Fe^0-based remediation system that takes advantage of the enhanced iron corrosion in the presence of Cl^- ions are possible. However, this does not mean that Cl^- ions generally increase the efficiency of Fe^0/H_2O systems. Similar results have been obtained with hybrid Fe^0/aggregate systems, including Fe^0/MnO_2 (Ghauch et al. 2010, Ghauch et al. 2011, Gheju and Balcu 2019, Cao et al. 2021c, Burghardt and Kassahun 2005), Fe^0/pumice (Bilardi et al. 2023, Moraci and Calabrò 2010), and Fe^0/sand (Gheju and Balcu 2023, Btatkeu-K et al. 2016, Kosmulski 2016, Btatkeu et al. 2013). In other words, designing a sustainable Fe^0 remediation system in a saline environment requires a careful consideration of the balance between acceptable Cl^- concentration and contaminant removal efficiency for each Fe^0 material.

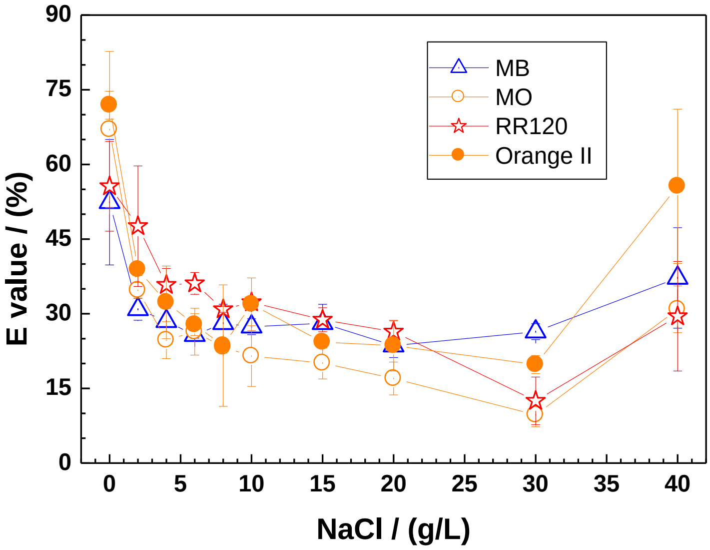

Figure 5. 3 Extent of dye discoloration after 45 days as a function of the NaCl concentration using ZVI1. Experimental conditions: m_{iron} = 0.1 g; m_{sand} = 0.5 g; $V_{solution}$ = 22 mL; (dye) = 10 mg L^{-1}. The lines shown are not fitting functions, they simply connect the points for ease of visualization.

5.2.3 Influence of Fe^0 Dosage on Dye Discoloration in Fe^0/H_2O Systems

Figure 5.4 summarizes the effect of 0.0 to 45.0 g L^{-1} Fe^0 on the extent of MB and MO discoloration over 45 days. The percentage discoloration of both dyes increased with increasing Fe^0 dosage, while the presence of salt (NaCl) typically reduced the extent of dye discoloration. The point at 0.0 g L^{-1} Fe^0 (sand only) corresponds to the Fe^0 free system in which dye discoloration is mediated solely by electrostatic interactions at the negatively charged sand surface (Miyajima 2012, Mitchell et al. 1955). Figure 5.4a shows that more than 20% of MB is discolored in the pure sand system, while there was no MO discoloration (E = 0%—Figure 5.4b). Another feature of Figure 5.4a is that the presence of salt reduces the extent of MB discoloration by sand. This is due to the increased availability of Fe^{2+} and Fe^{3+} ions, which are concurrent with MB (also positively charged) for adsorption onto the sand surface (Parks 1965).

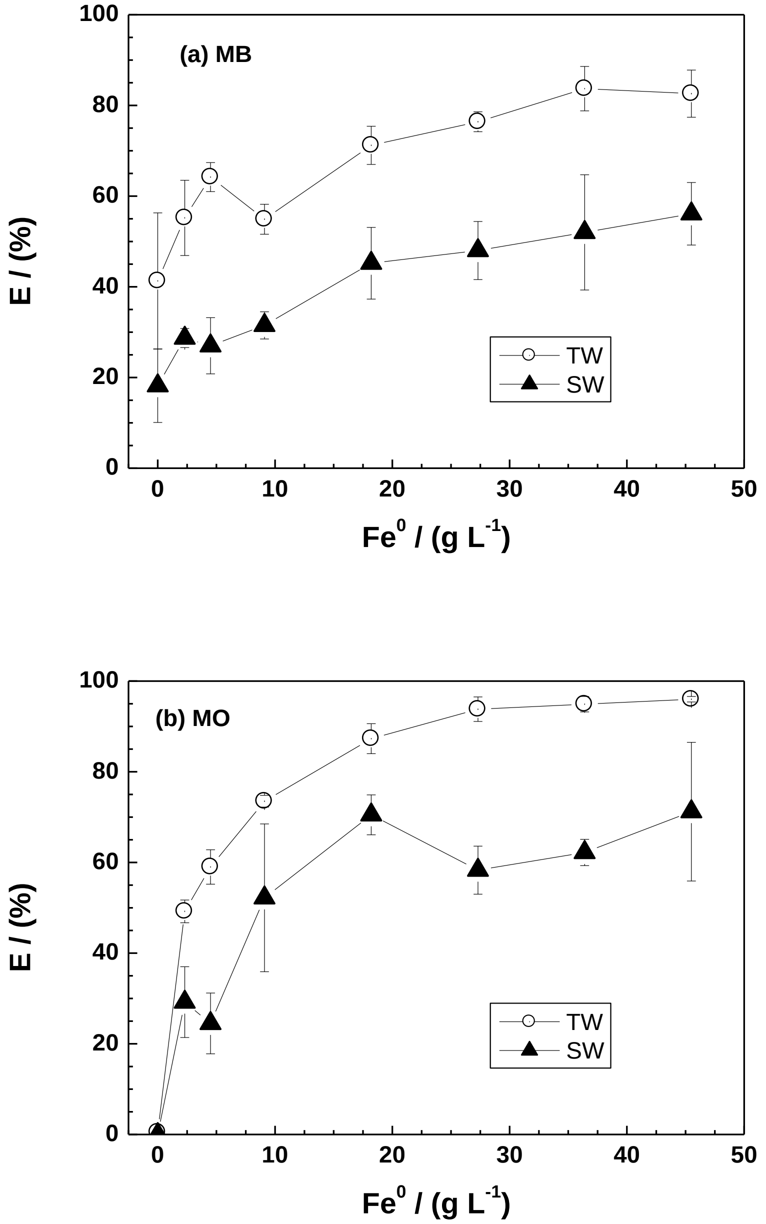

Figure 5. 4 Extent of dye discoloration after 45 days as a function of the Fe^0 dosage for methylene blue (**a**) and methyl orange (**b**) using ZVI1. Experimental conditions: $m_{sand} = 0.5$ g; $V_{solution} = 22$ mL; (dye) = 10 mg L^{-1}. The lines shown are not fitting functions, they simply connect the points for ease of visualization.

For Fe^0 dosages between 0 and 45 g L^{-1}, there is an increase in dye discoloration efficiency with increasing iron dosage (Figure 5.4a, b). This is primarily due to the availability of more active binding sites as a result of continuous iron corrosion, which produces solid iron corrosion products (FeCPs) for dye adsorption and co-precipitation. However, the discoloration percentage for both dyes become almost constant for (Fe^0) > 20.0 g L^{-1}. This behavior suggests a “splitting effect of the concentration gradient” between FeCPs and dye molecules (Aragaw et al. 2022). The different discoloration efficiencies of MB and MO as a function of the amount of FeCPs available are essentially due to differences in chemical structure, molecular size, and FeCPs–dye interactions (Miyajima 2012, Mitchell et al. 1955, Aragaw et al. 2022).

5.2.4. Influence of Fe^0 Type on Dye Discoloration in Fe^0/H_2O Systems

Figure 5.5 summarizes the extent of MB and discoloration after 45 days with four different Fe^0 materials in tap water ((NaCl) = 0 g L^{-1}) and in salt water ((NaCl) = 40 g L^{-1}). It can be seen that for all the 4 Fe^0 materials tested, the dye discoloration decreases in salt water compared to tap water, confirming the observations in Section 5.2.4 and further validating the working hypothesis.

For MB (Figure 5.5a), the most significant TW vs. SW variability between replicates was observed for ZVI1 (error bars), while the lowest was recorded for ZVI4. Considering the absolute values, the following increasing order of efficiency is observed: ZVI4 > ZVI3 > ZVI2 > ZVI1. This ranking confirms the information from the k_{AA} values (Table 4.2), showing that ZVI4 is significantly less reactive than the other three materials (Xin et al. 2018). Another feature of Figure 5.5a is that ZVI4 performed only slightly better than sand alone in SW and TW. Based on the information in Figure 5.5a, ZVI1 can be recommended as the most reactive material, while ZVI2 and ZVI3 are very close in their efficiency for MB discoloration. The results of MO discoloration (Figure 5.5b) confirm the trend observed in Figure 5.5a, with the exception that ZVI1 has a significantly lower efficiency in both TW and SW. While this difference is difficult to justify, the overall results reaffirm the importance of characterizing the diversity among the Fe^0 materials of environmental interest (Miehr et al. 2004, Li et al. 2019).

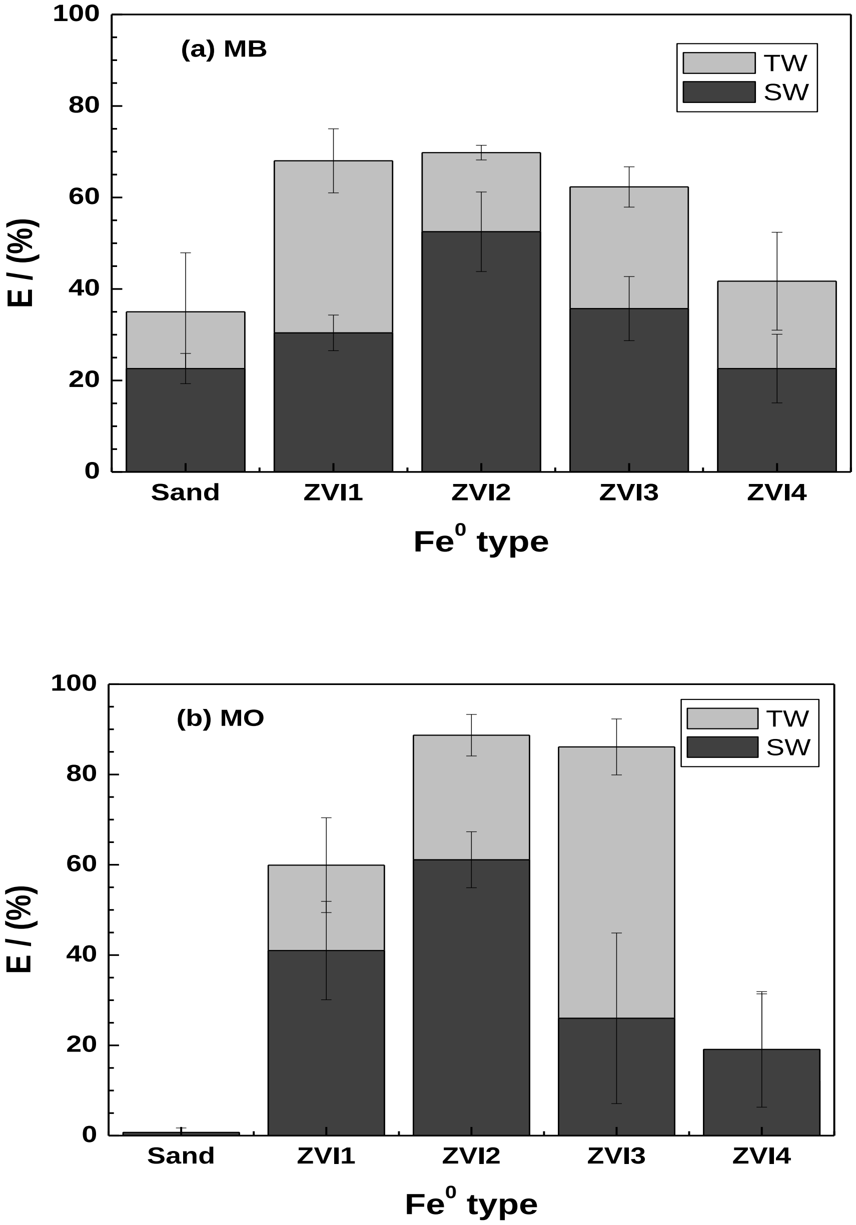

Figure 5. 5 Extent of MB discoloration after 45 days as a function of the Fe^0 type for methylene blue (**a**) and methyl orange (**b**). Experimental conditions: m_{iron} = 0.1 g; m_{sand} = 0.5 g; $V_{solution}$ = 22 mL; (MB) = 10 mg L^{-1}.

Despite a growing interest in the applications of Fe^0 for environmental remediation (Guan et al. 2015, Plessl et al. 2022, Singh et al. 2023) and safe drinking water supply (Tepong-Tsindé et al. 2019, Tepong-Tsindé 2021, Ndé-Tchoupé et al. 2022, Mueller et al. 2023), little progress has been made in characterizing the variability in reactivity among Fe^0 samples from different sources (Cui et al. 2023, Ndé-Tchoupé et al. 2020, Li et al. 2019, Ranjan et al. 2006, Naseri et al. 2017). The most important lesson from Figure 5.5 is that the extent to which saltwater affects the performance of a Fe^0/H_2O system depends on the used Fe^0 source used (Fe^0 quality). In particular, one investigator using ZVI4 might conclude that Cl^- ions have no effect on Fe^0 efficiency, while a colleague working under similar conditions using ZVI1 or ZVI2 would come to a different conclusion. As discussed by several authors, the diversity of contaminants and Fe^0 materials, as well as the lack of unified or standardized experimental procedures are the three most important factors hindering the progress of knowledge in the design of sustainable Fe^0-based remediation systems (Cao et al. 2022, Cui et al. 2023, Gheju and Balcu 2023, Cao et al. 2021c, Naseri et al. 2017).

5.3 Influences of common anions on the efficiency of Fe^0/H_2O systems

5.3.1 The mechanism of MB discoloration in the presence of anions

Figure 5.6a compares the extents of MB discoloration in the presence of ZVI1 as influenced by the presence of Cl^-, HCO_3^-, F^-, HPO_4^{2-}, and SO_4^{2-} as the equilibration time varied from 0 to 30 days. The results indicate that the extent of MB discoloration progressively increased in all systems, with the HCO_3^- system depicting the most significant increase of efficiency. The progressive increase of the MB discoloration with increasing experimental duration suggests that MB discoloration does not result from $FeCO_3$ precipitation. In other words, MB discoloration results from progressive generation of FeCPs. The other anions confirm this observation as the same trend is observed, but with a lower magnitude. Figure 5.6b compares the extents of pH variation in the five systems. It is seen that the pH of each system remains almost constant and equal to the initial value as the equilibration time varied from 0 to 30 days. This means that the pH changes accompanying the iron corrosion in the HCO_3^- system for example occurs in the vicinity of Fe^0 particles at the bottom of the assay tubes and cannot be recorded in the bulk solution. This observation corresponds to the real situation in iron filters and are observable only by the quiescent experimental design of this and related works (Miyajima 2012, Konadu-Amoah et al. 2023, Tao et al. 2023). In other words, mixing or shaking the experimental vessels would have enabled a record of pH variation in the bulk solution. However, the objective is to investigate the processes in a manner that can reflect natural conditions characterized by diffusive transport in the vicinity of the Fe^0 surface (Gheju and Balcu 2019).

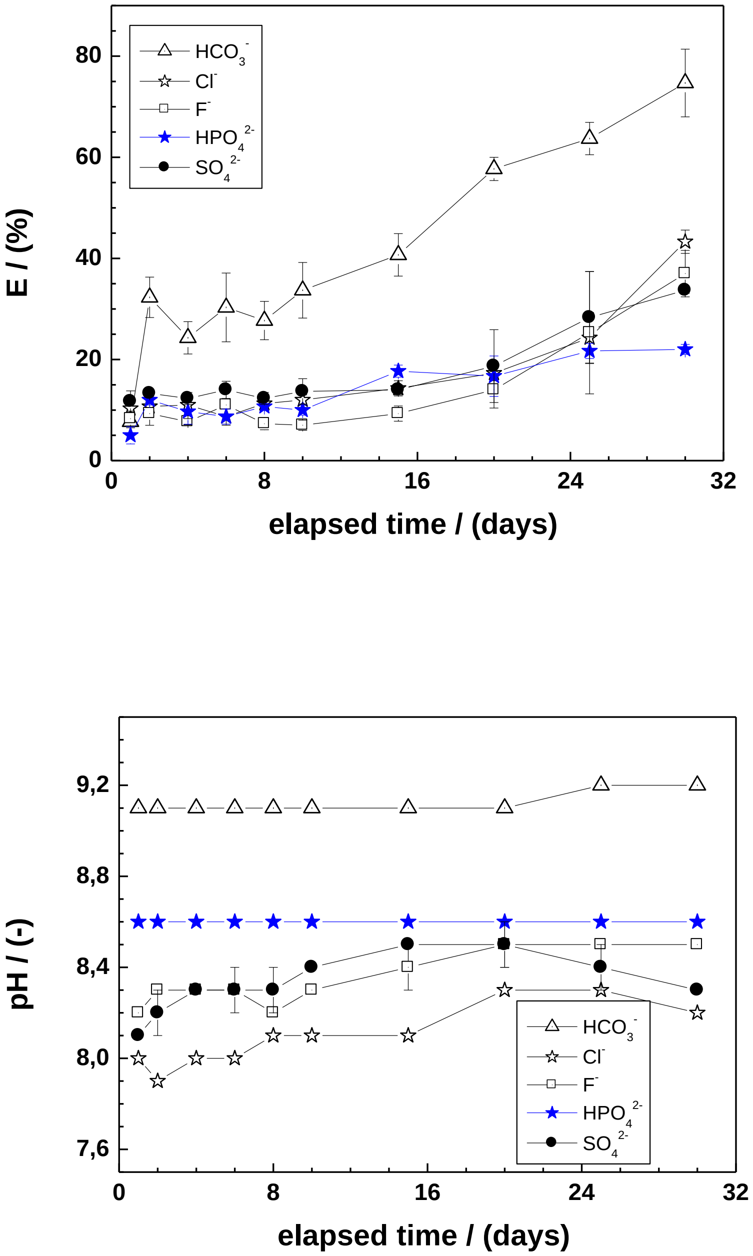

Figure 5. 6 Time-dependent extent of methylene blue discoloration (a), and variation of pH value (b) in Fe^0/sand systems as a function of the dissolved anion using ZVI1. Experimental conditions: m_{iron} = 0.1 g; m_{sand} = 0.5 g; $V_{solution}$ = 20 mL; (MB) = 10 mg L^{-1}; (Anion) corresponds to P = 25 % (Table 4.3). The lines shown are not fitting functions, they simply connect the points for ease of visualization.

The previous sections have corroborated the suitability of the MB method to investigate the complexity in Fe^0/H_2O systems. The originality of this method is twofold: (i) there are no redox interactions of MB and reactive species within the

Fe^0/H_2O system (Miyajima 2012), and (ii) there is no adsorptive affinity between MB and FeCPs (Chapter 3) (Mitchell et al. 1955). In essence, the MB method uses MB to trace the process of generation of FeCPs in a Fe^0/H_2O system. The results of this section suggest that an experimental duration of 30 days is enough to monitor changes induced by the presence and concentration of individual anions. Based on this evidence and past results (Miyajima 2012, Miyajima and Noubactep 2015, Tao et al. 2023), the remaining experiments were performed for an equilibration time of 45 days.

5.3.2 Effects of common anions on the reactivity of Fe^0/H_2O systems

Figure 5.7 compares the extents of MB discoloration in the presence of ZVI1 for 45 days as influenced by the presence of Cl^-, HCO_3^-, F^-, HPO_4^{2-}, and SO_4^{2-}. The initial concentration of each anion increased from 0 (TW) to 100 % (saturation concentration) (Table 4.3). The results indicate that, in all systems, the E value corresponding to TW (0 %) first decreased. In fact, E values for (salt) = 5 % were all inferior to those corresponding to (salt) = 0 %. This observation validates the working hypothesis: The presence of any salt decreases the amount of FeCPs for MB discoloration. For (salt) >5 %, there is no general trend in the magnitude on how MB discoloration is influenced by increasing anion concentration.

For example, in the HCO_3^- system, MB discoloration remains constant to about 62 % when (HCO_3^-) varied from 5 to 40 % (relative value). An E value of 5 % corresponds to 29 mM $NaHCO_3$ or 1743 mg L^{-1} HCO_3^-, while 40 % corresponds to 214 mM $NaHCO_3$ (13071 mg L^{-1} HCO_3^-) (Table 3). For (HCO_3^-) > 40 %, the E value sensibly increased to reach 90 % for (HCO_3^-) = 571 mM (33655 mg L^{-1}) which is the saturation concentration. The HPO_4^{2-} system presented a random fluctuation, with the lowest E value at saturation ((HPO_4^{2-}) = 271 mM or 26028 mg L^{-1}). The results in Fig. 5.7 show that practically, each anion influences MB discoloration by a different mechanism.

Previous studies have reported mixed trends (enhancement or inhibition) on the influence of the presence and the concentration of various anions on the efficiency of Fe^0/H_2O systems (Kim et al. 2007, Tao et al. 2023). To assess the plausibility of given arguments, the experiments of this study widely varied the anion concentrations (Table 4.3) in order to account for a wide range of natural and wastewaters. Arguments justifying the influences of anions on the efficiency of Fe^0/H_2O systems can be summarized as follows (Sun et al. 2016, Sun et al. 2023): (i) maintaining the Fe^0 reactivity by facilitating the breakdown of oxide scales (e.g. Cl^-), (ii) limiting access to reactive sites on Fe^0 or competing with contaminants for the same (e.g. HCO_3^-, PO_4^{3-}). SO_4^{2-} both promote the performance of Fe^0/H_2O systems by freeing the Fe^0 surface from oxide scales, and inhibit it by competing with some contaminants for adsorption sites within the system. The results in Fig. 5.7 are not confirming this trend, while the working hypothesis is validated. On the contrary, HCO_3^-, which is expected to inhibit MB discoloration is the single anion which has rather enhanced it for $(HCO_3^-) > 50$ % (286 mM or 17429 mg L^{-1}).

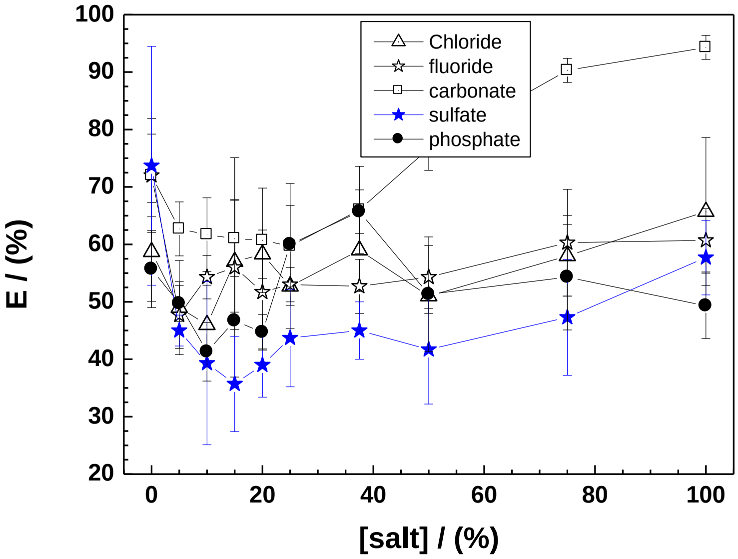

Figure 5. 7 Extent of dye discoloration after 45 days as a function of the dissolved anion using ZVI1. Experimental conditions: m_{iron} = 0.1 g; m_{sand} = 0.5 g; $V_{solution}$ = 20 mL; (MB) = 10 mg L^{-1}. The lines shown are not fitting functions, they simply connect the points for ease of visualization.

If relative concentration 5, 25 and 100 % (Table 4.3) are operationally considered to be relevant for groundwater, surface water and wastewater respectively, Figure 5.7 give the following order of increasing MB discoloration as influenced by the anions.

Groundwater: $SO_4^{2-} < Cl^- = F^- = HPO_4^{2-} < HCO_3^-$
Surface water: $SO_4^{2-} < Cl^- = F^- < HPO_4^{2-} = HCO_3^-$
Wastewater: $HPO_4^{2-} < SO_4^{2-} < F^- < Cl^- < HCO_3^-$

For the three concentrations, only HCO_3^- is confirmed as an enhancer of Fe^0 reactivity at all concentrations. This order of efficiency surprisingly shows that SO_4^{2-} inhibits Fe^0 reactivity in groundwater. The general trend from the literature (section 5.3.1) is that SO_4^{2-} improve the efficiency of the systems. To better understand the systems, the iron concentrations and the pH values were recorded at the end of the experiments.

Figure 5.8a shows that elevated iron concentrations (0.2 mg L^{-1}) were recorded only in F^- and Cl^- systems with higher concentrations in the F^- system. There should be a decrease of MB discoloration in both systems as observed, but because the solubility of the salts are just one influencing factors, neither of these systems was the best or the worse in impacting MB discoloration (Fig 5.7). The discussion above has shown that improved MB discoloration is in the HCO_3^- system. Actually, the HCO_3^- system depicted the lowest iron concentration (Figure 5.8a).

Figure 5.8b shows that the pH value of the Cl^- system remains constant and equal to that of the used tap water (8.2) This observation corroborated the view that changes related to iron corrosion at the bottom of the assay tubes could not be measured in the bulk solution. In other words, changes in pH values as recorded in Figure 5.8b are just a reflection of the buffer capacity of the used salt. It has already been pointed out that despite high pH values in HCO_3^- systems, MB discoloration is increased because protons are produced in the vicinity of Fe^0 granules.

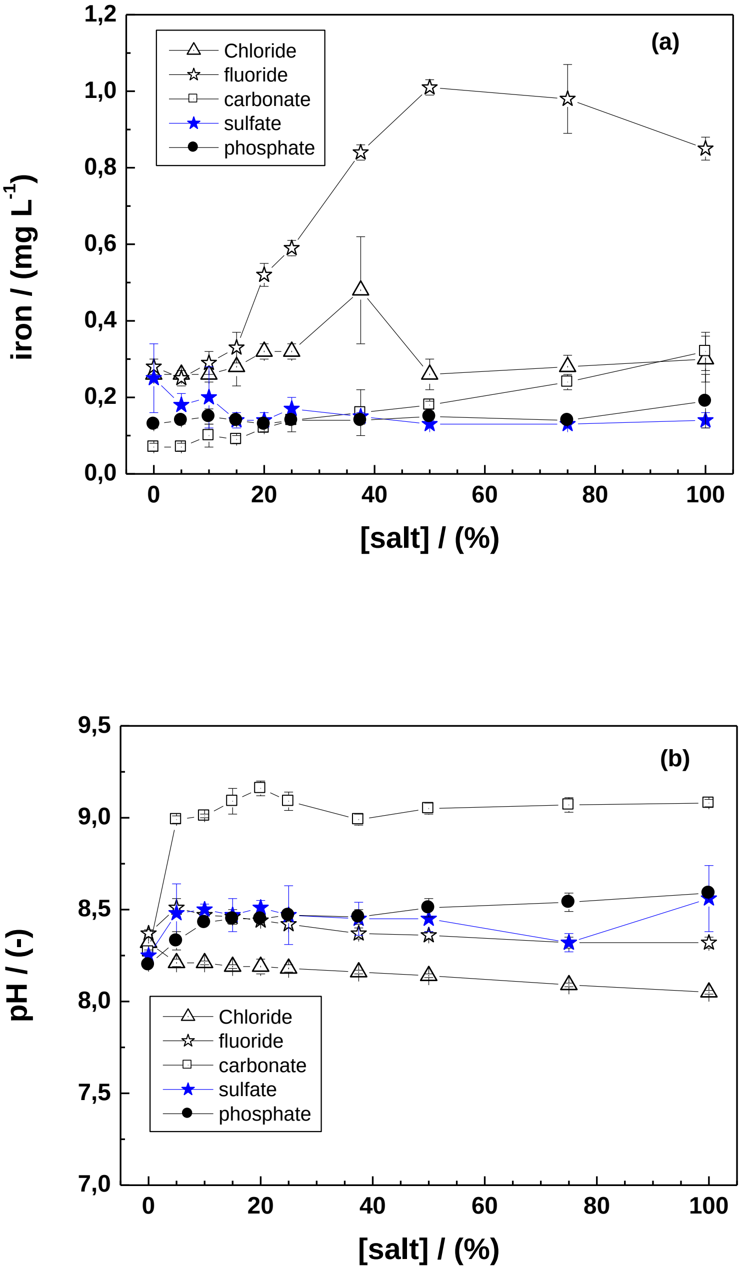

Figure 5. 8 Changes of iron concentration (a) and pH value (b) after 45 days as a function of the dissolved anion using ZVI1. Experimental conditions: m_{iron} = 0.1 g; m_{sand} = 0.5 g; $V_{solution}$ = 20 mL; (MB) = 10 mg L^{-1}. The lines shown are not fitting functions, they simply connect the points for ease of visualization.

5.3.3 Effects of the Fe^0 intrinsic reactivity

Table 5.3 compares the extents of MB discoloration in tap water and various anions as influenced by the Fe^0 type. The results confirm the trend that, the HCO_3^- system depicts the highest MB discoloration efficiency and the HPO_4^{2-} system the lowest. For other anions, there was no a clear trend, confirming that there is no single material for all situations (Yang et al. 2006, Li et al. 2016, Cui et al. 2023).

Table 5. 3 Extent of MB discoloration after 45 days as a function of the Fe^0 type for tap water and various anions. Experimental conditions: $m_{iron} = 0.1$ g; $m_{sand} = 0.5$ g; $V_{solution} = 22$ mL; (MB) = 10 mg L^{-1}; (Anion) corresponds to P = 100 % (Table 4.3). ΔE is the standard deviation from the triplicates. Larger ΔE values are a reflection of the fact that individual systems are far from any steady state.

	ZVI1		ZVI2		ZVI3		ZVI4	
	E	ΔE	E	ΔE	E	ΔE	E	ΔE
	(%)	(%)	(%)	(%)	(%)	(%)	(%)	(%)
TW	62.7	23.7	66.0	6.6	63.0	11.3	59.0	8.5
Cl^-	47.7	3.2	59.3	11.7	44.3	5.9	41.3	4.9
F^-	43.3	8.1	52.3	4.0	31.0	5.0	45.0	6.6
HCO_3^-	89.0	4.4	89.0	2.0	88.7	2.3	76.7	10.4
SO_4^{2-}	56.7	6.8	55.7	12.7	60.7	14.5	43.0	11.3
HPO_4^{2-}	35.0	14.0	23.3	1.5	28.0	9.5	23.3	1.5

The results in Table 5.3 confirm the trend observed in this study that HCO_3^- enhances MB discoloration for the 4 tested Fe^0 materials. The increasing order of efficiency reported in section 3.1 is roughly maintained: $HPO_4^{2-} < F^- < Cl^- < SO_4^{2-} < TW < HCO_3^-$. However, for F^-, Cl^-, and SO_4^{2-}, the trend was not evident. For example, for the least reactive material (ZVI4) there was no significant difference in the extent of MB discoloration in the three systems. In other words, a researcher working exclusively with ZVI4 would come to the following increasing order of efficiency: $HPO_4^{2-} < F^- = Cl^- = SO_4^{2-} < TW < HCO_3^-$. Thus, the results confirm the Fe^0 intrinsic reactivity as a standalone operational parameter for the design of remediation Fe^0/H_2O systems (Yang et al. 2006, Lufingo et al. 2019, Pavelková et al. 2020, Cui et al. 2023).

The increasing order of reactivity of the materials in the individual solutions was:

Cl^-:	ZVI4 < ZVI3 < ZVI1 < ZVI2
HCO_3^-:	ZVI4 < ZVI1 = ZVI2 = ZVI3
F^-:	ZVI3 < ZVI1 < ZVI4 < ZVI2
HPO_4^{2-}:	ZVI2 = ZVI4 < ZVI3 < ZVI1
SO_4^{2-}:	ZVI4 < ZVI2 = ZVI1 < ZVI3
TW:	ZVI4 < ZVI1 = ZVI3 < ZVI2.

This recalls that material selection is a highly site-specific issue. For example, in a carbonate rich groundwater, ZVI2 will be preferable to ZVI1. The inverse is valid for phosphate rich groundwater.

Summarized, the influence of the Fe^0 type on the efficiency of remediation Fe^0/H_2O systems depends on the (i) corrosion rate, (ii) solubility of the Fe-salt, and (iii) interactions (e.g. adsorptive affinity) between the anions and the contaminants of concern. It is essential to recall that the MB method used herein does not address the nature of the contaminant as it just traces the availability of FeCPs (Btatkeu-K et al. 2016, Konadu-Amoah et al. 2022).

5.3.4 Effects of the nature of contaminants

Figure 5.9 compares the extents of methylene blue (MB) and orange II (O-II) discoloration in the presence of ZVI1 as influenced by the presence of Cl^-, HCO_3^-, F^-, HPO_4^{2-}, and SO_4^{2-} (initial concentration 10 – Table 4.3). It is seen that orange II discoloration is significantly higher in tap water (H_2O), and in the presence of Cl^- and F^-. In the presence of HPO_4^{2-} and SO_4^{2-}, both dyes showed no significant difference in the extent of their discoloration by ZVI1, while the HCO_3^- system depicted a completely different behavior, MB discoloration been much higher. The results seem counterintuitive as it is documented that O-II has a larger affinity to FeCPs than MB (Miyajima 2012, Miyajima and Noubactep 2015, Phukan et al. 2015, Phukan et al. 2016). Similar results were obtained while comparing the discoloration of MB and methylorange in Fe^0/H_2O systems (Gatcha-Bandjun et al. 2017, Tsamo et al. 2018, Alyoussef 2019, Cao et al. 2021b)

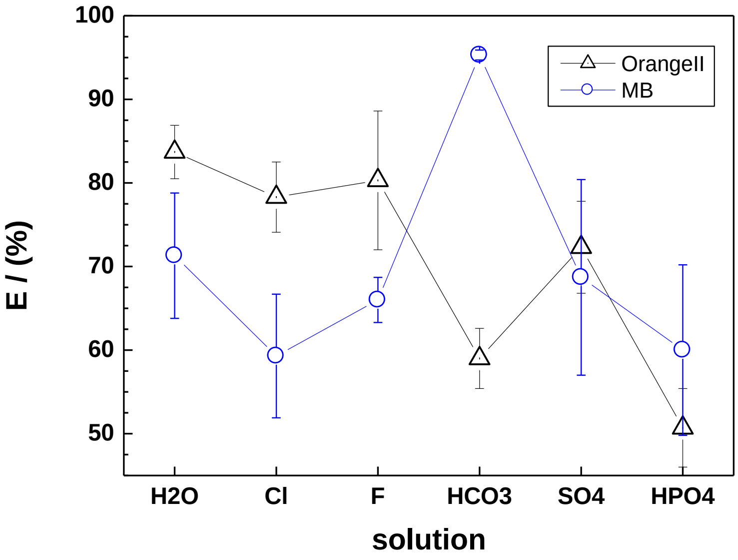

Figure 5. 9 Extent of MB and Orange II discoloration after 45 days as a function of the anion. Experimental conditions: m_{iron} = 0.1 g; m_{sand} = 0.5 g; $V_{solution}$ = 20 mL; (MB) = 10 mg L^{-1}; (Anion) corresponds to P = 100 % (Table 3). The lines shown are not fitting functions, they simply connect the points for ease of visualization.

The reason why MB discoloration is better than O-II removal in the investigated Fe^0/sand system (Figure 5.9) is given by considering the impact of contact time on processes causing dye discoloration (Alyoussef 2019). The presence of HCO_3^- is just an operational parameter that has enabled this observation for an equilibration duration of 45 days under given experimental conditions (chapter 4). As discussed in section 5.3.2, HCO_3^- sustains Fe^0 corrosion and produces FeCPs for MB discoloration by co-precipitation in the vicinity of the Fe^0 surface. This MB removal induces a diffusion of MB molecules from the bulk solution to the bottom of the essay tube and justifies recorded MB discoloration. Note that MB is already attracted to the bottom of the assay tube by sand (Mitchell et al. 1955, Miyajima 2012). In other words, increased MB discoloration is justified by MB adsorptive accumulation by sand and co-precipitation with native FeCPs. Under the same experimental conditions, O-II with higher affinity to FeCPs could not be removed because O-II has no adsorptive affinity to sand (Phukan et al. 2015, 2016).

The argument that the observed better MB discoloration relative to O-II (Figure 5.9) is just a "statistic snapshot" is supported by recent results by Tsamo et al. (2018). These authors investigated the effects of Fe^0 pre-corrosion by Cl^-, H_2O, HCO_3^-, HPO_4^{2-}, and SO_4^{2-} on methylene blue (MB) and methyl orange (MO) discoloration in assay tubes and under quiescent conditions. The Fe^0 pre-corrosion time varied from 0 to 44 days and the equilibration time with dye solutions was 28 days. Their overall results showed that all tested anions have low impact on MB discoloration but negative impact on MO removal. In particular, in the HCO_3^- system "severely affects MO discoloration". The extents of MO discoloration (E value) for the Cl^-, H_2O, HCO_3^-, and SO_4^{2-} systems were very similar and closed to 80 % for $t_{pre\text{-}corrosion} = 3$ days. For $t_{pre\text{-}corrosion} > 3$, While the E value remained almost constant for all other systems. E for the HCO_3^- system decreased to values reaching 40 % for 44 days of pre-corrosion. Clearly, extending the equilibration time herein would have enable the observation of the "natural trend" (validating the working hypothesis) of enhanced MO discoloration in Fe^0/H_2O systems by virtue of increase availability of FeCPs (Phukan et al. 2016).

5.4 Discussion

5.4.1 General aspects

Investigating the effects of common anions on the efficiency of Fe^0/H_2O systems has been plagued by the same problems of the post-1990 Fe^0 literature and the view that Fe^0 is a reducing agent for some dissolved contaminants (Lawrinenko et al. 2023a, Xiao et al. 2023, Xiao et al. 2024). In other words, some attempts were made to perform some systematic investigations to better characterized the influence of individual anions (Sun et al. 2016). However, the experimental designs were faulty (e.g. vigorously shaken batches) and the results mistakenly interpreted (e.g. Fe^0 as electron donor) (Hu et al. 2021, Xiao et al. 2023, Xiao et al. 2024). Accordingly, there has been no guide to inform the discussion of independent results, achieved under very different conditions. There is still no standardized or unified experimental protocol, and no reference Fe^0 material to ease comparison of independent results. In addition, most of the observations reported in the literature are static snap-shots and the choice of the time of their realization (e.g. end of the experiment) is pragmatically fixed by individual investigators (Westerhoff 2003, Lim and Zhu 2008). This is not the ideal starting point for the investigation of dynamic processes within Fe^0/H_2O systems, especially as these dynamics processes occur over an enormous range of time scales – from some hours in batch experiments to some years or decades in the field (Alyoussef 2019, Cao et al 2021b, Singh et al. 2023). The present work has introduced a guide which stipulates that a suitable experimental design should reproduce the theory of the system (Chapter 3). This implies that any report on the lack of effects on any salt on the efficiency of a Fe^0/H_2O system is faulty. Such an observation just means that the operational conditions used (e.g. too high Fe^0 loading or mixing intensity) are not appropriate to reproduce the theory of the system. A common bias in investigating the Fe^0/H_2O system is the application of

non-relevant mixing procedures, e.g. stirring at intensities higher than 75 rpm (Noubactep 2009a, Noubactep et al. 2009b)
The present study has used the MB method to invalidate some mixed findings on the influence of common anions on the efficiency of Fe^0/H_2O systems, this corresponds to deconstruct views that have been pragmatically established using the observations from very independent systems, without any guide. In particular, the inhibiting effects of HCO_3^- ions could only be established by combining the observations of this work (enhanced MB discoloration) and those made by Tsamo et al. (2018) (inhibited MB discoloration). Another contribution of this work is to have considered fluoride ions that are rarely considered although they are abundant in many regions of the world (Ali et al. 2016, Patrick and Sahu 2023, Yadav et al. 2023). The results of the effects of F^- on the efficiency of Fe^0/H_2O systems confirm the non-suitability of Fe^0-based systems for water defluoridation as reported by Heimann et al. (2018) and Ndé-Tchoupé et al. (2019).

5.4.2 Revisiting the effects of chloride addition on the Fe^0/H_2O system

The results presented in section 5.2 and 5.3 clearly demonstrate that Cl^- addition fundamentally hinders the process of contaminant removal in Fe^0/H_2O systems. The rationale for this is that the formation of FeCl-complexes primarily hinders the availability of FeCPs (the contaminant scavengers). This observation is in tune with the historical work of whitney (1903) stating that aqueous Fe^0 corrosion produces oxides/hydroxides (FeCPs) or salts (working hypothesis). The observation made herein clearly contradict published findings over the past 20 years claiming that Cl^- addition typically enhances water treatment with granular Fe^0 (Kim et al. 2007, Hwang et al. 2015, Li et al. 2019, Hernandez et al. 2004). For example, Kim et al. (2007) tested halide salts to sustain the Fe^0 efficiency for explosive "degradation" and concluded that Fe^0 PRBs "installed in aquifers with chloride-rich groundwater are likely to perform and maintain reactivity better than those installed in aquifers with low chloride concentrations". Many other researchers have reached similar conclusions for chloride-rich wastewater (Sun et al. 2016, Hernandez et al. 2004, Zhang et al. 2005, Ansaf et al. 2016) and even more confusing conclusion with other anions (Table 5.4). The question is – how can both views be reconciled?

The key point is to consider that Fe^0 would "passivate" earlier without Cl^- addition. Due to the high solubility of Fe(II) and Fe(III) chlorides relative to iron hydroxides, Cl^- addition sustains Fe^0 corrosion and produces more contaminant scavengers because Fe^0 is in large stoichiometric excess. All of these reactions are enhanced by mixing operations, such as shaking and stirring (Table 5.4). A similar situation has been reported for the addition of MnO_2 to Fe^0 and Fe^0 amendment with sand (Burghardt and Kassahun 2005, Ghauch et al. 2010, Ghauch et al. 2011, Gheju and

Balcu 2019). Here, MnO_2 promotes the Fe^{2+} oxidation and increases the formation of contaminant scavengers (FeCPs) compared to the pure Fe^0 system (Cao et al. 2021b, Alyoussef 2019). Obviously, there is no contradiction between the retardation of contaminant removal in the presence of chloride ions and the improved efficiency of the same systems compared to the operational reference (Cl^- free Fe^0/H_2O).

Table 5. 4 Representative batch studies on the influence of anions on the efficiency of Fe^0/H_2O system for water treatment using microscale Fe^0 materials from 2001 to 2020. References are given in the chronological order of publication from the top. The concentration ranges of anions (g L^{-1}) is specified, together with the mixing/stirring intensities. "p" stands for positive effect, "n" for negative, "n/p" for both positive and negative, "u" for unaffected, and "n.c." for non-considered.

X	Bicarbonate	Chloride	Nitrate	Phosphate	Sulfate	Mixing operations	Reference
Arsenic	1.22 - 122 n	7.1 p	1.24 n	0.19 - 1.9 p	1.920 n	Shaking: 50 rpm	(Su and Puls 2001)
Bromate	0.047 n	n.c.	0.075 p	0.005 n	0.11 p	Rotating: 47 rpm	(Xie and Shang 2007)
p-CNB	0 - 10.0 n/p	0 - 10.0 p	0 - 10.0 p	0 - 0.004 n	0 - 10.0 p	Agitation: 120 rpm	(Le et al. 2011)
NB	0 - 1.0 n/p	0 - 1.0 p	0 - 0.5 p	0 - 008 n	0 - 1.0 p	Agitation: 50 rpm	(Yin et al. 2012)
Acid orange 7	30.5 n	17.75 n	31.0 n	48.0 n	48.0 n	Shaking: 180 rpm	(Li et al. 2015)
Lindane	6.1 - 61.0 p	8.9 - 88.8 p	n.c.	n.c.	1.0 - 9.6 u	Shaking: 100 rpm	(Dominguez et al. 2016)
TCE	0.04 - 0.1 p	0.004 - 0.006 u	n.c.	n.c.	0.05 - 0.57 p	Stirring: 125 rpm	(Velimirovic et al. 2017)
MB	2.83 p	1.65 p	n.c.	4.45 p	4.45 p	Quiescent	(Tsamo et al. 2018)
MO	2.83 u	1.65 n	n.c.	4.45 u	4.45 n	Quiescent	(Tsamo et al. 2018)
CCl_4	0.18 - 0.61 p	0.11 - 0.51 n/p	n.c.	n.c.	0.14 - 0.58 p	Shaking: 200 rpm	(Zhu et al. 2020)

NB = Nitrobenzene, MB = Methylene blue, MO = Methyl orange, p-CNB = p-chloronitrobenzene, TCE = Tetrachloroethylene.

Table 5.4 summarizes the experimental conditions of selected publications on the effects of the five anions on the performance of Fe^0/H_2O systems. Studies presented in Table 5.4 recall that the nature (X) and concentrations (mg L^{-1}) of anions in polluted waters may significantly influence the remediation performance of Fe^0 (Klausen et al. 2003, Liu et al. 2007, Sun et al. 2023). Nitrate is redox-active in the Fe^0/H_2O system while the 4 other anions are redox inert. In general, anions interact with Fe^0 reaction products (e.g. Fe^{2+}, Fe hydroxides, H_2) and other dissolved species (e.g. cations, natural organic matter) to form soluble complexes or mineral precipitates that influence the efficiency of the Fe^0/H_2O system by many different mechanisms. Despite more than two decades of extensive research controversies exist on the effects of all anions as recently reported by Sun et al. (2016) in a critical review article. Table 5.4 illustrates the state of confusion based on 9 selected publications between 2001 and 2020 using microscale Fe^0 (mFe^0). It is seen that practically each researcher employs a different experimental procedure for characterizing the effects of anions on the remediation efficiency of Fe^0/H_2O systems. These procedures typically differ in Fe^0 type and pre-treatment, Fe^0 particle size (mFe^0 versus nano-Fe^0), volume of the reaction vessels used, volume of the solution added, nature and concentration of the contaminants, mixing type and intensities, and equilibration time allowed. The net result is that, in Table 5.4, no trend is observed for any single anion (e.g. n, p, n/p for each anion).

5.4.3 Revisiting the effects of F^-, HCO_3^-, HPO_4^{2-}, and SO_4^{2-} addition on the Fe^0/H_2O system

The results presented in section 5.3 show that F^-, HCO_3^-, HPO_4^{2-}, and SO_4^{2-} significantly impact MB discoloration in Fe^0/H_2O systems when the concentration of the anions varied widely. The general trend for all anions was an inhibition of MB discoloration. This tangible observation seems to contradict literature reports on mixed effects (enhancement and inhibition) of individual anions (Sun et al. 2016, Sun et al. 2023). The mechanism of the observed inhibition of MB discoloration was proposed as follows, validating the working hypothesis: anions form more or less stable complexes (e.g. FeF_6^{3-}) with Fe^{II} and Fe^{III} ions delaying the formation of FeCPs (Fe oxides and hydroxides). Because FeCPs remove MB from the aqueous phase by adsorption and co-precipitation, there is no quantitative MB discoloration before enough FeCPs becomes available (Konadu-Amoah et al. 2022). This explanation is valid whether there is a local acceleration of iron corrosion (e.g. pitting by Cl^-) or not. It also remains valid for redox active species (e.g. NO_3^-) or species with good adsorptive affinities to FeCPs (e.g. Orange II). In other words, the fundamental mechanism by which the presence of anions influences the decontamination process in Fe^0/H_2O systems is an inhibition or a delay (relative to the anion-free system). Taking this as a premise, the actual impact of individual anions, or generally individual co-solutes (including natural organic matter - NOM) can be better characterized. After the establishment of the operating mode of hybrid systems (e.g. Fe^0/FeS_2, Fe^0/MnO_2, Fe^0/sand) (Miyajima and Noubactep 2015, Cao et al. 2021b, Cao et al. 2021c) for water remediation, the MB method has established with this study a sound basis for the characterization of the influence of co-solutes on the performance of remediation Fe^0/H_2O systems. This section revisits the impacts of individual ions, mainly based on a recent review article by Sun et al. (2016).

5.4.3.1 Bicarbonate (HCO_3^-)

The influence of HCO_3^- on the performance of Fe^0-based systems has been found to be typically dependent on its concentration and the equilibration time (Agrawal et al. 2002, Bi et al. 2009a). As a rule of thumb, the performance is initially enhanced, but subsequently deteriorated due to formation of passive iron carbonate precipitates (Bi et al. 2009a). Another common argument for the ambivalent behavior of Fe^0/HCO_3^- systems is the concentration (and pH) dependent speciation of carbonate (e.g. H_2CO_3, HCO_3^-, CO_3^{2-}) (King 1998).

Under the experimental conditions of the present work, only enhanced MB discoloration was observed although the HCO_3^- concentration varied widely. This observation was irritating as it was contradicting the working hypothesis. Fortunately, Tsamo et al. (2018), working under similar conditions for a longer equilibration time (up to 74 days) could observe inhibited MB discoloration in Fe^0/HCO_3^- systems, confirming the crucial importance of the equilibration time (Cao et al. 2021b). In other words, HCO_3^- ions basically deteriorate the performance of Fe^0-based systems for water treatment. However, selected operational parameters (including the initial HCO_3^- concentration) may at least temporarily enhance this performance.

5.4.3.2 Fluoride (F^-)

F^- has not typically investigated for its impact on the performance of Fe^0-based systems (Zhou et al. 2008). Zhou et al. (2008) reported on significant enhancement of Cr^{VI} removal in Fe^0/H_2O systems as result of NaF addition with and increased Cr^{VI} removal with increasing NaF concentration. This observation was justified by the formation of stable FeF_6^{3-} (and $Cr\ F_6^{3-}$), which diminishes the precipitation of Fe^{III} and Cr^{III} hydroxides. However, NaF addition also leads to shifts of the electrode potentials of Fe^{III}/Fe^{II} and Cr^{VI}/Cr^{III} (Naka et al. 2008, Song et al. 2017), which also contribute to increased Cr^{VI} removal. In this constellation, it is difficult to segregate between the individual contributions of complex formation and redox reactivity on the extend of Cr^{VI} removal. This is an issue that has been already elegantly addressed by the MB method (Tao et al. 2023).

The results presented herein support the working hypothesis that Fe-F complexes delay/inhibit the availability of FeCPs and the decontamination process. Again, an enhancement or inhibition of the decontamination depends on the individual operational conditions (Table 5.4)). One key feature of the results presented herein, is that an additional argument to justify the non-suitability of Fe^0-based systems for water defluoridation (Heimann et al. 2018, Ndé-Tchoupé et al. 2019). In this context, it is important to notice that Ndé-Tchoupé et al. (2015) have introduced as a concept to test Fe^0-based filters for decentralized water defluoridation. All reasons for the failure of such filters (e.g. size of $F^–$ ions, stability of $FeF_6^{3–}$ complexes) were already documented in the scientific literature. Nevertheless, the concept was presented and carefully investigated. The results that Fe^0 filters were not suitable for water defluoridation was the starting point to investigate rainwater harvesting in the hills of the Kilimanjaro (Marwa et al. 2018). In retrospect, Ndé-Tchoupé et al. (2015) was a "good mistake" which has opened the rainwater harvesting world to the research group of Dr. Noubactep (Göttingen, Germany). In other words, in an era of multidisciplinary research, it can happen that wrong concepts are introduced. However, systematic investigations always restore the scientific truth.

5.4.3.3 Phosphate ($HPO_4^{2–}$)

$HPO_4^{2–}$ has been constantly presented as depicting the largest inhibitory effect on the performance of Fe^0-based systems for water treatment (Su and Puls 2001, Xie and Shang 2007). $HPO_4^{2–}$ is mostly reported to form inner-sphere complexes with dissolved Fe and co-precipitates on the Fe^0 surface. The whole process inhibits electron transfer from Fe^0 to the individual pollutants (Su and Puls 2004, Xie and Shang 2007). The precipitation of phosphate-bearing minerals also reportedly inhibits pollutants to access to the active sites on the Fe^0 surface. The results presented herein confirm this observation while questioning the importance of the access of the pollutants to the Fe^0 surface because these effects have been observed while MB is not redox active, thus no electron transfer is in play.

5.4.3.4 Sulfate ($SO_4^{2–}$)

Like $Cl^–$, $SO_4^{2–}$ is commonly associated with an enhancement of the performance of Fe^0-based systems (Johnson et al. 1998, Devlin and Allin 2005). However, the exact mechanism of this process has not been conclusively established (Sun et al. 2016). $SO_4^{2–}$ cannot be as aggressive as $Cl^–$ toward destabilizing the oxide scale on Fe^0. For this reason, it has been postulated that $SO_4^{2–}$ promotes Fe oxide dissolution (Sun et al. 2016). The deterioration effects of $SO_4^{2–}$ for Fe^0-based systems is also reported in the literature and justified by some competitive process for adsorption onto the oxide scale (Liu et al. 2007, Yu et al. 2013).

The present work has established that SO_4^{2-} basically delays the process of contaminant removal in Fe^0/H_2O systems because the stability of $FeSO_4$ delays the availability of FeCPs which are the effective contaminant scavengers (Tao et al. 2023). This demonstration shows that confusing reports are rooted on experiments under different operational conditions of which some are even non-relevant for natural systems.

5.5 Environmental significance

5.5.1 The suitability of quiescent batch experiments for investigating the Fe^0/H_2O system

This study has justified why under quiescent experimental conditions, MB discoloration in Fe^0/H_2O systems is inhibited by the presence of Cl^-, F^-, HPO_4^{2-}, and SO_4^{2-}. The reason for enhanced MB discoloration in the presence of HCO_3^- is also justified while considering a recent publication by Tsamo et al. (2018). The used MB method has enabled explanation of reported discrepancies on the effects of common anions on the performance of Fe^0-based systems in the real world. The investigated anions and the concentrations tested are relevant for natural waters and wastewaters. However, natural organic matter (NOM) (Rao et al. 2009) has not been addressed, and polluted waters are invariably a mixed solution of several anions. Therefore, additional investigations to study the effects of mixed anions and NOM are needed for the rational design of more sustainable Fe^0-based remediation systems. Some few such studies already exist (Klausen et al. 2001, Holm 2002, Bi et al. 2009a). However, they have been performed and discussed while considering Fe^0 as a reducing agent, and in-situ generated minerals physical barriers for electron transfer (Xie and Shang 2007, Lawrinenko et al. 2023a, 2023b). The results presented herein recalled that Fe^0-based filtration systems should be regarded as local coagulation units in the vicinity of Fe^0 particles. In other words, the discussion of processes causing contaminant removal in Fe^0 filters are better addressed while considering the similitude between the Fe^0/H_2O system and coagulation (Bojic et al. 2009, Noubactep and Schöner 2010, Noubactep 2011a). In this context, it is essential to remember that Fe^0/particles were anciently used in flocculation (Baker 1934, 1948).

5.5.2 Fe^0/H_2O system as a myriad of coagulation cells

The most important finding of the research is that common anions should be considered as standalone influencers of the Fe^0 corrosion process. This is because, just like a contaminant to be removed, each anion is initially present in the polluted water and thus acts concurrently either as:

1. A complexing agent for generated Fe^{II} ions, thus delaying the availability of FeCPs;
2. An adsorbate for adsorption sites at the surface of in-situ generated FeCPs; and
3. A particle to be occluded by precipitating FeCPs (co-precipitation).

All these three processes occur simultaneously in all Fe^0/H_2O systems and their respective magnitudes depend on several inter-dependent operational parameters, including: (i) the Fe^0 intrinsic reactivity (Cui et al. 2023), (ii) the stability of the Fe-anion complexes (Zhou et al. 2008), and (iii) the adsorptive affinity of the anions to FeCPs (Touomo-Wouafo et al. 2020). The redox reactivity of individual anions, the manner how they influence the redox reactivity of the Fe^{III}/Fe^{II} redox electrode, and the redox reactivity of contaminants are three complicating factors justifying the need of holistic investigations under relevant experimental conditions for the design of more sustainable Fe^0/H_2O systems. In other words, this work is just the starting point for a systematic investigation of the influences of common co-solutes (anions, cations, NOM) on the performance of Fe^0-based remediation systems. The next step, using relevant contaminant for natural waters can be guided by the seminal works of Crawford et al. (1993a, 1993b) clarifying the relationship between adsorption and co-precipitation of heavy metal ions onto the hydrated oxides. In fact, a Fe^0/H_2O system is the homestead of aged and nascent iron oxides and hydroxides, depicting differential adsorptive affinity to various solutes, including common anions and contaminants (Sikora and MacDonald 2000, Noubactep 2010, Noubactep 2011b).

Chapter 6: Synthesis and Conclusions

Sustainable and effective remediation using metallic iron-based systems (Fe^0/H_2O systems) have proven efficient in order to (i) improve environmental quality, and (ii) supply decentralized safe drinking water. The further optimization of the performance of Fe^0/H_2O systems is thus necessary. One main open issue is the lack of data on the long-term behavior of Fe^0 materials under environmental conditions. That is the iron corrosion rate and its changes over the time. This thesis focused on two selected aspects of the sustainability of Fe^0-based filtration systems: (i) the suitability of hybrid Fe^0/aggregates systems, and (ii) the influences of common environmental anions on their performance.

6.1 Synthesis

6.1.1 The suitability of hybrid Fe^0/aggregates systems

Mixing Fe^0 with one or several non-expansive aggregates is the most suitable option to warrant long-term hydraulically efficient Fe^0-based filtration systems, including subsurface Fe^0 PRBs for groundwater remediation. Unfortunately, the hydraulic aspects were not properly considered while designing the first-generation Fe^0 PRBs in the 1990s and the early 2000s. Moreover, published results on long-term sustainable Fe^0 PRBs often do not monitor the permeability loss in a before/after perspective of the operation of PRBs. For this reason, the Fe^0 remediation research community has yet to consider this fundamental aspect in the procedure of designing laboratory experiments to investigate the performance of Fe^0-based filtration systems.

This thesis started about a decade after the practical importance of mixing granular Fe^0 with (inert or reactive) non-expansive materials (e.g. gravel, pumice, pyrite, sand) was established. Prior to 2011, several field projects have been implemented using such mixtures (mostly Fe^0/sand), with achieved results difficult to justify while considering Fe^0 as a reducing agent. In fact, if Fe^0 was a reducing agent, systems with higher Fe^0:sand ratios would have exhibited better remediation performance because they have higher amount of reactive material per unit volume. The second reason to expect a lower performance from hybrid Fe^0/aggregates systems is that Fe^0 particles become separated by additive aggregates, and thus diminished mass transport (longer diffusion path) of contaminants to the Fe^0 surface occurs. The fact that the opposite was observed (hybrid systems more efficient) validates the view that Fe^0 is a generator of FeCPs which coat the sand surface and offer more adsorptive sites to contaminants. Adsorbed contaminants can still be reductively transformed by H_2 and other reducing species omnipresent within the Fe^0/H_2O system (e.g. Fe^{II} species, Fe_3O_4). Unfortunately, research has continued while still considering the reductive transformation concept. The net result is that it is difficult to discern good from falsified results through the Fe^0 literature of the past decade (post 2010). This state of affairs was the motivation for the critical literature review on the suitability of hybrid Fe^0/aggregate filtration systems for water treatment (Tao et al. 2022).

Tao et al. (2022) showed that any enhanced contaminant removal efficiency in Fe^0/aggregate/H_2O systems relative to the Fe^0/H_2O system is related to the avoidance/delay of particle cementation by virtue of the non-expansive nature of the aggregates. The argument that aggregate addition sustains any reductive transformation of contaminants mediated by electrons from Fe^0 was disproved by the evidence that Fe^0/sand systems are equally more efficient than pure Fe^0 systems. This demonstration corroborates the concept that aqueous contaminant removal in iron/water systems is not a process mediated by electrons from Fe^0. To sum up, Tao et al. (2022) has reiterated that only hybrid Fe^0/H_2O filtration systems are sustainable.

For future research, each Fe^0/aggregates system should be characterized using the following steps:

(i) Grain size and grain size distribution of Fe^0 and aggregates used;

(ii) Chemical reactivity of Fe^0 and aggregates (e.g. sand is inert, while MnO_2 is reactive);

(iii) The optimum Fe^0:aggregate ratio. Ideally, this ratio should be given in a vol: vol percent basis;

(iv) Determine the optimum thickness of the reactive zone for long-term efficiency for decontamination, and maintained hydraulic conductivity;

(v) Because Fe^0/H_2O systems are ion-selective, the extent of removal of selected model contaminants needs to be assessed in long-term experiments, for example ≥ 12 months.

(vi) Finally, because the Fe^0/sand system performs better that pure Fe^0, investigating any hybrid system involving reactive materials (e.g. Fe_3O_4, FeS_2, MnO_2) should use a Fe^0/sand system as reference.

The analysis in Tao et al. (2022) has established clearly that long-term column tests (laboratory and pilot) should be carried out before reliable mathematical modelling and numerical simulations can be performed. This is because a comprehensive assessment of the remediation performance of Fe^0/H_2O systems is yet to be realized. Only such assessments, grounded on systematic investigations would facilitate the further development and optimization of this still innovative remediation technology. This assessment should consider all environmental factors affecting the performance of the systems. The presence of common anions is such an environmental factor.

6.1.2 The influences of common anions on the performance of Fe^0/H_2O systems

The effects of common anions on the performance of Fe^0/H_2O systems have been largely discussed in the Fe^0 remediation literature. However, a detailed comprehensive assessment is still lacking. In this thesis, the methylene blue method (MB method), a method fundamentally based on the law of conservation of mass, has for the first time been systematically used to assess the influences of common anions on the performance of Fe^0/H_2O systems. For the sake of clarity, the $Fe^0/Cl^-/MB/H_2O$ system was first systematically investigated (Tao et al. 2023). The optimized experimental procedure was then exploited to investigate the Fe^0/anion/MB/H_2O system for F^-, Cl^-, HCO_3^-, HPO_4^{2-}, and SO_4^{2-} (Tao et al. 2024). The MB method performed in this work enabled an indirect quantification of the amounts of solid iron corrosion (FeCPs) generated in individual Fe^0/H_2O systems as response of the nature and concentration of each anion. Each of the investigated anions (e.g. F^-, Cl^-, HCO_3^-, HPO_4^{2-}, SO_4^{2-}) influences the Fe corrosion process as well as the availability of FeCPs. This evidence was exploited to formulate the working hypothesis: "The presence of each anion primarily inhibits the decontamination performance of Fe^0/H_2O systems". The detailed assessment revealed that the remediation Fe^0/H_2O system can be regarded as a myriad of coagulation cells, each operating in the vicinity of a Fe^0 particle. In these cells, all solutes (including contaminants and indicators) compete with each other to influence the process of iron corrosion and FeCPs precipitation. This new perspective of the Fe^0/H_2O system (coagulation cells) has elucidated all published discrepancies.

The results presented in this thesis furthermore confirmed the suitability of the MB method as a tool for assessment of the extent of iron corrosion within a Fe^0/H_2O system. The principle of the MB method can be applied on a routine basis, since it roughly allows evaluation of the remediation effectiveness. By systematically monitoring Fe concentration and pH value, the MB method also provides an overview of the processes occurring in a Fe^0 reactive zone during the time course of remediation. In particular, in the presence of F^-, the formation of very stable FeF_6^{3-} complexes has impaired the MB discoloration and provided a further reason why Fe^0/H_2O systems are not suitable for water defluoridation.

The results presented in this thesis elegantly confirm that Fe^0 is a generator of contaminant scavengers. Fe^0 would "passivate" earlier without Cl^- addition. Due to the high solubility of Fe^{II} and Fe^{III} chlorides relative to iron hydroxides, Cl^-

addition sustains Fe^0 corrosion and produces more contaminant scavengers because Fe^0 is in large stoichiometric excess. The presence of NaCl delays the precipitation of iron oxides and hydroxides, thus delaying the decontamination process. This was observed for all four dyes and at all NaCl concentrations. These results clearly underscore the importance of pitting corrosion effects (for Cl^-) and the capacity to remove precipitation as the rationale for the positive role of chloride and sulfate in improving the efficiency of Fe^0/H_2O systems respectively. The results also present a better explanation of the ambivalent role of HCO_3^- (e.g. inhibitory at high concentrations, and enhancing at lower ones). In fact, the impact of HCO_3^- is not limited to a concentration-dependent buffering effect but reveals the kinetics of the formation of a $FeCO_3$ scale on Fe^0. Phosphate as an inhibitor of Fe^0 reactivity was observed as expected.

6.2 Conclusion and Outlook

The research presented in this work has addressed some of the hydraulic issues associated with the longevity of Fe^0 filtration systems and has provided evidence for the suitability of hybrid Fe^0/aggregate systems from a hydraulic perspective. This research has shown that the interplay between the Fe^0 intrinsic reactivity, the size of Fe^0 particles, the nature and size of the aggregates used, and the Fe^0: aggregate ratio is responsible for the sustainability of Fe^0 filters. It has been shown that the Fe^0:aggregate ratio is one of the key players in hydraulic conductivity loss. More so, pure Fe^0 filters (100 % Fe^0 systems) are definitively not sustainable due to loss of permeability/clogging, while research on hybrid systems is yet to be systematically performed. Systems with 50 % Fe^0 (w/w) were widely investigated and some few systems with less than 5 % Fe^0 (w/w or vol/vol) were presented. Systems with lower Fe^0:aggregate ratios have typically not presented any permeability loss. Therefore, one of the most productive areas for future work would involve investigating the suitability of lower than 10% (vol/vol). Related small-scale experiments should last for several months or years. This is because the long-term corrosion kinetics is not known and is expected to further change with decreased pore space (porosity loss).

As concerning the influence of commonly occurring anions on the performance of Fe^0 filters, this study has established the science of the Fe^0/anion/H_2O system. This science-based approach has enabled the elucidation of published controversies. However, this achievement is only the first step in efforts to understand environmental systems as highly artificial single-anion-systems were characterized, while multi-anion systems were not addressed in the present study. More systematic research is needed to design efficient and sustainable real-world Fe^0-based systems characterized by multi-anion-compositions (e.g. HCO_3^--Cl^--

SO_4^{2-} or HCO_3^--F^--SO_4^{2-}). A beneficial next step can be to investigate the influences of mixed anions systems.

Chapter 7: Epilogue

The presented work corresponds to the original manuscript evaluated by two referees. Minor revisions were performed, strictly limited to actualizing bibliographic references. The major concern raised during the defense was the lack of diffusion coefficient to support the mechanistic discussion. This concern was addressed during the preliminary works based on the rule of thumb: "lower agitation speed requires longer contact time than higher ones". Tao et al. (2023) established that, under the experimental conditions used (no agitation at all), there was no difference in the extent of methylene blue discoloration between pure sand and Fe^0/sand systems during the 20 first days (3 weeks) of equilibration. This was the rationale for using equilibration times larger than 21 days (Chapter 5).

Four steps are involved during the MB discoloration by Fe^0 and sand: (i) bulk diffusion, (ii) external mass transfer or film diffusion, (iii) intra-particle transport within the particle, and (iv) MB discoloration at the liquid/solid interface. Film diffusion occurs between the external surface of the adsorbent particles and the surrounding fluid phase (Hamdaoui and Chiha 2007, Fernandes et al. 2007, Worch 2012, Elgarahy et al. 2023). Hamdaoui and Chiha (2007) tested agitation speeds of 100, 250, 400, 600, and 1000 rpm, respectively and reported that only external and internal diffusions significantly impact the kinetics of MB discoloration. Several other authors came to a similar conclusion (Zeng et al. 2021a, Manoko et al. 2022, Elgarahy et al. 2023, Zeghioud and Mouhamadou 2023, Dubey et al. 2024) which is highly qualitative and corresponds to the named rule of thumb ("lower agitation requires longer contact time"). This is because experiments investigating the impacts of the mixing speed on the efficiecy of MB discoloration in Fe^0/H_2O systems have not considered any accompanying quiescent batch experiments (mixing speed: 0 rpm). The considered mixing intensities were all larger than 100 rpm which corresponds to the optimal mixing intensities for flocculation (Polasek 2007, Polasek 2011, Nurmawati et al. 2022). More so, the experiments were not designed to establish any reaction mechanism, but rather to optimize the operational conditions in treatability tests (Zawaideh and Zhang 1998, Choe et al. 2000, Sun et al. 2006, Xie and Shang 2007, Hwang et al. 2011, Stieber et al. 2011). In other words, the crucial influence of the agitation speed on the molecular transport of cationic MB to the adsorption sites was not thoroughly investigated. However, under experimental conditions limiting the manifestation of electrostatic interactions between adsorbents and charged MB, no mechanistic investigations are possible (Noubactep 2007, 2008, Makota et al. 2017, Noubactep et al. 2017, Ebelle et al. 2019). Clearly, some few apparent diffusion coefficients have been published (Fernandes et al. 2007), but cannot be used to discuss the results achieved in this work. This is because no other research group has used MB in test tubes. The diffusion coefficient depends certaunly on the size of the diffusing molecule but also on the geometry of the reaction vessels used (Jacops et al. 2017, Asaad et al. 2021). The concern of the jury is absolutely justified: In order to compute reliable models for the description of processes occuring in Fe^0-based filters or Fe^0/H_2O remediation systems in general, correct estimates for contaminant (e.g. RCl) diffusion coefficients are essential. Moreover, the diffusion coefficients of reaction products (e.g. H_2, RH) also need to be established (Zhou 2021).

With regard to the impact of anions on MB discoloration in Fe^0/H_2O systems, Leaist (1988) characterized MB diffusion in water as influenced by the presence of $Cl^–$ (NaCl). Their results showed that as MB concentration increased from 0.0006 to 0.02 mol $L^{–1}$, corresponding to 191 to 6397 mg $L^{–1}$, aggregation of MB monomers and binding of the $Cl^–$ counterions cause the MB's binary diffusion coefficient to drop from 0.83 x 10^{-9} to 0.63 x 10^{-9} m^2 s^{-1}. These results also show that adding 0.005 or 0.01 mol $L^{–1}$ of $Cl^–$ ions (292 or 584 mg $L^{–1}$) sharply reduces the MB diffusivity, and that each mole of diffusing MB cotransports 0.2-0.7 mol NaC1. Clearly, the apparent MB diffusion coefficient decreases with the presence and amount of $Cl^–$ ions. This corresponds to the decreased MB discoloration as result of ligand addition as reported herein. The results of Leaist (1988) also validate the concern of the jury and indicate that determining the apparent diffusion coefficients would have eased the discussion of the results of the present work. Since diffusion coefficients obtained under quiescent batch conditions are not available, an optimization of the discussion in Chapter 5 is not possible at this time. On the other hand, the results of Sedláček et al. (2013, 2014) demonstrate that in Fe^0/H_2O systems, structural parameters like effective porosity and tortuosity increase the diffusion coefficients and delays MB discoloration.

A second concern of the jury was about the redox reactivity of the Fe^0 ($E^0 = –0.44$ V) for MB ($E^0 = –0.02$ V) and the mechanism of MB discoloration. It should be made clear why the MB method stands despite repeated reports on MB electrochemical reduction by electrons from Fe^0 (Frost et al. 2010, Sun et al. 2015, Elkady et al. 2019, Trinh et al. 2019, Pujar 2022, Abd El-Monaem et al. 2024, Fan et al. 2024).

MB has been used as a redox indicator in chemistry and biochemistry for more than one century (Clark et al. 1925). MB reversibly turns to colorless leucomethylene blue (LMB) when the redox potential decreases (Pujar 2022). This implicitely means that the blue colour alone indicates that MB reduction (Eq A.1) is not quantitative. Considering this evidence, the presentation of the MB method has constantly seggregated between "MB discoloration" and "MB removal" (Miyajima 2012, Phukan 2016, Alyoussef 2019, Tepong-Tsind é 2021). Despite this decade-old knowledge, largely published and reviewed (Btatkeu-K et al. 2016, Konadu-Amoah et al. 2021) in the recent literature, independent reports on MB reduction by Fe^0 (Eq. A.2) are still published (Elkady et al. 2019, Pujar 2022, Abd El-Monaem et al. 2024, Fan et al. 2024).

$$\mathrm{MB} + n\ e \Leftrightarrow \mathrm{LMB} \qquad (A.1)$$

$$\mathrm{Fe}^0 \Leftrightarrow \mathrm{Fe}^{2+} + 2\ e \qquad (A.2)$$

$$\mathrm{MB} + n\ \mathrm{Fe_x(OH)_y}^{(3x-y)} \Rightarrow [\mathrm{MB}[\mathrm{Fe_x(OH)_y}^{(3x-y)}]_n] \qquad (A.3)$$

The present works has reiterated that MB discoloration by Fe^0 is not possible while MB discoloration by co-precipitation with solid iron corrosion products (Eq. A.3) (Abd El-Monaem et al. 2024) can be quantitative despite electrostatic repulsion between cationic MB and positively charged FeCPs. From a pure thermodynamic perspective, Fe^0 can exchange electron with MB because the electrode potential of the Fe^{II}/Fe^0 electrode ($E^0 = -0.44$ V) is lower than that of MB ($E^0 = -0.02$ V). However, as discussed herein on the basis of Whitney (1903), only H^+ can access the Fe^0 surface. In other words, reduction of MB (A.1), when it occurs, is mediated by other reducings agents, for example structural Fe^{II} (White and Peterson 1996, Charlet et al. 1998, Liger et al. 1999, Mettler et al. 2009). In fact, White and Peterson (1996) have reported that the electrode potential of adsorbed Fe^{III}/Fe^{II} ranges from −0.34 to −0.65 V, making structural Fe^{II} a stronger reducing agent than aqueous Fe^{2+} ($E^0 = 0.77$ V). In some cases, ($E < -0.44$ V), structural Fe^{II} is even a stronger reducing agent than Fe^0.

References

Abd El-Monaem E.M., Omer A.M., El-Subruiti G.M., Mohy Eldin M.S., Eltaweil A.S. (2024): Zero-valent iron supported-lemon derived biochar for ultra-fast adsorption of methylene blue. Biomass Conv. Bioref. Biomass Conv. Bioref. 14, 1697–1709.

Aghazadeh M., Zakeri A., Bafghi M .Sh. (2012): Modeling and optimization of surface quality of copper deposits recovered from brass scrap by direct electrowinning. Hydrometallurgy 111–112,103–108.

Agrawal A., Ferguson W.J., Gardner B.O., Christ J., Bandstra J.Z., Tratnyek P.G. (2002): Effects of carbonate on contaminant reduction by zero-valent iron. Environ. Sci. Technol. 36, 4326–4333.

Ali S., Thakur S.K., Sarkar A., Shekhar S. (2016): Worldwide contamination of water by fluoride. Environ. Chem. Lett. 14, 291–315.

Alyoussef G. (2019): Characterizing the impact of contact time in investigating processes in Fe^0/H_2O systems. Master Dissertation, University of Göttingen, Germany.

Anderson W. (1886): On the purification of water by agitation with iron and by sand filtration. Journal of the Society for Arts 35 (1775), 29–38.

Angst U.M. (2019): A critical review of the science and engineering of cathodic protection of steel in soil and concrete. Corrosion 75, 1420–1433.

Ansaf, K.V.K.; Ambika, S.; Nambi, I.M. (2016): Performance enhancement of zero valent iron based systems using depassivators: Optimization and kinetic mechanisms. Water Res. 102, 436–444.

Aragaw T.A., Alene A.N. A. (2022): Comparative study of acidic, basic, and reactive dyes adsorption from aqueous solution onto kaolin adsorbent: Effect of operating parameters, isotherms, kinetics, and thermodynamics. Emerg. Contam. 8, 59–74.

Asaad A., Hubert F., Ferrage E., Dabat T., Paineau E., Porion P., Savoye S., Gregoire B., Dazas B., Delville A., Tertre E. (2021): Role of interlayer porosity and particle organization in the diffusion of water in swelling clays. Appl. Clay Sci. 207, 106089.

Bafghi M.Sh., Zakeri A., Ghasemi Z., Adeli M. (2008): Reductive dissolution of manganese ore in sulfuric acid in the presence of iron metal. Hydrometallurgy 90, 207–212.

Baker M.N. (1934): Sketch of the history of water treatment. J. Am. Water Works Assoc. 26, 902–938.

Baker M.N. (1948): The Quest for Pure Water: The History of Water Purification from the Earliest Records to the Twentieth Century. American Water Works Association, New York, USA.

Bandyopadhyay S. (Ed.) (2024): Advances in Drinking Water Purification: Small systems and emerging issues. Elsevier, Amsterdam, The Netherlands.

Bi E., Bowen I., Devlin J.F. (2009a): Effect of mixed anions (HCO_3^--SO_4^{2-}-ClO_4^-) on granular iron (Fe^0) reactivity. Environ. Sci. Technol. 43, 5975–5981.

Bi E., Devlin J.F., Huang B. (2009b): Effects of mixing granular iron with sand on the kinetics of trichloroethylene reduction. Ground Water Monit. Remed. 29, 56–62.

Bilardi S., Calabrò P.S., Moraci N. (2019): The removal efficiency and long-term hydraulic behaviour of zero valent iron/lapillus mixtures for the simultaneous removal of Cu^{2+}, Ni^{2+} and Zn^{2+}. Sci. Tot. Environ. 675, 490-500.

Bilardi S., Calabrò P.S., Moraci N. (2023): A review of the hydraulic performance of permeable reactive barriers based on granular zero valent iron. Water 15, 200.

Birke, V.; Schuett, C.; Burmeier, H.; Friedrich, H.-J. (2015): Impact of trace elements and impurities in technical zero-valent iron brands on reductive dechlorination of chlorinated ethenes in groundwater. In Permeable Reactive Barrier Sustainable Groundwater Remediation; Naidu, R., Birke, V., Eds.; CRC Press: Boca Raton, FL, USA, pp. 87–98, ISBN 978-1-4822-2447-4.

Bischof G. (1877): On putrescent organic matter in potable water. Proc. R. Soc. Lond. 26, 258–261.

Bischof G. (1973): On the purification of water. Proceedings of the Royal Philosophical Society of Glasgow, Band 8, 357–372.

Bojic A.Lj., Bojic D., Andjelkovic T. (2009): Removal of Cu^{2+} and Zn^{2+} from model wastewaters by spontaneous reduction–coagulation process in flow conditions. J. Hazard. Mater. 168, 813–819.

Bojic A.Lj., Purenovic M., Bojic D., Andjelkovic T. (2007): Dehalogenation of trihalomethanes by a micro-alloyed aluminium composite under flow conditions. Water SA 33, 297–304.

Brenner S. (2010): Sequences and consequences. Phil. Trans. R. Soc. B 365, 207–212.

Btatkeu K.B.D., Miyajima K., Noubactep C., Caré S. (2013): Testing the suitability of metallic iron for environmental remediation: Discoloration of methylene blue in column studies. Chem. Eng. J. 215–216, 959–968.

Btatkeu-K. B.D., Olvera-Vargas H., Tchatchueng J.B., Noubactep C. Caré S. (2014a): Determining the optimum Fe^0 ratio for sustainable granular Fe^0/sand water filters. Chem. Eng. J. 247, 265–274.

Btatkeu-K. B.D., Olvera-Vargas H., Tchatchueng J.B., Noubactep C., Caré S. (2014b): Characterizing the impact of MnO2 on the efficiency of Fe0-based filtration systems. Chem. Eng. J. 250, 416–422.

Btatkeu-K. B.D., Tchatchueng J.B., Noubactep C. Caré S. (2016): Designing metallic iron based water filters: Light from methylene blue discoloration. J. Environ. Manage. 166, 567–573.

Burghardt D., Kassahun A. (2005): Development of a reactive zone technology for simultaneous in situ immobilisation of radium and uranium. Environ. Geol. 49, 314–320.

Butler C.E., Hayes F.K. (2001): Factors influencing rates and products in the transformation of trichloroethylene by iron sulfide and iron metal. Environ. Sci. Technol. 35, 3884–3891.

Cao V., Alyoussef G., Gatcha-Bandjun N., Gwenzi W., Noubactep C. (2021b): The key role of contact time in elucidating the mechanism of enhanced decontamination by Fe^0/MnO_2/sand systems. Sci. Rep. 11, 12069.

Cao V., Alyoussef G., Gatcha-Bandjun N., Gwenzi W., Noubactep C. (2021c): Characterizing the impact of MnO_2 addition on the efficiency of Fe^0/H_2O systems. Sci. Rep. 11, 9814.

Cao V., Bakari O., Kenmogne-Tchidjo J.F., Gatcha-Bandjun N., Ndé-Tchoupé A.I., Gwenzi W., Njau K.N., Noubactep C. (2022): Conceptualizing the Fe^0/H_2O system: A call for collaboration to mark the 30th anniversary of the Fe^0-based permeable reactive barrier technology. Water 14, 3120.

Cao V., Ndé-Tchoupé A.I., Hu R., Gwenzi W., Noubactep C. (2021a): The mechanism of contaminant removal in $Fe(0)/H_2O$ systems: The burden of a poor literature review. Chemosphere 280, 130614.

Caré S., Crane R., Calabrò P.S., Ghauch A., Temgoua E., Noubactep C. (2013): Modeling the permeability loss of metallic iron water filtration systems. CLEAN – Soil, Air, Water 41, 275–282.

Caré S., Nguyen Q.T., L'Hostis V., Berthaud Y. (2008): Mechanical properties of the rust layer induced by impressed current method in reinforced mortar. Cement Concrete Res. 38, 1079–1091.

Charlet L., Liger E., Gerasimo P. (1998): Decontamination of TCE- and U-rich waters by granular iron: role of sorbed Fe (II). J. Environ. Eng., 124, 25–30.

Chaves L.H.G. (2005): The role of green rust in the environment: A review. Rev. Bras. Eng. Agríc. Ambient.9, 284–288.

Choe S., Chang Y.Y., Hwang K.Y., Khim J. (2000): Kinetics of reductive denitrification by nanoscale zero-valent iron. Chemosphere 41, 1307–1311.

Clark W.M., Cohen B., Gibbs H.D. (1925): Studies on oxidation-reduction: VIII. Methylene blue. Public Health Reports 40, 1131–1201.

Crawford R.J., Harding I.H., Mainwaring D.E. (1993a): Adsorption and coprecipitation of single heavy metal ions onto the hydrated oxides of iron and chromium. Langmuir 9, 3050–3056.

Crawford R.J., Harding I.H., Mainwaring D.E. (1993b): Adsorption and coprecipitation of multiple heavy metal ions onto the hydrated oxides of iron and chromium. Langmuir 9, 3057–3062.

Cui X., Xiao M., Tao R., Hu R., Ruppert H., Gwenzi W., Noubactep C. (2023): Developing the ascorbic acid test: A candidate standard tool for characterizing the intrinsic reactivity of metallic iron for water remediation. Water 15, 1930.

Devlin J.F., Allin K.O. (2005): Major anion effects on the kinetics and reactivity of granular iron in glass-encased magnet batch reactor experiments. Environ. Sci. Technol. 39, 1868–1874.

Devlin J.F., Klausen J., Schwarzenbach R.P. (1998): Kinetics of nitroaromatic reduction on granular iron in recirculating batch experiments. Environ. Sci. Technol, 32, 1941–1947.

Devonshire E. (1890): The purification of water by means of metallic iron. J. Frankl. Inst. 129, 449–461.

Domga R., Togue-Kamga F., Noubactep C., Tchatchueng J.B. (2015): Discussing porosity loss of Fe^0 packed water filters at ground level. Chem. Eng. J. 263, 127–134.

Dominguez C.M., Parchao J., Rodriguez S., Lorenzo D., Romero A., Santos A. (2016): Kinetics of lindane dechlorination by zerovalent iron microparticles: Effect of different salts and stability study. Ind. Eng. Chem. Res. 55, 12776–12785.

Du M., Zhang Y., Hussain I., Du X., Huang S., Wen W. (2019): Effect of pyrite on enhancement of zero-valent iron corro-sion for arsenic removal in water: A mechanistic study. Chemosphere 233, 744–753.

Du M., Zhang Y., Zeng X., Kuang H., Huang S. (2020): Enhancement of ballmiling on pyrite/zero-valent iron for arsenic removal in water: A mechanistic study. Chemosphere 249, 126130.

Dubey S., Rekhate C., Sharma A., Joshi A., Prajapati A.K. (2024): Optimizing distillery effluent treatment through sono-electrocoagulation: A response surface methodology approach, Tot. Environ. Adv. 9, 200093.

Duff M.C., Coughlin J.U., Hunter B.D. (2002): Uranium co-precipitation with iron oxide minerals. Geochim. Cosmochim. Acta 66, 3533–3547.

Ebelle T.C., Makota S., Tepong-Tsindé R., Nassi A., Noubactep C. (2019): Metallic iron and the dialogue of the deaf. Fresenius Environ. Bull. 28, 8331–8340.

Elgarahy A.M., Mostafa H.Y., Zaki E.G., ElSaeed S.M., Elwakeel K.Z., Akhdhar A., Guibal E. (2023): Methylene blue removal from aqueous solutions using a biochar/gellan gum hydrogel composite: Effect of agitation mode on sorption kinetics. Int. J. Biol. Macromol. 232, 123355.

Elkady M., Shokry H., El-Sharkawy A., El-Subruiti G., Hamad H. (2019): New insights into the activity of green supported nanoscale zero-valent iron composites for enhanced acid blue-25 dye synergistic decolorization from aqueous medium. J. Mol. Liq. 294, 111628.

Erickson A.J., Gulliver J.S., Weiss P.T. (2007): Enhanced sand filtration for storm water phosphorus removal. J. Environ. Eng. 133, 485–497.

Fan M., Zhang P., Wang C., Sun H. (2024): Highly efficient removal of ionic dyes in aqueous solutions using magnetic 3D reduced graphene oxide aerogel supported nano zero-valent iron. Environ. Eng. Res. 29, 230149.

Farjami E., Clima L., Gothelf K.V., Ferapontova E.E. (2010): DNA interactions with a Methylene Blue redox indicator depend on the DNA length and are sequence specific. Analyst135, 1443–1448

Farrell J., Wang J., O'Day P., Conklin M. (2001): Electrochemical and spectroscopic study of arsenate removal from water using zero-valent iron media. Environ. Sci. Technol. 35, 2026–2032.

Fernandes A.N., Almeida C.A.P., Menezes C.T.B., Debacher N.A., Sierra M.M.D. (2007): Removal of methylene blue from aqueous solution by peat. J. Hazard. Mater. 144, 412–419.

Fortune W.B., Mellon M.G. (1938): Determination of iron with o-phenanthroline: A spectrophotometric study. Ind. Eng. Chem. Anal. Ed. 10, 60–64.

Fronczyk J. (2020): Properties of reactive materials for application in runoff water treatment systems. J. Ecol. Eng. 21, 185-197.

Frost R.L., Xi Y., He H. (2010): Synthesis, characterization of palygorskite supported zero-valent iron and its application for methylene blue adsorption. J. Colloid Interface Sci. 341, 153–161.

Gaspar D.J., Lea A.S., Engelhard M.H., Baer D.R., Miehr R., Tratnyek P.G. (2002): Evidence for localization of reaction upon reduction of carbon tetrachloride by granular iron. Langmuir 18, 7688–7693.

Gatcha-Bandjun N., Noubactep C., Loura B.B. (2017): Mitigation of contamination in effluents by metallic iron: The role of iron corrosion products. Environ. Technol. Innov. 8, 71–83.

Ghaedi M., Nasab A.G., Khodadoust S., Sahraei R., Daneshfar A. (2015): Characterization of zinc oxide nanorods loaded on activated carbon as cheap and efficient adsorbent for removal of methylene blue. J. Ind. Eng. Chem. 21, 986–993.

Ghauch A.; Abou Assi, H.; Baydoun, H.; Tuqan, A.M.; Bejjani, A. (2011): Fe^0-based trimetallic systems for the removal of aqueous diclofenac: Mechanism and kinetics. Chem. Eng. J. 172, 1033–1044.

Ghauch, A.; Abou Assi, H.; Bdeir, S. (2010): Aqueous removal of diclofenac by plated elemental iron: Bimetallic systems. J. Hazard. Mater.182, 64–74.

Gheju M., Balcu I. (2019): Sustaining the efficiency of the Fe(0)/H_2O system for Cr(VI) removal by MnO_2 amendment. Chemosphere 214, 389–398.

Gheju M.; Balcu I. (2023): Effect of sand co-presence on Cr^{VI} removal in Fe^0-H_2O system. Water 15, 777.

Gillham R.W. (2010): Development of the granular iron permeable reactive barrier technology (good science or good fortune). In "Advances in environmental geotechnics: proceedings of the International Symposium on Geoenvironmental Engineering in Hangzhou, China, September 8-10, 2007"; Y. Chen, X. Tang, L. Zhan (Eds); Springer Berlin/London, pp. 5–15.

Gillham R.W., O'Hannesin S.F (1994): Enhanced degradation of halogenated aliphatics by zero-valent iron. Ground Water 32, 958–967.

Groysman A. (2010): Corrosion for Everybody. Springer Dordrecht, Heidelberg, London, New York, 368 pp.

Gu B., Phelps T.J., Liang L., Dickey M.J., Roh Y. Kinsall B.L., Palumbo A.V., Jacobs K. (1999): Biogeochemical dynamics in zero-valent iron columns: Implications for permeable reactive barriers. Environ Sci. Technol., 33, 2170–2177.

Guan X., Sun Y., Qin H., Li J., Lo I.M.C., He D., Dong H. (2015): The limitations of applying zero-valent iron technology in contaminants sequestration and the corresponding countermeasures: The development in zero-valent iron technology in the last two decades (1994–2014). Water Res. 75, 224–248.

Hamdaoui O., Chiha M. (2007): Removal of methylene blue from aqueous solutions by wheat bran. Acta Chimica Slovenica 54, 407–418.

Hamdy A., Mostafa M.K., Nasr M. (2018): Zero-valent iron nanoparticles for methylene blue removal from aqueous solutions and textile wastewater treatment, with cost estimation. Water Sci. Technol. 78, 367–378.

Heimann S., Ndé-Tchoupé A.I., Hu R., Licha T., Noubactep C. (2018): Investigating the suitability of Fe^0 packed-beds for water defluoridation. Chemosphere 209, 578–587.

Henderson A.D., Demond A.H. (2007): Long-term performance of zero-valent iron permeable reactive barriers: a critical review. Environ. Eng. Sci. 24, 401–423.

Henderson A.D., Demond A.H. (2011): Impact of solids formation and gas production on the permeability of ZVI PRBs. J. Environ. Eng. 137, 689–696.

Henderson A.D., Demond A.H. (2013): Permeability of iron sulfide (FeS)-based materials for groundwater remediation. Water Res. 47, 1267–1276.

Hering J.G., Maag S., Schnoor J.L. (2016): A call for synthesis of water research to achieve the sustainable development goals by 2030. Environ. Sci. Technol. 50, 6122–6123.

Hernandez R., Zappi M., Kuo C.H. (2004): Chloride effect on TNT degradation by zerovalent iron or zinc during water treatment. Environ. Sci. Technol. 38, 5157–5163.

Holm T.R. (2002): Effects of CO_3^{2-}/bicarbonate, Si, and PO_4^{3-} on arsenic sorption to HFO. Journal AWWA 94, 174–181.

Hu R., Ndé-Tchoupé A.I., Cao C., Gwenzi W., Noubactep C. (2021): Metallic iron for environmental remediation: The fallacy of the electron efficiency concept. Frontiers Environ. Chem. 2, 677813.

Huang Y.H., Tang C., Zeng H. (2012): Removing molybdate from water using a hybridized zero-valent iron/magnetite/Fe(II) treatment system. Chem. Eng. J. 200–202, 257–263.

Hussam A. (2009): Contending with a development disaster: Sono filters remove arsenic from well water in Bangladesh. Innovations 4, 89–102.

Hussam A., Munir A.K.M. (2007): A simple and effective arsenic filter based on composite iron matrix: Development and deployment studies for groundwater of Bangladesh. J. Environ. Sci. Health A 42, 1869–1878.

Hwang Y.; Kim D.; Shin H.-S. (2015): Inhibition of nitrate reduction by NaCl adsorption on a nano-zero-valent iron surface during a concentrate treatment for water reuse. Environ. Technol. 36, 1178–1187.

Hwang Y.H., Kim D.G., Shin H.S. (2011): Effects of synthesis conditions on the characteristics and reactivity of nano scale zero valent iron. Appl. Catal. B: Environ. 105, 144–150.

ITRC (Interstate Technology & Regulatory Council) (2005): Permeable Reactive Barriers: Lessons Learned/New Directions. PRB-4. Washington, D.C.: Interstate Technology & Regulatory Council, Permeable Reactive Barriers Team. www.itrcweb.org (access: 09.03.2012).

ITRC (Interstate Technology & Regulatory Council) (2011): Permeable Reactive Barrier: Technology Update. PRB-5. Washington, D.C.: Interstate Technology & Regulatory Council, PRB: Technology Update Team. www.itrcweb.org (access: 09.03.2012).

Jacops E., Aertsens M., Maes N., Bruggeman C., Swennen R., Krooss B., Amann-Hildenbrand A., Littke R. (2017): The dependency of diffusion coefficients and geometric factor on the size of the diffusing molecule: observations for different clay-based materials. Geofluids 2017, 8652560.

James B.R., Rabenhorst M.C., Frigon G.A. (1992): Phosphorus sorption by peat and sand amended with iron oxides or steel wool. Water Environ. Res. 64, 699–705.

Jia Y., Aagaard P., Breedveld G.D. (2007): Sorption of triazoles to soil and iron minerals. Chemosphere 67, 250–258.

Jiao Y., Qiu C., Huang L., Wu K., Ma H., Chen S., Ma L., Wu L. (2009): Reductive dechlorination of carbon tetrachloride by zero-valent iron and related iron corrosion. Appl. Catal. B: Environ. 91, 434–440.

Johnson T.L., Fish W., Gorby Y.A., Tratnyek P.G. (1998): Degradation of carbon tetrachloride by iron metal: Complexation effects on the oxide surface. J. Cont. Hydrol. 29, 379–398.

Kaplan D.I., Gilmore T.J. (2004): Zero-valent iron removal rates of aqueous Cr(VI) Measured under flow conditions. Water Air Soil Pollut. 155, 21–33.

Kara H.K., Anshebo S.T., Sabir F.K., Workineh G.A. (2021): Removal of methylene blue dye from wastewater using periodiated modified nanocellulose. Int. J. Chem. Eng. 2021, 9965452.

Kenneke J.F., McCutcheon S.C. (2003): Use of pretreatment zones and zero-valent iron for the remediation of chloroalkenes in an oxic aquifer. Environ. Sci. Technol. 37, 2829–2835.

Kim J.S., Shea P.J., Yang J.E., Kim J.E. (2007): Halide salts accelerate degradation of high explosives by zerovalent iron. Environ. Pollut. 147, 634–641.

King D.W. (1998): Role of carbonate speciation on the oxidation rate of Fe(II) in aquatic systems. Environ. Sci. Technol. 32, 2997–3003.

Klausen J., Ranke J., Schwarzenbach R.P. (2001): Influence of solution composition and column aging on the reduction of nitroaromatic compounds by zerovalent iron. Chemosphere 44, 511–517.

Klausen J., Vikesland P.J., Kohn T., Burris D.R., Ball W.P., Roberts A.L. (2003): Longevity of granular iron in groundwater treatment processes: Solution composition effects on reduction of organohalides and nitroaromatic compounds. Environ. Sci. Technol. 37, 1208–1218.

Konadu-Amoah B. (2023): Decontamination in Fe^0-based systems: Understanding phosphate removal in Fe^0/H_2O system using the MB method. PhD Dissertation, Hohai University, Najing, China.

Konadu-Amoah B., Hu R., Cui X., Tao R., Ndé-Tchoupé A.I., Gwenzi W., Noubactep C. (2023): Characterizing the process of phosphate removal in Fe^0/H_2O systems. Chem. Eng. J. 465, 143042.

Konadu-Amoah B., Ndé-Tchoupé A.I., Hu R., Gwenzi W., Noubactep C. (2022): Investigating the Fe^0/H_2O systems using the methylene blue method: Validity, applications and future directions. Chemosphere 291, 132913.

Kosmulski M. (2016): Isoelectric points and points of zero charge of metal (hydr)oxides: 50 years after Parks' review. Adv. Colloid Interface Sci. 238, 1–61.

Koutsoumpeli E., Murray J., Langford D., Bon R.S., Johnson S. (2015): Probing molecular interactions with methylene blue derivatized self-assembled monolayers. Sensing and Bio-Sensing Research 6, 1–6.

Lauderdale R.A., Emmons A.H. (1951): A method for decontaminating small volumes of radioactive water. Journal American Water Works Association 43, 327–331.

Lawrinenko M., Kurwadkar S., Wilkin R.T. (2023a): Long–term performance evaluation of zero-valent iron amended permeable reactive barriers for groundwater remediation – A mechanistic approach. Geosci. Front. 14, 101494.

Lawrinenko M., Kurwadkar S., Wilkin R.T. (2023b): Reply to comment by C. Noubactep on "Long-term performance evaluation of zero-valent iron amended permeable reactive barriers for groundwater remediation: A mechanistic approach". Geosci. Front. 14, 101583.

Le C., Wu J.H., Deng S.B., Li P., Wang X.D., Zhu N.W., Wu P.X. (2011): Effects of common dissolved anions on the reduction of para-chloronitrobenzene by zero-valent iron in groundwater. Water Sci. Technol. 63, 1485–1490.

Leaist D.G. (1988): The effects of aggregation, counterion binding, and added NaCl on diffusion of aqueous methylene blue. Can. J. Chem. 66, 2452–2457.

Lee G., Rho S., Jahng D. (2004): Design considerations for groundwater remediation using reduced metals. Korean J. Chem. Eng. 21, 621–628.

Li H., Wan J., Ma Y., Wang Y., Guan Z. (2015): Role of inorganic ions and dissolved natural organic matters on persulfate oxidation of acid orange 7 with zero-valent iron. RSC Adv. 5, 99935–99943.

Li J.; Dou X.; Qin H.; Sun Y.; Yin D.; Guan X. (2019): Characterization methods of zerovalent iron for water treatment and remediation. Water Res. 148, 70–85.

Li L., Benson C.H. (2010): Evaluation of five strategies to limit the impact of fouling in permeable reactive barriers. J. Hazard. Mater. 181, 170–180.

Li L., Benson C.H., Lawson E.M. (2005): Impact of mineral fouling on hydraulic behavior of permeable reactive barriers. Ground Water 43, 582– 596.

Li L., Benson C.H., Lawson E.M. (2006): Modeling porosity reductions caused by mineral fouling in continuous-wall permeable reactive barriers, J. Contam. Hydrol. 83, 89–121,

Li S., Ding Y., Wang W., Lei H. (2016): A facile method for determining the Fe(0) content and reactivity of zero valent iron. Anal. Methods 8, 1239–1248.

Liger E., Charlet L., van Cappellen P. (1999): Surface catalysis of uranium(VI) reduction by iron(II). Geochim. Cosmochim. Acta 63, 2939–2955.

Lim T.T., Zhu B.W. (2008): Effects of anions on the kinetics and reactivity of nanoscale Pd/Fe in trichlorobenzene dechlorination. Chemosphere 73, 1471–1477.

Lipczynska-Kochany E., Harms S., Milburn R., Sprah G., Nadarajah N. (1994): Degradation of carbon tetrachloride in the presence of iron and sulphur containing compounds. Chemosphere 29, 1477–1489.

Liu Y.Q., Phenrat T., Lowry G.V. (2007): Effect of TCE concentration and dissolved groundwater solutes on NZVI-promoted TCE dechlorination and H_2 evolution. Environ. Sci. Technol. 41, 7881–7887.

Lu J., Zhou Z., Zhou Y. (2023): Recent advance in enhanced adsorption of ionic dyes from aqueous solution: A review, Crit. Rev. Environ. Sci. Technol. 53, 1709–1730.

Lü Y., Li J., Li Y., Liang L., Dong H., Chen K., Yao C., Li Z., Li J., Guan X. (2019): The roles of pyrite for enhancing reductive removal of nitrobenzene by zero-valent iron. Appl. Catal. B Environ. 242, 9–18.

Lü Y., Li Z., Li J., Chen K., Dong H., Shou J., Li Y. (2018): Synergetic effect of pyrite on Cr(VI) removal by zero valent iron in column experiments: an investigation of mechanisms. Chem Eng J 349, 522–529.

Lufingo M., Ndé-Tchoupé A.I., Hu R., Njau K.N., Noubactep C. (2019): A novel and facile method to characterize the suitability of metallic iron for water treatment. Water 11, 2465.

Luo P., Bailey E.H., Mooney S.J. (2013): Quantification of changes in zero valent iron morphology using X-ray computed tomography. J. Environ. Sci. 25, 2344–2351.

Makota S., Ndé-Tchoupé A.I., Mwakabona H.T., Tepong-Tsindé R., Noubactep C., Nassi A., Njau K.N. (2017): Metallic iron for water treatment: Leaving the valley of confusion. Appl. Water Sci. 7, 4177–4196.

Manoko M.C., Chirwa E.M., Makgopa K. (2022): Non-demineralized paper waste sludge derived magnetic biochar as sorbs for removal of methylene blue, phosphorus, and selenate in wastewater. Clean. Chem. Eng. 3, 100048.

Marwa J., Lufingo M., Noubactep C., Machunda R. (2018): Defeating fluorosis in the East African Rift Valley: Transforming the Kilimanjaro into a rainwater harvesting park. Sustainability 10, 4194.

Matheson L.J., Tratnyek P. (1994): Reductive dehalogenation of chlorinated methanes by iron metal. Environ. Sci. Technol. 28, 2045–2053.

McCreery R.L. (2008): Advanced carbon electrode materials for molecular electrochemistry. Chem. Rev. 108, 2646–2687.

McGeough K.L., Kalin R.M., Myles P. (2007): Carbon disulfide removal by zero valent iron. Environ. Sci. Technol. 41, 4607–4612.

McGuire M.M., Carlson D.L., Vikesland P.J., Kohn T., Grenier A.C., Langley L.A., Roberts A.L., Fairbrother D.H. (2003): Applications of surface analysis in the environmental sciences: dehalogenation of chlorocarbons with zero-valent iron and iron-containing mineral surfaces. Anal. Chim. Acta 496, 301–313.

Melchers R.E., Petersen R.B. (2018): A reinterpretation of the Romanoff NBS data for corrosion of steels in soils, Corros. Eng. Sci. Technol. 53, 131–140.

Mettler S., Wolthers M., Charlet L., von Gunten U. (2009): Sorption and catalytic oxidation of Fe(II) at the surface of calcite. Geochim. Cosmochim. Acta 73, 1826 –1840.

Miehr, R.; Tratnyek, G.P.; Bandstra, Z.J.; Scherer, M.M.; Alowitz, J.M.; Bylaska, J.E. (2004): Diversity of contaminant reduction reactions by zerovalent iron: Role of the reductate. Environ. Sci. Technol. 38, 139–147.

Mitchell G., Poole P., Segrove H.D. (1955): Adsorption of methylene blue by high-silica sands. Nature 176, 1025–1026.

Miyajima K. (2012): Optimizing the design of metallic iron filters for water treatment. Freiberg Online Geosci. 32, 1–60.

Miyajima K., Noubactep C. (2012): Effects of mixing granular iron with sand on the efficiency of methylene blue discoloration. Chem. Eng. J. 200–202, 433–438.

Miyajima K., Noubactep C. (2013): Impact of Fe^0 amendment on methylene blue discoloration by sand columns. Chem. Eng. J. 217, 310–319.

Miyajima K., Noubactep C. (2015): Characterizing the impact of sand addition on the efficiency of granular iron for water treatment. Chem. Eng. J. 262, 891–896.

Moraci N., Calabrò P.S. (2010): Heavy metals removal and hydraulic performance in zero-valent iron/pumice permeable reactive barriers. J. Environ. Manage. 91, 2336–2341.

Moraci N., Lelo D., Bilardi S., Calabrò P.S. (2016): Modelling long-term hydraulic conductivity behaviour of zero valent iron column tests for permeable reactive barrier design. Canadian Geotech. J. 53, 946–961.

Mos Y.M., Zorzano K.B., Buisman C.J., Weijma J. (2018): Magnetite synthesis from ferrous iron solution at pH 6.8 in a continuous stirred tank reactor. Water Sci. Technol. 77, 1870–1878.

Mueller B., Chan M.C.K., Hug S.J. (2023): Unique geochemistry of arsenic-contaminated groundwater and corresponding mitigation efforts in Southern Nepal. ACS EST Water 3, 1527–1535.

Mwakabona H.T., Ndé-Tchoupé A.I., Njau K.N., Noubactep C., Wydra K.D. (2017): Metallic iron for safe drinking water provision: Considering a lost knowledge. Water Res. 117, 127–142.

Naidu R., Bekele D.N., Birke V. (2014): Permeable reactive barriers: cost-effective and sustainable remediation of groundwater. In: Naidu, R., Birke, V. (Eds.), Permeable Reactive Barrier: Sustainable Groundwater Remediation. CRC Press, Boca Raton, Florida, U.S.A, pp. 1–23 https://doi.org/10.1201/9781351228886-1.

Naka D., Kim D., Carbonaro R.F., Strathmann T.J. (2008): Abiotic reduction of nitroaromatic contaminants by iron(II) complexes with organothiol ligands. Environ. Toxicol. Chem. 27, 1257–1266.

Naseri E., Ndé-Tchoupé A.I., Mwakabona H.T., Nanseu-Njiki C.P., Noubactep C., Njau K.N., Wydra K.D. (2017): Making Fe^0-based filters a universal solution for safe drinking water provision. Sustainability 9, 1224.

Ndé-Tchoupé A.I, Makota S., Nassi A., Hu R., Noubactep C. (2018): The suitability of pozzolan as admixing aggregate for Fe0-based filters. Water 10, 417.

Ndé-Tchoupé A.I., Crane R.A., Hezron T. Mwakabona, Noubactep C., Njau K.N. (2015): Technologies for decentralized fluoride removal: Testing metallic iron based filters. Water 7, 6750–6774.

Ndé-Tchoupé A.I., Hu R., Gwenzi W., Nassi A., Noubactep C. (2020): Characterizing the reactivity of metallic iron for water treatment: H_2 evolution in H_2SO_4 and uranium removal efficiency. Water 12, 1523.

Ndé-Tchoupé A.I., Nanseu-Njiki C.P., Hu R., Nassi A., Noubactep C., Licha T. (2019): Characterizing the reactivity of metallic iron for water defluoridation in batch studies. Chemosphere 219, 855–863.

Ndé-Tchoupé, A.I.; Konadu-Amoah, B.; Gatcha-Bandjun, N.; Hu, R.; Gwenzi, W.; Noubactep, C. (2022): Kanchan arsenic filters for household water treatment: Unsuitable or unsustainable? Water 14, 2318.

Nesic S. (2007): Key issues related to modelling of internal corrosion of oil and gas pipelines – A review. Corros. Sci. 49, 4308–4338.

Noubactep C. (2007): Processes of contaminant removal in "Fe^0–H_2O" systems revisited. The importance of co-precipitation. Open Environ. Sci. 1, 9–13.

Noubactep C. (2008): A critical review on the mechanism of contaminant removal in Fe^0–H_2O systems. Environ. Technol. 29, 909–920.

Noubactep C. (2009a): Characterizing the effects of shaking intensity on the kinetics of metallic iron dissolution in EDTA. J. Hazard. Mater. 170, 1149–1155.

Noubactep C. (2009c): An analysis of the evolution of reactive species in Fe^0/H_2O systems. J. Hazard. Mater. 168, 1626–1631.

Noubactep C. (2010): Metallic iron for safe drinking water worldwide. Chem. Eng. J. 165, 740–749.

Noubactep C. (2011a): Aqueous contaminant removal by metallic iron: Is the paradigm shifting? Water SA 37, 419–426.

Noubactep C. (2011b): Metallic iron for safe drinking water production. Freiberg Online Geosci. 27, 1–38.

Noubactep C. (2012): Investigating the processes of contaminant removal in Fe^0/H_2O systems. Korean J. Chem. Eng. 29, 1050–1056.

Noubactep C. (2013a): Metallic iron for environmental remediation: the long walk to evidence. Corros. Rev. 31, 51–59.

Noubactep C. (2013b): Metallic iron for water treatment: A critical review. Clean - Soil, Air, Water 41, 702–710.

Noubactep C. (2013c): Relevant reducing agents in remediation Fe^0/H_2O systems. Clean – Soil, Air, Water 41, 493–502.

Noubactep C. (2013d): Water remediation by metallic iron: Much ado about nothing - As profitless as water in a sieve? Clean - Soil, Air, Water 42, 1177–1178.

Noubactep C. (2014): Flaws in the design of Fe(0)-based filtration systems? Chemosphere 117, 104–107.

Noubactep C. (2015): Metallic iron for environmental remediation: a review of reviews. Water Res. 85, 114–123.

Noubactep C. (2016a): Predicting the hydraulic conductivity of metallic iron filters: Modeling gone astray. Water 8, 162.

Noubactep C. (2016b): Research on metallic iron for environmental remediation: Stopping growing sloppy science. Chemosphere 153, 528–530.

Noubactep C. (2016c): No scientific debate in the zero-valent iron literature. Clean – Soil, Air, Water 44, 330–332.

Noubactep C. (2016d): Designing metallic iron packed-beds for water treatment: A critical review. Clean – Soil, Air, Water 44, 411–421.

Noubactep C. (2018a): Metallic iron (Fe^0) provide possible solution to universal safe drinking water provision. J. Water Technol. Treat. Mthods. 1(1):102.

Noubactep C. (2018b): Metallic iron for environmental remediation: How experts maintain a comfortable status quo. Fresenius Environ. Bull. 27, 1379–1393.

Noubactep C. (2019): The operating mode of Fe^0/H_2O systems: Hidden truth or repeated nonsense? Fresenius Environ. Bull. 28, 8328–8330.

Noubactep C. (2020): Metallic Iron for Environmental Remediation: Prospects and Limitations. Chap. 36, A Handbook of Environmental Toxicology: Human Disorders and Ecotoxicology. J.P.F. D’Mello (ed), CAB International, 531–544.

Noubactep C. (2021): Metallic iron for the removal of metals and metalloids from aqueous solutions: An old-timer view. Curr. Opin. Environ. Sci. Health 22, 100256.

Noubactep C. (2023): Comments on "Long-term performance evaluation of zero-valent iron amended permeable reactive barriers for groundwater remediation: A mechanistic approach" by Lawrinenko et al., Geoscience Frontiers 14 (2023) 101494, Geosci. Front. 14, 101582.

Noubactep C. (2024): Metallic iron for decentralized safe drinking water supply: Self-reliance is possible. In: "Advances in drinking water purification: Small systems and emerging issues", Bandyopadhyay S. (Ed.), Elsevier, Amsterdam, Netherlands, 231–251.

Noubactep C., Caré S. (2010a): Dimensioning metallic iron beds for efficient contaminant removal. Chem. Eng. J. 163, 454–460.

Noubactep C., Caré S. (2010b): Enhancing sustainability of household water filters by mixing metallic iron with porous materials. Chem. Eng. J. 162, 635–642.

Noubactep C., Licha T., Scott T.B., Fall M., Sauter M. (2009b): Exploring the influence of operational parameters on the reactivity of elemental iron materials. J. Hazard. Mater. 172, 943–951.

Noubactep C., Makota S., Bandyopadhyay A. (2017): Rescuing Fe^0 remediation research from its systemic flaws. Res. Rev. Insights 1, 1–8.

Noubactep C., Meinrath G., Dietrich P., Merkel B. (2003): Mitigating uranium in groundwater: Prospects and limitations. Environ. Sci. Technol. 37, 4304–4308.

Noubactep C., Meinrath G., Dietrich P., Sauter M., Merkel B. (2005a): Testing the suitability of zerovalent iron materials for reactive Walls. Environ. Chem. 2, 71–76.

Noubactep C., Meinrath G., Merkel J. B. (2005b): Investigating the mechanism of uranium removal by zerovalent iron materials. Environ. Chem. 2, 235–242.

Noubactep C., Schöner A. (2010): Metallic iron: dawn of a new era of drinking water treatment research? Fresenius Envi-ron. Bull. 19, 1661–1668.

Noubactep C., Schöner A., Meinrath G. (2006): Mechanism of uranium (VI) fixation by elemental iron. J. Hazard Mater. 132, 202–212.

Noubactep C., Schöner A., Woafo P. (2009): Metallic iron filters for universal access to safe drinking water. Clean: Soil Air Water 37, 930–937.

Nurmawati A., Wahyusi K.N., Dewati R., Hilmy J. (2022): The effect of velocity gradient and camp number on solids removal using bio-coagulant from corbula faba hinds shells. Int. J. Eco-Innov. Sci. Eng. 3, 15–20.

Oldright G.L., Keyes H.E., Miller V., Sloan W.A. (1928): Precipitation of lead and copper from solution on sponge iron. BuMines B 281, 131 pp.

Parks G.A. (1965): The isoelectric points of solid oxides, solid hydroxides, and aqueous hydroxo complex systems. Chem. Rev. 65,177–198.

Patrick M., Sahu O. (2023): Origins, mechanisms, and remedies of fluoride ions from ground and surface water: A Review. Chemistry Africa, https://doi.org/10.1007/s42250-023-00694-4.

Pavelková A., Stejskal V., Vološčuková O., Nosek J. (2020): Cost-effective remediation using microscale ZVI: Comparison of commercially available products. Ecol. Chem. Eng. S. 27, 211–224.

Phukan M. (2015): Characterizing the Fe^0/sand system by the extent of dye discoloration. Freiberg Online Geosci. 40, 1–70.

Phukan M., Noubactep C., Licha T. (2015): Characterizing the ion-selective nature of Fe^0-based filters using azo dyes. Chem. Eng. J. 259, 481–491.

Phukan M., Noubactep C., Licha T. (2016): Characterizing the ion-selective nature of Fe0-based filters using three azo dyes in batch systems. Journal of Environmental Chemical Engineering 4, 65–72.

Pilling N.B., Bedworth R.E. (1923): The oxidation of metals at high temperatures. J. Inst. Metals, 29 529–591.

Plessl K., Russ A., Vollprecht D. (2023): Application and development of zero-valent iron (ZVI) for groundwater and wastewater treatment. Int. J. Environ. Sci. Technol. 20, 6913–6928.

Polasek P. (2007): Differentiation between different kinds of mixing in water purification – Back to basics. Water SA 33, 249–251.

Polasek P. (2007): Differentiation between different kinds of mixing in water purification – Back to basics. Water SA 33, 249–251.

Polasek P. (2011): Influence of velocity gradient on optimisation of the aggregation process and physical properties of formed aggregates. J. Hydrol. Hydromech. 59, 107–117.

Pujar G. (2022): Reduction of methylene blue dye from aqueous solution using zero valent iron. Int. Res. J. Eng. Technol. 9, 3036–3039.

Pullin H., Crane R.A., Morgan D.J., Scott T.B. (2017): The effect of common groundwater anions on the aqueous corrosion of zero-valent iron nanoparticles and associated removal of aqueous copper and zinc. J. Environ. Chem. Eng. 5, 1166–1173.

Raghav M., Saez A.E., Ela W.P. (2015): Understanding abiotic ferrihydrite re-mineralization by ferrous ions. Int. J. Environ. Sci. Technol. 12, 1945–1956.

Rahman M.A., Karmakar S., Salama H., Gactha-Bandjun N., Btatkeu K. B.D., Noubactep C. (2013): Optimising the design of Fe^0-based filtration systems for water treatment: The suitability of porous iron composites. J. Appl. Solution Chem. Modeling 2, 165–177.

Ranjan, S.P.; Kazama, S.; Sawamoto, M. (2006): Effects of climate and land use changes on groundwater resources in coastal aquifers. J. Environ. Manag. 80, 25–35.

Rao P., Mak M.S.H., Liu T., Lai K.C.K., Lo I.M.C. (2009): Effects of humic acid on arsenic(V) removal by zero-valent iron from groundwater with special references to corrosion products analyses. Chemosphere 75, 156–162.

Reardon E.J. (2005): Zerovalent irons: Styles of corrosion and inorganic control on hydrogen pressure buildup. Environ. Sci. Tchnol. 39, 7311–7317.

Reardon J.E. (1995): Anaerobic corrosion of granular iron: Measurement and interpretation of hydrogen evolution rates. Environ. Sci. Technol. 29, 2936–2945.

Reynolds G.W., Hoff J.T., Gillham R.W. (1990): Sampling bias caused by materials used to monitor halocarbons in groundwater. Environ. Sci. Technol. 24, 135–142.

Richardson J.P., Nicklow J.W. (2002): In situ permeable reactive barriers for groundwater contamination. Soil and Sediment Contamination 11, 241–268.

Roccamante M., Ruiz-Delgado A., Cabrera-Reina A., Oller I., Malato S., Miralles-Cuevas S. (2022): Removal of microcontaminants by zero-valent iron solar processes at natural pH: Water matrix and oxidant agents effect. Sci. Tot. Environ. 819, 153152.

Rose J., Flank A.-M., Masion A., Bottero J.-Y., Elmerich P. (1997a): Nucleation and growth mechanisms of Fe oxyhydroxide in the presence of PO_4 ions. 2. P K-Edge EXAFS Study. Langmuir 13, 1827–1834.

Rose J., Manceau A., Bottero J.-Y., Masion A., Garcia F. (1996): Nucleation and growth mechanisms of Fe oxyhydroxide in the presence of PO_4 Ions. 1. Fe K-Edge EXAFS Study. Langmuir 12, 6701–6707.

Rose J., Manceau A., Masion A., Bottero J.-Y. (1997b): Structure and mechanisms of formation of FeOOH(NO_3) oligomers in the early stages of hydrolysis. Langmuir 13, 3240–3246.

Ruhl A.S., Ünal N., Jekel M. (2012): Evaluation of two-component Fe(0) fixed bed filters with porous materials for reductive dechlorination. Chem. Eng. J. 209, 401–406.

Saadatpour M., Goeini M., Afshar A., Shahmirnoori A. (2023): A preliminary approach based on numerical simulation modelling and evaluation of permeable reactive barrier for aquifer remediation susceptible to selenium contaminant. J. Environ. Manage. 331, 117242.

Santisukkasaem U., Das D.B. (2019): A non-dimensional analysis of permeability loss in zero-valent iron permeable reactive barrier (PRB). Transp. Porous Media 126, 139–159.

Santisukkasaem U., Olawuyi F., Oye P., Das D.B. (2015): Artificial Neural Network (ANN) for evaluating permeability decline in permeable reactive barrier (PRB). Environ. Process. 2, 291–307.

Sarr D. (2001): Zero-valent-iron permeable reactive barriers - how long will they last? Remediation 11, 1–18.

Saywell L.G., Cunningham B.B. (1937): Determination of iron: colorimetric o-phenanthroline method. Ind. Eng. Chem. Anal. Ed. 9, 67–69.

Scherer M.M., Richter S., Valentine R.L., Alvarez P.J.J. (2000): Chemistry and microbiology of permeable reactive barriers for in situ groundwater clean-up. Rev. Environ. Sci. Technol. 30, 363–411.

Scott T.B., Popescu I.C., Crane R.A., Noubactep C. (2011): Nano-scale metallic iron for the treatment of solutions containing multiple inorganic contaminants. J. Hazard. Mater. 186, 280–287.

Sedláček P., Smilek J., Klučáková M. (2013): How the interactions with humic acids affect the mobility of ionic dyes in hydrogels – Results from diffusion cells. Reactive & Functional Polymers 73, 1500–1509.

Sedláček P., Smilek J., Klučáková M. (2014): How the interactions with humic acids affect the mobility of ionic dyes in hydrogels–2. Non-stationary diffusion experiments. Reactive & Functional Polymers 75, 41–50.

Seng S., Tabelin C.B., Kojima M., Hiroyoshi N., Ito M. (2019): Galvanic microencapsulation (GME) using zero-valent aluminum and zero-valent iron to suppress pyrite oxidation. Mater. Trans. 60, 277–286.

Sikora E., Macdonald D.D. (2000): The passivity of iron in the presence of ethylenediaminetetraacetic acid I. General electrochemical behavior. J. Electrochem. Soc. 147, 4087–4092.

Singh R., Chakma S., Birke V. (2023): Performance of field-scale permeable reactive barriers: An overview on potentials and possible implications for in-situ groundwater remediation applications, Sci. Tot. Environ. 858, 158838.

Song D.-I., Kim Y.H., Shin W.S. (2005): A simple mathematical analysis on the effect of sand in Cr(VI) reduction using zero valent iron. Korean J. Chem. Eng. 22, 67–69.

Song X., Chen Z., Wang X., Zhang S. (2017): Ligand effects on nitrate reduction by zero-valent iron: Role of surface complexation. Water Res. 114, 218–227.

Stieber M., Putschew A., Jekel M. (2011): Treatment of pharmaceuticals and diagnostic agents using zero-valent iron–kinetic studies and assessment of transformation products assay. Environ. Sci. Technol. 45, 4944–4950.

Su C., Puls R.W. (2001): Arsenate and arsenite removal by zerovalent iron: Effects of phosphate, silicate, carbonate, borate, sulfate, chromate, molybdate and nitrate, relative to chloride. Environ. Sci. Technol. 35, 4562–4568.

Su C., Puls R.W. (2004): Nitrate reduction by zerovalent iron: Effects of formate, oxalate, citrate, chloride, sulfate, borate and phosphate. Environ. Sci. Technol. 38, 2715–2720.

Sun S., Xu X., Jiang X., Yue Y., Dai Y., Yang X., Xiu Q., Duan L., Zhao S. (2023): Unveiling the neglected roles of chloride and sulfate in the removal of nitro compounds by sulfidated zero-valent iron/ferrous ion systems. ACS ES&T Water 3, 1212–1222.

Sun X., Kurokawa T., Suzuki M., Takagi M., Kawase Y. (2015): Removal of cationic dye methylene blue by zero-valent iron: Effects of pH and dissolved oxygen on removal mechanisms. J. Environ. Sci. Health Part A 50, 1057–1071.

Sun Y., Li J., Huang T., Guan X. (2016): The influences of iron characteristics, operating conditions and solution chemistry on contaminants removal by zero-valent iron: A review. Water Res. 100, 277–295.

Sun Y.-P., Li X., Cao J., Zhang W.-x., Wang H.P. (2006): Characterization of zero-valent iron nanoparticles. Adv. Colloid Interface Sci. 120, 47–56

Tabelin C.B., Park I., Li X., Seng S., Villacorte-Tabelin M., Igarashi T., Ito M., Hiroyoshi N. (2019): Development of ad-vanced pyrite passivation strategies towards sustainable management of acid mine drainage. IOP Conf. Ser.: Earth Envi-ron. Sci.351, 012010.

Tao R., Cui X., Xiao M., Hu R., Gwenzi W., Ruppert H., Noubactep C. (2023): Influence of water salinity on the efficiency of Fe^0-based systems for water treatment. Water 15, 2466.

Tao R., Hu R., Gwenzi W., Ruppert H., Noubactep C. (2024): Effects of common dissolved anions on the efficiency of Fe^0-based remediation systems. Journal of Environmental Management. (Submitted).

Tao R., Yang H., Cui X., Xiao M., Gatcha-Bandjun N., Kenmogne-Tchidjo J.F., Lufingo M., Konadu-Amoah B., Tepong-Tsindé R., Ndé-Tchoupé A.I., Touomo-Wouafo M., Btatkeu-K B.D., Gwenzi W., Hu R., Tchatchueng J.B., Ruppert H., Noubactep C. (2022): The suitability of hybrid Fe^0/aggregate filtration systems for water treatment. Water 14, 260.

Tepong-Tsindé R. (2021): Designing and Piloting a household filter for the peri-urban population of Douala (Cameroon). Freiberg Online Geosci. 61, 1–80.

Tepong-Tsindé R., Ndé-Tchoupé A.I., Noubactep C., Nassi A., Ruppert H. (2019): Characterizing a newly designed steel-wool-based household filter for safe drinking water provision: Hydraulic conductivity and efficiency for pathogen re-moval. Processes 7, 966.

Tepong-Tsindé R., Phukan M., Nassi A., Noubactep C., Ruppert H. (2015): Validating the efficiency of the MB discoloration method for the characterization of Fe^0/H_2O systems using accelerated corrosion by chloride ions. Chem. Eng. J. 279, 353–362.

Touomo-Wouafo M., Donkeng-Dazie J., Jirka I., Btatkeu-K B.D., Tchatchueng J.B., Noubactep C., Ludvík J. (2020): Electrochemical monitoring of metal ions removal in Fe^0/H_2O systems: competitive effects of cations Zn^{2+}, Pb^{2+}, and Cd^{2+}. Monatshefte für Chemie-Chemical Monthly 151, 1511–1523.

Trinh B.-S., Le P.T., Werner D., Phuong N.H., Luu T.L. (2019): Rice husk biochars modified with magnetized iron oxides and nano zero valent iron for decolorization of dyeing wastewater. Processes 7, 660.

Tsamo C., Meali D.S., Assaouka H.T. (2018): Studying the impact of anions pregenerated iron corrosion products on the efficiency of contaminant removal in Fe^0/H_2O systems. J. Environ. Sci. Eng. B7, 1e10.

Tseng H.H., Su J.G., Liang C. (2011): Synthesis of granular activated carbon/zero valent iron composites for simultane-ous adsorption/dechlorination of trichloroethylene. J Hazard Mater. 30, 192, 500-506.

Velimirovic M., Auffan M., Carniato L., Batka V.M., Schmid D., Wagner S., Borschneck D., Proux O., von der Kammer F., Hofmann T. (2018): Effect of field site hydrogeochemical conditions on the corrosion of milled zerovalent iron particles and their dechlorination efficiency. Sci. Tot. Environ. 618, 1619–1627.

Vidic R.D., Suidan M.T., Traegner U.K., Nakhla G.F. (1990): Adsorption isotherms: illusive capacity and role of oxygen. War. Res. 24, 1187–1195.

Wakatsuki T., Esumi H., Omura S. (1993): High performance and N, P removable on-site domestic wastewater treatment system by multi-soil-layering method. Water Sci. Technol. 27, 31–40.

Wang Y., Zhao Y., Liu Y. (2021): Effect of solution chemistry on aqueous As(III) removal by titanium salts coagulation. Environ. Sci. Pollut. Res. 28, 21823–21834.

Weber E.J. (1996): Iron-mediated reductive transformations: investigation of reaction mechanism. Environ. Sci. Technol. 30, 716–719.

Werner J. (1959): Amination by Reduction. Ind. Eng. Chem. 51 (9), 1065–1066.

Westerhoff P. (2003): Reduction of nitrate, bromate, and chlorate by zero valent iron (Fe^0). J. Environ. Eng. 129, 10–16.

Westerhoff P., James J. (2003): Nitrate removal in zero-valent iron packed columns. Water Res. 37, 1818–1830.

White A.F., Peterson M.L. (1996): Reduction of aqueous transition metal species on the surfaces of Fe(II)-containing oxides. Geochim. Cosmochim. Acta 60, 3799–3814.

Whitman G.W., Russel R.P., Altieri V.J. (1924): Effect of hydrogen-ion concentration on the submerged corrosion of steel. Indust. Eng. Chem. 16, 665–670.

Whitney W.R. (1903): The corrosion of iron. J. Am. Chem. Soc. 25, 4, 394–406.

Whitney W.R. (1947): The corrosion of iron. Corrosion 3, 331–340.

Wielinski J., Jimenez-Martinez J., Göttlicher J., Steininger R., Mangold S., Hug S.J., Berg M., Voegelin A. (2022): Spatiotemporal mineral phase evolution and arsenic retention in microfluidic models of zerovalent iron-based water treatment. Environ. Sci. Technol. 56, 13696−13708.

Wilkin R.T., Puls R.W., Sewell G.W. (2002): Long-term performance of permeable reactive barriers using zero-valent iron: An evaluation at two sites. EPA 600-S-02-001, Environmental Research Brief. United States Environmental Protection Agency, Cincinnati, Ohio.

Wilkin R.T., Puls R.W., Sewell G.W. (2003): Long-term performance of permeable reactive barriers using zero-valent iron: geochemical and microbiological effects. Ground Water 41, 493–503.

Wilopo W., Sasaki K., Hirajima T. (2010): Contribution of sheep manurebacteria in the immobilization ofarsenic from groundwater usingzero-valent iron. J. SE Asian Appl. Geol. 2, 1–11.

Wolfe N.L., Cipollone M.G. (2001): Remediation of environmental contaminants using a metal and a sulfur-containing compound. US Patent US6207073B1.

Worch E. (2012): Adsorption Technology in Water Treatment. Walter de Gruyter GmbH & Co. KG, Berlin/Boston, 345 pp.

Wu Q., Zheng C., Zhang J., Zhang F. (2017): Nitrate removal by a permeable reactive barrier of Fe^0: A model-based evaluation. J. Earth Sci. 28, 447–456.

Xiao M., Cui X., Hu R., Gwenzi W., Noubactep C. (2020a): Validating the efficiency of the FeS_2 method for elucidating the mechanisms of contaminant removal using Fe^0/H_2O systems. Processes 8, 1162.

Xiao M., Hu R., Cui X., Gwenzi W., Noubactep C. (2020b): Understanding the operating mode of Fe^0/Fe-sulfide/H_2O systems for water treatment. Processes 8, 409.

Xiao M., Hu R., Gwenzi W., Tao R., Cui X., Yang H., Noubactep C. (2024): Designing sustainable Fe0–based water filters: The crucial role of material selection. Environ. Chem. Lett. (ECLE-D-23-01068, in revision).

Xiao M., Hu R., Tao R., Cui X., Konadu-Amoah B., Yang H., Ndé-Tchoupé A.I., Gwenzi W., Noubactep C., Ruppert H. (2023): Metallic iron for environmental remediation: The still overlooked iron chemistry. Appl. Water Sci. 13, 222.

Xie L., Shang C. (2007): The effects of operational parameters and common anions on the reactivity of zero-valent iron in bromate reduction. Chemosphere 66, 1652–1659.

Xie L., Shang C. (2007): The effects of operational parameters and common anions on the reactivity of zero-valent iron in bromate reduction. Chemosphere 66, 1652–1659.

Xin J., Tang F., Yan J., La C., Zheng X., Liu W. (2018): Investigating the efficiency of microscale zero valent iron-based in situ reactive zone (mZVI-IRZ) for TCE removal in fresh and saline groundwater. Sci. Total Environ. 626, 638–649.

Xin J., Tang F., Zheng X., Shao H., Koldito O., Lu X. (2016): Distinct kinetics and mechanisms of mZVI particles aging in saline and fresh groundwater: H_2 evolution and surface passivation. Water Res. 100, 80–87.

Yadav A., Kumari N., Kumar R., Kumar M., Yadav S. (2023): Fluoride distribution, contamination, toxicological effects and remedial measures: a review. Sustain. Water Resour. Manag. 9, 150.

Yang H. (2022): Modelling the porosity loss of metallic iron beds for water treatment. PhD Dissertation, University of Göttingen, Germany.

Yang H., Hu R., Ndé-Tchoupé A.I., Gwenzi W., Ruppert H., Noubactep C. (2020): Designing the next generation of Fe^0-based filters for decentralized safe drinking water treatment. Processes 8, 745.

Yang H., Hu R., Ruppert H., Noubactep C. (2021): Modeling porosity loss in Fe^0-based permeable reactive barriers with Faraday’s law. Sci. Rep. 11, 16998.

Yang H., Liu Q., Hu R., Ptak T., Taherdangkoo R., Liu Y., Noubactep C. (2022). Numerical case studies on long-term effectiveness of metallic iron based permeable reactive barriers: Importance of porosity heterogeneity of the barrier. Journal of Hydrology, 612, 128148.

Yang J.E., Kim J.S., Ok Y.S., Kim S.J., Yoo K.Y. (2006): Capacity of Cr (VI) reduction in an aqueous solution using different sources of zerovalent irons. Korean J. Chem. Eng. 23, 935–939.

Yin W., Wu J., Li P. (2012): Experimental study of zero-valent iron induced nitrobenzene reduction in groundwater: The effects of pH, iron dosage, oxygen and common dissolved anions. Chem. Eng. J. 184, 198– 204.

You Y., Han J., Chiu P.C., Jin Y. (2005): Removal and inactivation of waterborne viruses using zerovalent iron. Environ. Sci. Technol. 39, 9263–9269.

Yu J., Liu W.X., Zeng A.B., Guan B.H., Xu X.H. (2013): Effect of SO on 1,1,1-trichloroethane degradation by Fe^0 in aqueous solution. Ground Water 51, 286–292.

Yu Y., Root R.A., Sierra-Alvarez R., et al. (2023): Treatment of the insensitive munitions compound, 3-nitro-1,2,4-triazol-5-one (NTO), in flow-through columns packed with zero-valent iron. Environ. Sci. Pollut. Res. 30, 64606–64616.

Zawaideh L.L., Zhang T.C. (1998): The effects of pH and addition of an organic buffer (HEPES) on nitrate transformation in Fe0-water systems. Water Sci. Technol. 38, 107–115.

Zeghioud H., Mouhamadou S. (2023): Dye removal characteristics of magnetic biochar derived from sewage sludge: Isotherm, thermodynamics, kinetics, and mechanism. Water Air Soil Pollut. 234, 233.

Zeng H., Qi W., Zhai L., Wang F., Zhang J., Li D. (2021a): Magnetic biochar synthesized with waterworks sludge and sewage sludge and its potential for methylene blue removal. J. Environ. Chem. Eng. 9, 105951.

Zeng H., Qi W., Zhai L., Wang F., Zhang J., Li D. (2021b): Preparation and characterization of sludge-based magnetic biochar by pyrolysis for methylene blue removal. Nanomaterials 11, 2473.

Zhang D., Wei Y., Wu S., Dong Y., Zhou B., Liang J., Zhou L. (2023): Synergetic interactions between zero-valent iron and schwertmannite for enhanced arsenic (III) removal: Role of morphological variations. Chem. Eng. J. 477, 146934.

Zhang P., Simunek J., Bowman R.S. (2004): Nonideal transport of solute and colloidal tracers through reactive zeo-lite/iron pellets. Water Resour. Res. 40, W04207.

Zhang X., Wu Y. (2017): Application of coupled zero-valent iron/biochar system for degradation of chlorobenzene-contaminated groundwater. Water Sci. Technol. 75, 571–580.

Zhang Y., Wang J., Amrhein C., Frankenberger W.T. Jr. (2005): Removal of selenate from water by zerovalent iron. J. Environ. Qual. 34, 487–495.

Zhao Y., Yu J., Jin W. (2011): Damage analysis and cracking model of reinforced concrete structures with rebar corrosion. Corros. Sci. 53, 3388–3397.

Zhou H., He Y., Lan Y., Mao J., Chen S. (2008). Influence of complex reagents on removal of chromium (VI) by zero-valent iron. Chemosphere 72, 870-874.

Zhou X. (2021): Numerical modeling of granular materials and multiphysical processes in porous media. PhD Dissertation, University of Colorado at Boulder, USA.

Zhu X., Han B., Feng Q. (2020): Common anions affected removal of carbon tetrachloride in groundwater using granular sponge zerovalent iron. Water Air Soil Pollut. 231, 138.

Appendix 1

2 published papers and 1 submitted manuscript

As first author:

1. Tao R., Cui X., Xiao M., Hu R., Gwenzi W., Ruppert H., Noubactep C. (2023): Effects of commonly occurring anions on the efficiency of Fe^0-based remediation systems. Journal of Environmental Management (submitted).
2. Tao R., Cui X., Xiao M., Hu R., Gwenzi W., Ruppert H., Noubactep C. (2023): Influence of water salinity on the efficiency on Fe^0-based systems for water treatment. Water 15, 2466.
3. Tao R., Yang H., Cui X., Xiao M., Gatcha-Bandjun N., Kenmogne-Tchidjo J.F., Lufingo M., Konadu-Amoah B., Tepong-Tsindé R., Ndé-Tchoupé A.I., Touomo-Wouafo M., Btatkeu-K B.D., Gwenzi W., Hu R., Tchatchueng J.B., Ruppert H., Noubactep C. (2022): The suitability of hybrid Fe^0/aggregate filtration systems for water treatment. Water 14, 260.

As co-authors:

1. Xiao M., Hu R., Tao R., Cui X., Konadu-Amoah B., Yang H., Ndé-Tchoupé A.I., Gwenzi W., Noubactep C., Ruppert H. (2023): Metallic iron for environmental remediation: The still overlooked iron chemistry. Appl. Water Sci. 13, 222.
2. Cui X., Tao R., Xiao M., Hu R., Ruppert H., Gwenzi W., Noubactep C. (2023): Developing the ascorbic acid test: A candidate standard tool for characterizing the intrinsic reactivity of metallic iron for water remediation. Water 15, 1930.
3. Konadu-Amoah B., Hu R., Cui X., Cao V., Tao R., Yang H., Ndé-Tchoupé A.I., Gwenzi W., Ruppert H., Noubactep C (2022): Realizing the potential of metallic iron for the mitigation of toxics: Flee or adapt? Appl Water Sci. 12, 217.
4. Konadu-Amoah B., Hu R., Cui X., Tao R., Ndé-Tchoupé A.I., Gwenzi W., Noubactep C (2023): Characterizing the process of phosphate removal in Fe^0/H_2O systems. Chem. Eng. J. 465, 143042.
5. Hu R., Yang H., Tao R., Cui X., Xiao M., Konadu-Amoah B., Cao V., Lufingo M., Soppa-Sangue N.P., Ndé-Tchoupé A.I., Gatcha-Bandjun N., Sipowo-Tala V.R., Gwenzi W., Noubactep C. (2020): Metallic iron for environmental remediation: Starting an overdue progress in knowledge. Water 12, 641.
6. Yang H., Hu R., Qiu P., Liu Q., Xing Y., Tao R., Thomas P (2020): Application of Wavelet De-Noising for Travel-Time Based Hydraulic Tomography, Water 12(6), 1533.

Appendix 2

Tables presenting ALL results used in the presentation

Experiment 1: Influence of Cl^- Concentration on MB Discoloration in Fe^0/H_2O Systems

NaCl = 0g/L										
Run	**MB1**	**MB2**	**MB3**	**MB**	**dMB**	**MB1**	**MB2**	**MB3**	**MB**	**dMB**
(-)	(mg/L)	(mg/L)	(mg/L)	(mg/L)	(mg/L)	(%)	(%)	(%)	(%)	(%)
1	4.7	2.4	4.6	3.9	1.3	51.0	75.0	52.1	59.4	13.5
2	4.2	6.1	4.5	4.9	1.0	56.3	36.5	53.1	48.6	10.6
3	3.6	2.8	3.7	3.4	0.5	62.5	70.8	61.5	64.9	5.1
4	6.2	5.3	4.9	5.5	0.7	35.4	44.8	49.0	43.1	6.9
5	5.3	6.1	4.7	5.4	0.7	44.8	36.5	51.0	44.1	7.3
6	7.1	6.8	7.7	7.2	0.5	26.0	29.2	19.8	25.0	4.8
7	7.7	7.8	6.7	7.4	0.6	19.8	18.8	30.2	22.9	6.3
8	8.3	8.4	8.7	8.5	0.2	13.5	12.5	9.4	11.8	2.2
9	8.6	8.9	8.1	8.5	0.4	10.4	7.3	15.6	11.1	4.2
10	9.6	9.4	9.4	9.5	0.1	0.0	2.1	2.1	1.4	1.2

NaCl = 8g/L										
Run	MB1	MB2	MB3	MB	dMB	MB1	MB2	MB3	MB	dMB
(-)	(mg/L)	(mg/L)	(mg/L)	(mg/L)	(mg/L)	(%)	(%)	(%)	(%)	(%)
1	7.0	7.0	7.2	7.1	0.1	27.1	27.1	25.0	26.4	1.2
2	8.1	8.1	7.9	8.0	0.1	15.6	15.6	17.7	16.3	1.2
3	8.4	8.2	8.1	8.2	0.2	12.5	14.6	15.6	14.2	1.6
4	7.6	7.8	7.4	7.6	0.2	20.8	18.8	22.9	20.8	2.1
5	8.6	8.3	8.4	8.4	0.2	10.4	13.5	12.5	12.2	1.6
6	9.0	8.9	9.0	9.0	0.1	6.3	7.3	6.3	6.6	0.6
7	9.0	9.1	9.2	9.1	0.1	6.3	5.2	4.2	5.2	1.0
8	9.0	9.3	9.2	9.2	0.2	6.3	3.1	4.2	4.5	1.6
9	9.4	9.4	9.1	9.3	0.2	2.1	2.1	5.2	3.1	1.8
10	9.4	9.6	9.5	9.5	0.1	2.1	0.0	1.0	1.0	1.0

NaCl = 40/L										
Run	MB1	MB2	MB3	MB	dMB	MB1	MB2	MB3	MB	dMB
(-)	(mg/L)	(mg/L)	(mg/L)	(mg/L)	(mg/L)	(%)	(%)	(%)	(%)	(%)
1	4.8	5.1	5.7	5.2	0.5	42.2	38.6	31.3	37.3	5.5
2	7.5	7.5	6.2	7.1	0.8	9.6	9.6	25.3	14.9	9.0
3	7.7	7.5	5.9	7.0	1.0	7.2	9.6	28.9	15.3	11.9
4	7.7	7.8	7.8	7.8	0.1	7.2	6.0	6.0	6.4	0.7
5	8.0	7.8	7.9	7.9	0.1	3.6	6.0	4.8	4.8	1.2
6	7.8	7.8	8.0	7.9	0.1	6.0	6.0	3.6	5.2	1.4
7	8.1	8.1	8.0	8.1	0.1	2.4	2.4	3.6	2.8	0.7
8	8.1	7.9	8.0	8.0	0.1	2.4	4.8	3.6	3.6	1.2
9	8.2	8.1	8.2	8.2	0.1	1.2	2.4	1.2	1.6	0.7
10	8.3	8.2	8.2	8.2	0.1	0.0	1.2	1.2	0.8	0.7

Experiment 2: Influence of Cl^- Concentration on Dye Discoloration in Fe^0/H_2O Systems

MB										
Run	**MB1**	**MB2**	**MB3**	**MB**	**dMB**	**MB1**	**MB2**	**MB3**	**MB**	**dMB**
(-)	(mg/L)	(mg/L)	(mg/L)	(mg/L)	(mg/L)	(%)	(%)	(%)	(%)	(%)
1	5.5	3.2	5.0	4.6	1.2	42.7	66.7	47.9	52.4	12.6
2	6.8	6.7	6.4	6.6	0.2	29.2	30.2	33.3	30.9	2.2
3	6.6	7.1	6.9	6.9	0.3	31.3	26.0	28.1	28.5	2.6
4	7.1	7.2	7.1	7.1	0.1	26.0	25.0	26.0	25.7	0.6
5	7.0	7.2	6.5	6.9	0.4	27.1	25.0	32.3	28.1	3.8
6	7.1	7.0	6.8	7.0	0.2	26.0	27.1	29.2	27.4	1.6
7	7.2	6.5	7.0	6.9	0.4	25.0	32.3	27.1	28.1	3.8
8	7.2	7.6	7.2	7.3	0.2	25.0	20.8	25.0	23.6	2.4
9	6.9	7.2	7.1	7.1	0.2	28.1	25.0	26.0	26.4	1.6
10	7.1	5.8	5.2	6.0	1.0	26.0	39.6	45.8	37.2	10.1

MO										
Run	**MO1**	**MO2**	**MO3**	**MO**	**dMO**	**MO1**	**MO2**	**MO3**	**MO**	**dMO**
(-)	(mg/L)	(mg/L)	(mg/L)	(mg/L)	(mg/L)	(%)	(%)	(%)	(%)	(%)
1	4.9	2.4	2.2	3.2	1.5	49.0	75.0	77.1	67.0	15.7
2	6.1	6.3	6.4	6.3	0.2	36.5	34.4	33.3	34.7	1.6
3	7.6	6.9	7.2	7.2	0.4	20.8	28.1	25.0	24.7	3.7
4	6.6	7.5	7.1	7.1	0.5	31.3	21.9	26.0	26.4	4.7
5	7.5	7.3	7.3	7.4	0.1	21.9	24.0	24.0	23.3	1.2
6	8.2	7.1	7.3	7.5	0.6	14.6	26.0	24.0	21.5	6.1
7	8.0	7.6	7.4	7.7	0.3	16.7	20.8	22.9	20.1	3.2
8	7.6	8.2	8.1	8.0	0.3	20.8	14.6	15.6	17.0	3.3
9	8.8	8.8	8.4	8.7	0.2	8.3	8.3	12.5	9.7	2.4
10	6.2	6.6	7.1	6.6	0.5	35.4	31.3	26.0	30.9	4.7

RR120										
Run	**RR1**	**RR2**	**RR3**	**RR**	**dRR**	**RR1**	**RR2**	**RR3**	**RR**	**dRR**
(-)	(mg/L)	(mg/L)	(mg/L)	(mg/L)	(mg/L)	(%)	(%)	(%)	(%)	(%)
1	5.2	4.1	3.5	4.3	0.9	45.8	57.3	63.5	55.6	9.0
2	3.7	5.6	5.8	5.0	1.2	61.5	41.7	39.6	47.6	12.1
3	5.8	6.3	6.4	6.2	0.3	39.6	34.4	33.3	35.8	3.3
4	5.9	6.2	6.3	6.1	0.2	38.5	35.4	34.4	36.1	2.2
5	6.6	6.6	6.7	6.6	0.1	31.3	31.3	30.2	30.9	0.6
6	6.6	6.4	6.5	6.5	0.1	31.3	33.3	32.3	32.3	1.0
7	7.1	6.7	6.7	6.8	0.2	26.0	30.2	30.2	28.8	2.4
8	7.3	7	6.9	7.1	0.2	24.0	27.1	28.1	26.4	2.2
9	8.3	8	8.9	8.4	0.5	13.5	16.7	7.3	12.5	4.8
10	7.9	5.8	6.6	6.8	1.1	17.7	39.6	31.3	29.5	11.0

OII										
Run	**OII1**	**OII2**	**OII3**	**OII**	**dOII**	**OII1**	**OII2**	**OII3**	**OII**	**dOII**
(-)	(mg/L)	(mg/L)	(mg/L)	(mg/L)	(mg/L)	(%)	(%)	(%)	(%)	(%)
1	2.9	2.8	2.4	2.7	0.3	69.8	70.8	75.0	71.9	2.8
2	5.8	6.0	5.8	5.9	0.1	39.6	37.5	39.6	38.9	1.2
3	6.0	6.2	7.3	6.5	0.7	37.5	35.4	24.0	32.3	7.3
4	7.0	7.1	6.7	6.9	0.2	27.1	26.0	30.2	27.8	2.2
5	6.3	7.1	8.6	7.3	1.2	34.4	26.0	10.4	23.6	12.2
6	6.4	7.1	6.1	6.5	0.5	33.3	26.0	36.5	31.9	5.3
7	7.4	7.2	7.2	7.3	0.1	22.9	25.0	25.0	24.3	1.2
8	7.0	7.9	7.1	7.3	0.5	27.1	17.7	26.0	23.6	5.1
9	7.6	7.6	7.9	7.7	0.2	20.8	20.8	17.7	19.8	1.8
10	5.9	3.9	3.0	4.3	1.5	38.5	59.4	68.8	55.6	15.5

Experiment 3: Influence of Fe^0 Dosage on Dye Discoloration in Fe^0/H_2O Systems

MB							
Run	**System**	**ZVI**	**Solution**	**MB**	**deltaMB**	**MB**	**deltaMB**
(-)		(g)	(-)	(mg/L)	(mg/L)	(%)	(%)
1	None	0.00	TW	9.60	0.10	0.00	1.04
2	Sand	0.00	TW	5.63	1.44	41.32	14.96
3	ZVI1-Sand	0.05	TW	4.30	0.79	55.21	8.27
4	ZVI1-Sand	0.10	TW	3.43	0.31	64.24	3.18
5	ZVI1-Sand	0.20	TW	4.33	0.32	54.86	3.35
6	ZVI1-Sand	0.40	TW	2.77	0.40	71.18	4.21
7	ZVI1-Sand	0.60	TW	2.27	0.21	76.39	2.17
8	ZVI1-Sand	0.80	TW	1.57	0.47	83.68	4.92
9	ZVI1-Sand	1.00	TW	1.67	0.50	82.64	5.24

MB

Run	System	ZVI	Solution	MB	deltaMB	MB	deltaMB
(-)		(g)	(-)	(mg/L)	(mg/L)	(%)	(%)
1	None	0.00	SW	8.27	0.06	0.04	0.70
2	Sand	0.00	SW	6.77	0.67	18.18	8.05
3	ZVI1-Sand	0.05	SW	5.90	0.17	28.66	2.09
4	ZVI1-Sand	0.10	SW	6.03	0.51	27.05	6.21
5	ZVI1-Sand	0.20	SW	5.67	0.25	31.48	3.04
6	ZVI1-Sand	0.40	SW	4.53	0.65	45.18	7.87
7	ZVI1-Sand	0.60	SW	4.30	0.53	48.00	6.40
8	ZVI1-Sand	0.80	SW	3.97	1.05	52.04	12.70
9	ZVI1-Sand	1.00	SW	3.63	0.57	56.07	6.88

MO

Run	System	ZVI	Solution	MB	deltaMB	MB	deltaMB
(-)		(g)	(-)	(mg/L)	(mg/L)	(%)	(%)
1	None	0.00	TW	9.17	0.06	0.15	0.63
2	Sand	0.00	TW	9.13	0.06	0.51	0.63
3	ZVI1-Sand	0.05	TW	4.67	0.23	49.16	2.52
4	ZVI1-Sand	0.10	TW	3.77	0.35	58.97	3.83
5	ZVI1-Sand	0.20	TW	2.43	0.12	73.49	1.26
6	ZVI1-Sand	0.40	TW	1.17	0.31	87.29	3.33
7	ZVI1-Sand	0.60	TW	0.57	0.25	93.83	2.74
8	ZVI1-Sand	0.80	TW	0.47	0.15	94.92	1.66
9	ZVI1-Sand	1.00	TW	0.37	0.06	96.01	0.63

MO

Run	System	ZVI	Solution	MB	deltaMB	MB	deltaMB
(-)		(g)	(-)	(mg/L)	(mg/L)	(%)	(%)
1	None	0.00	SW	9.27	0.75	0.04	8.10
2	Sand	0.00	SW	9.60	0.10	3.56	1.08
3	ZVI1-Sand	0.05	SW	6.57	0.72	29.16	7.80
4	ZVI1-Sand	0.10	SW	7.00	0.62	24.49	6.74
5	ZVI1-Sand	0.20	SW	4.43	1.51	52.18	16.34
6	ZVI1-Sand	0.40	SW	2.73	0.40	70.51	4.36
7	ZVI1-Sand	0.60	SW	3.87	0.49	58.29	5.32
8	ZVI1-Sand	0.80	SW	3.50	0.26	62.24	2.85
9	ZVI1-Sand	1.00	SW	2.67	1.42	71.23	15.27

Experiment 4: Influence of Fe^0 Type on Dye Discoloration in Fe^0/H_2O Systems

MB								
Run	**System**	**Sand**	**ZVI**	**Solution**	**MB**	**deltaMB**	**MB**	**deltaMB**
(-)		(g)	(g)	(-)	(mg/L)	(mg/L)	(%)	(%)
1	None	0.00	0.00	TW	9.37	0.15	0.14	1.63
2	Sand	0.50	0.00	TW	6.10	1.21	34.97	12.93
3	ZVI1-Sand	0.50	0.10	TW	3.00	0.66	68.02	6.99
4	ZVI2-Sand	0.50	0.10	TW	2.83	0.15	69.79	1.63
5	ZVI3-Sand	0.50	0.10	TW	3.53	0.42	62.33	4.44
6	ZVI4-Sand	0.50	0.10	TW	5.47	1.00	41.72	10.68

MB								
Run	**System**	**Sand**	**ZVI**	**Solution**	**MB**	**deltaMB**	**MB**	**deltaMB**
(-)		(g)	(g)	(-)	(mg/L)	(mg/L)	(%)	(%)
1	None	0.00	0.00	SW	8.13	0.06	0.08	0.71
2	Sand	0.50	0.00	SW	6.30	0.26	22.60	3.25
3	ZVI1-Sand	0.50	0.10	SW	5.67	0.32	30.38	3.95
4	ZVI2-Sand	0.50	0.10	SW	3.87	0.71	52.50	8.72
5	ZVI3-Sand	0.50	0.10	SW	5.23	0.57	35.71	6.99
6	ZVI4-Sand	0.50	0.10	SW	6.30	0.61	22.60	7.47

MO								
Run	**System**	**Sand**	**ZVI**	**Solution**	**MB**	**deltaMB**	**MB**	**deltaMB**
(-)		(g)	(g)	(-)	(mg/L)	(mg/L)	(%)	(%)
1	None	0.00	0.00	TW	9.13	0.12	0.07	1.26
2	Sand	0.50	0.00	TW	9.17	0.06	-0.29	0.63
3	ZVI1-Sand	0.50	0.10	TW	3.67	0.96	59.88	10.51
4	ZVI2-Sand	0.50	0.10	TW	1.03	0.42	88.69	4.56
5	ZVI3-Sand	0.50	0.10	TW	1.27	0.57	86.14	6.22
6	ZVI4-Sand	0.50	0.10	TW	8.03	1.76	12.11	19.27

MO								
Run	**System**	**Sand**	**ZVI**	**Solution**	**MB**	**deltaMB**	**MB**	**deltaMB**
(-)		(g)	(g)	(-)	(mg/L)	(mg/L)	(%)	(%)
1	None	0.00	0.00	SW	9.77	0.06	0.03	0.59
2	Sand	0.50	0.00	SW	9.70	0.10	0.72	1.02
3	ZVI1-Sand	0.50	0.10	SW	5.77	1.07	40.98	10.94
4	ZVI2-Sand	0.50	0.10	SW	3.80	0.61	61.11	6.23
5	ZVI3-Sand	0.50	0.10	SW	7.23	1.85	25.96	18.94
6	ZVI4-Sand	0.50	0.10	SW	7.90	1.25	19.14	12.78

Experiment 5: The mechanism of MB discoloration in the presence of anions

Iron	Carbonate		Chloride		Fluoride		Phosphate		Sulfate	
Duration	**E**	**delta**	**E**	**delta**	**E**	**delta**	**E**	**delta**	**E**	**delta**
(day)	(%)	(%)	(%)	(%)	(%)	(%)	(%)	(%)	(%)	(%)
1	7.7	1.2	10.3	1.5	8.3	1.5	5.0	1.7	11.7	2.1
2	32.3	4.0	10.7	1.2	9.3	2.3	12.0	1.0	13.3	0.6
4	24.3	3.2	11.0	1.0	7.7	0.6	9.7	2.5	12.3	1.2
6	30.3	6.8	8.7	1.5	11.0	4.0	8.7	1.5	14.0	1.7
8	27.7	3.8	11.3	1.2	7.3	1.2	10.7	0.6	12.3	1.2
10	33.7	5.5	12.0	1.0	7.0	1.0	10.0	1.0	13.7	2.5
15	40.7	4.2	14.3	1.5	9.3	1.5	17.7	1.2	14.0	1.0
20	57.7	2.3	17.3	1.5	14.0	3.6	16.7	4.0	18.7	7.2
25	63.7	3.2	24.3	5.0	25.3	12.1	21.7	1.5	28.3	9.1
30	74.7	6.7	43.3	2.3	37.0	4.6	22.0	1.0	33.7	0.6

pH	Carbonate		Chloride		Fluoride		Phosphate		Sulfate	
Duration	**pH**	**delta**	**pH**	**delta**	**pH**	**delta**	**pH**	**delta**	**pH**	**delta**
(day)	(-)	(-)	(-)	(-)	(-)	(-)	(-)	(-)	(-)	(-)
1	9.1	0.0	8.0	0.0	8.2	0.0	8.6	0.0	8.1	0.0
2	9.1	0.0	7.9	0.0	8.3	0.0	8.6	0.0	8.2	0.1
4	9.1	0.0	8.0	0.0	8.3	0.0	8.6	0.0	8.3	0.0
6	9.1	0.0	8.0	0.0	8.3	0.0	8.6	0.0	8.3	0.1
8	9.1	0.0	8.1	0.0	8.2	0.0	8.6	0.0	8.3	0.1
10	9.1	0.0	8.1	0.0	8.3	0.0	8.6	0.0	8.4	0.0
15	9.1	0.0	8.1	0.0	8.4	0.1	8.6	0.0	8.5	0.0
20	9.1	0.0	8.3	0.0	8.5	0.1	8.6	0.0	8.5	0.1
25	9.2	0.0	8.3	0.0	8.5	0.0	8.6	0.0	8.4	0.1
30	9.2	0.0	8.2	0.0	8.5	0.0	8.6	0.0	8.3	0.0

Experiment 6: Effects of common anions on the reactivity of Fe^0/H_2O systems

Iron	**NaCl**		**NaF**		**$NaHCO_3$**		**Na_2SO4**		**Na_2HPO_4**	
Run	**Fe**	**Delta**	**Fe**	**Delta**	**Fe**	**Delta**	**Fe**	**Delta**	**Fe**	**Delta**
(-)	(mg/L)	(mg/L)	(mg/L)	(mg/L)	(mg/L)	(mg/L)	(mg/L)	(mg/L)	(mg/L)	(mg/L)
1	0.26	0.02	0.28	0.02	0.07	0.01	0.25	0.09	0.13	0.01
2	0.26	0.01	0.25	0.02	0.07	0.01	0.18	0.03	0.14	0.01
4	0.26	0.02	0.29	0.03	0.10	0.03	0.20	0.08	0.15	0.02
6	0.28	0.05	0.33	0.04	0.09	0.01	0.14	0.02	0.14	0.01
8	0.32	0.02	0.52	0.03	0.12	0.01	0.14	0.02	0.13	0.01
10	0.32	0.02	0.59	0.02	0.14	0.03	0.17	0.03	0.14	0.01
15	0.48	0.14	0.84	0.02	0.16	0.06	0.15	0.01	0.14	0.01
20	0.26	0.04	1.01	0.02	0.18	0.01	0.13	0.01	0.15	0.00
25	0.28	0.03	0.98	0.09	0.24	0.02	0.13	0.01	0.14	0.01
30	0.30	0.06	0.85	0.03	0.32	0.05	0.14	0.02	0.19	0.07

E	**NaCl**		**NaF**		**$NaHCO_3$**		**Na_2SO4**		**Na_2HPO_4**	
Run	**Fe**	**Delta**	**Fe**	**Delta**	**Fe**	**Delta**	**Fe**	**Delta**	**Fe**	**Delta**
(-)	(%)	(%)	(%)	(%)	(%)	(%)	(%)	(%)	(%)	(%)
1	58.7	8.6	72.0	9.9	72.0	7.2	73.7	20.8	55.7	6.7
2	49.0	8.2	47.7	5.8	62.7	4.7	45.0	2.7	49.7	3.1
4	46.0	6.9	54.3	3.8	61.7	6.4	39.3	14.2	41.3	5.1
6	57.0	10.8	56.0	19.1	61.0	6.6	35.7	8.3	46.7	1.5
8	58.3	4.2	51.7	9.9	60.7	9.1	39.0	5.6	44.7	3.1
10	52.7	7.4	53.0	3.0	59.7	7.1	43.7	8.5	60.0	10.6
15	59.0	7.2	52.7	4.7	66.0	7.6	45.0	5.0	65.7	3.8
20	51.0	3.0	54.3	5.5	76.7	3.8	41.7	9.5	51.3	10.0
25	58.0	7.0	60.3	9.3	90.3	2.1	47.3	10.1	54.3	9.2
30	65.7	12.9	60.7	5.5	94.3	2.1	57.7	6.5	49.3	5.7

pH	$NaCl$		NaF		$NaHCO_3$		Na_2SO4		Na_2HPO_4	
Run	**Fe**	**Delta**	**Fe**	**Delta**	**Fe**	**Delta**	**Fe**	**Delta**	**Fe**	**Delta**
(-)	(-)	(-)	(-)	(-)	(-)	(-)	(-)	(-)	(-)	(-)
1	8.32	0.04	8.37	0.02	8.27	0.01	8.25	0.02	8.20	0.01
2	8.21	0.02	8.51	0.05	8.99	0.02	8.48	0.16	8.33	0.05
4	8.21	0.01	8.47	0.02	9.01	0.01	8.50	0.03	8.43	0.00
6	8.19	0.01	8.46	0.04	9.09	0.07	8.47	0.09	8.45	0.01
8	8.19	0.04	8.44	0.02	9.16	0.04	8.51	0.04	8.45	0.02
10	8.18	0.02	8.42	0.02	9.09	0.05	8.47	0.16	8.47	0.02
15	8.16	0.01	8.37	0.03	8.99	0.03	8.45	0.09	8.46	0.04
20	8.14	0.01	8.36	0.02	9.05	0.03	8.45	0.07	8.51	0.05
25	8.09	0.01	8.32	0.03	9.07	0.04	8.32	0.05	8.54	0.05
30	8.05	0.01	8.32	0.03	9.08	0.02	8.56	0.18	8.59	0.01

Experiment 7: Effects of the Fe^0 intrinsic reactivity

	ZVI1		**ZVI2**		**ZVI3**		**ZVI4**	
	E	**ΔE**	**E**	**ΔE**	**E**	**ΔE**	**E**	**ΔE**
	(%)	(%)	(%)	(%)	(%)	(%)	(%)	(%)
TW	62.7	23.7	66.0	6.6	63.0	11.3	59.0	8.5
$Cl^–$	47.7	3.2	59.3	11.7	44.3	5.9	41.3	4.9
$F^–$	43.3	8.1	52.3	4.0	31.0	5.0	45.0	6.6
$HCO_3^–$	89.0	4.4	89.0	2.0	88.7	2.3	76.7	10.4
$SO_4^{2–}$	56.7	6.8	55.7	12.7	60.7	14.5	43.0	11.3
$HPO_4^{2–}$	35.0	14.0	23.3	1.5	28.0	9.5	23.3	1.5

Experiment 8: Effects of the nature of contaminants

MB	**Fe**	**Delta**	**E**	**Delta**	**pH**	**Delta**
	(mg/L)		(%)	(%)		
TW	0.14	0.01	71.33	7.51	8.37	0.06
Cl^-	0.22	0.07	59.33	7.37	7.96	0.02
F^-	0.84	0.07	66	2.65	8.31	0.04
HCO_3^-	0.32	0.07	95.33	0.58	9.14	0.06
SO_4^{2-}	0.21	0.02	68.67	11.68	8.32	0.08
HPO_4^{2-}	0.19	0.03	60	10.15	8.58	0.03

OII	**Fe**	**Delta**	**E**	**Delta**	**pH**	**Delta**
	(mg/L)		(%)	(%)		
TW	0.15	0.01	83.67	3.21	8.25	0.02
Cl^-	0.18	0.01	78.33	4.16	7.94	0.01
F^-	0.83	0.08	80.33	8.33	8.26	0.06
HCO_3^-	0.33	0.04	59	3.61	9.11	0.06
SO_4^{2-}	0.26	0.11	72.33	5.51	8.25	0.09
HPO_4^{2-}	0.2	0.01	50.67	4.73	8.65	0.06